NACA TN 2809

NATIONAL ADVISORY COMMITTEE FOR AERONAUTICS

TECHNICAL NOTE 2809

EXPERIMENTAL INVESTIGATION OF ECCENTRICITY RATIO, FRICTION, AND OIL FLOW OF SHORT JOURNAL BEARINGS

By G. B. DuBois and F. W. Ocvirk

Cornell University

Washington
November 1952

NATIONAL ADVISORY COMMITTEE FOR AERONAUTICS

TECHNICAL NOTE 2809

EXPERIMENTAL INVESTIGATION OF ECCENTRICITY RATIO, FRICTION, AND OIL FLOW OF SHORT JOURNAL BEARINGS

By G. B. DuBois and F. W. Ocvirk

SUMMARY

An experimental investigation of the performance of a full journal bearing under steady load was conducted at Cornell University to provide experimental data for comparison with an analytical solution which includes end leakage and offers advantages for the short bearing lengths commonly used. A $1\frac{3}{8}$-inch-diameter journal was tested at length-diameter ratios of 2, 1, 1/2, and 1/4, at speeds up to 6000 rpm, and with unit loads from 0 to 900 pounds per square inch using SAE 10 oil and AN-09-1010 oil. The eccentricity ratio, or the relative displacement of the shaft in the bearing clearance, was measured for comparison with the theoretical curves by a system of levers and sensitive dial indicators. Friction and oil flow data were also obtained.

The elastic deflection of the journal was found to affect the eccentricity ratio considerably, and the data were corrected for this effect. The corrected experimental data were in good agreement with the theoretical curves for length-diameter ratios of 1, 1/2, and 1/4. The data for a length-diameter ratio of 2 were insufficient to warrant a conclusion.

Changes in inlet oil pressure at light loads affected the angle of displacement more than the eccentricity ratio. A semiempirical method of plotting oil flow as affected by inlet oil pressure gave a single line for all of these tests and for data reported by Mr. S. A. McKee.

The experimental data on eccentricity ratio and friction followed single lines when plotted against a theoretically derived capacity number equal to the Sommerfeld number times the square of the length-diameter ratio. The form of the capacity number indicates that under certain conditions the eccentricity ratio is theoretically independent of bearing diameter.

Single-line summary curves may be used as charts which facilitate simple solutions of bearing performance at a known or an assumed operating temperature. Methods of approximating a maximum bearing temperature are discussed, and a method of evaluating the effect of deflection or misalinement on the eccentricity ratio at the ends of a bearing is explained.

INTRODUCTION

In recent years, intensive efforts have been made to include end leakage in the analysis of plain bearings of commonly used short lengths. The most recent mathematical analyses of the effect of length-diameter ratio and end leakage on bearing performance have been made by Cameron and Wood (reference 1) and by Ocvirk (reference 2). Comparison of experimental data with theoretical predictions has been meager because of the lack of experimental data, especially in the region of length-diameter ratios of less than unity.

An experimental investigation was conducted at the School of Mechanical Engineering of Cornell University at Ithaca, New York, in order to make available performance data on bearings of length-diameter ratios of 2, 1, 1/2, and 1/4. The project was conducted under the sponsorship and with the financial aid of the National Advisory Committee for Aeronautics. The specific objectives of the investigation and the methods of plotting the experimental data were developed from the mathematical analysis of the short-bearing approximation as proposed in reference 2. The short-bearing approximation is an extension of the film pressure distribution function by Michell (reference 3) and Cardullo (reference 4) resulting in theoretical performance curves in which the basic nondimensional quantity is the capacity number C_n. This capacity number is the product of the well-known Sommerfeld number and the square of the length-diameter ratio. The following performance characteristics are theoretically shown to be single-curve functions of this capacity number: (1) Eccentricity ratio, (2) attitude angle, (3) friction, (4) required oil flow rate, (5) peak pressure in the oil film, and (6) angular location of the peak pressure. Experimental data were obtained for comparison with the first four theoretical curves as shown in figures 1 to 4.

The method of measuring journal position with respect to the bearing is of major importance, because this is the principal variable in the theoretical analysis and because this measurement has been difficult in experimental investigations of the past. Also of special interest are the measurements of clearance at room temperature and at elevated temperatures under running conditions. Measurements of bearing friction,

temperatures near the bearing surface, oil flow rate, applied load, and journal speed are less difficult to determine.

Feeding oil under pressure through a single hole on the unloaded side of the bearing was adopted for the tests reported herein as the simplest configuration for lubrication. The analytical expression for oil flow deals only with the flow from the 180° of the converging film. This flow has been called the "required" oil flow to distinguish it from the "total" flow from the 360° bearing which could be measured experimentally. Inlet oil pressure materially affects the total oil flow, especially that which is discharged from the unloaded side. As shown in figure 5, the total oil flow approximates a single line when the ratio of total to required oil flow is plotted against C_{p_o}, a non-dimensional variable empirically arranged to include inlet oil pressure.

Considerable averaging of data was achieved. In friction and oil flow measurements, data for clockwise and counterclockwise rotations were averaged. Measurements of journal displacement were averages of the data taken for the two directions of rotation, for increasing and decreasing applications of load, and for the two ends of the bearing.

SYMBOLS

The geometric relationship of the journal and bearing is shown diagrammatically in figure 6.

Dimensional quantities:

l	bearing length, inches
d	bearing diameter, inches
r	bearing radius, inches
c_d	diametral bearing clearance, inches
c_r	radial bearing clearance, inches $(c_d/2)$
e	eccentricity, inches
h	oil film thickness, inches
h_{min}	minimum oil film thickness, inches
ϕ	attitude angle, angle between load line and line of centers, degrees

M_t friction torque, inch-pounds

F_c friction calibration factor, inch-pounds per inch of mercury

N journal speed, rpm

N' journal speed, rps

P net bearing load, pounds

p unit pressure on projected area, pounds per square inch (P/ld)

p_o inlet oil pressure, pounds per square inch

p_c capsule pressure, pounds per square inch

Q experimental total rate of oil flow, cubic inches per second

Q_{req} theoretically required rate of oil flow, cubic inches per second

T temperature, ^oF

Z oil viscosity, centipoises

μ oil viscosity, reyns $\left(\frac{Z}{6.9 \times 10^6}\right)$

Nondimensional quantities:

n eccentricity ratio or attitude $\left(\frac{e}{c_r}\right)$

$\frac{c_d}{d}$ clearance ratio

$\frac{l}{d}$ length-diameter ratio

C_n capacity number $\left(\frac{\mu N'}{p}\left(\frac{d}{c_d}\right)^2\left(\frac{l}{d}\right)^2\right)$

f friction coefficient $\left(\frac{M_t}{Pr}\right)$

f_v friction variable $\left(f\left(\frac{d}{c_d}\right)\left(\frac{l}{d}\right)^2\right)$

q_n oil flow number $\left(\frac{Q}{\pi\, d l c_d \frac{N'}{2}}\right)$

q oil flow factor $\left(\frac{Q}{Q_{req}} = \frac{Q}{\pi\, d l c_d \frac{N'}{2} n} = \frac{q_n}{n}\right)$

C_{p_o} inlet-pressure capacity number $\left(\frac{\mu N'}{p_o}\left(\frac{d}{c_d}\right)^2\left(\frac{l}{d}\right)^2\right)$

DESCRIPTION OF APPARATUS

A photograph of the bearing testing machine used in the experiments appears in figure 7. The manner in which the test elements were supported and loaded is shown in figures 8, 9, and 10. In addition, figure 10 illustrates diagrammatically the torquemeter used for friction-torque measurements and the means for collecting the oil flowing through the test bearing. Figures 11 and 12 show the mechanical system which measured the displacements of the journal at the ends of the bearing. The locations of thermocouples measuring bearing temperatures are given in figure 13.

Test Bearing and Journals

A bronze bearing and two steel shafts of $1\frac{3}{8}$-inch nominal diameter were used as shown in figures 8 and 9. One of the shafts served as a test element for length-diameter ratios l/d of 2 and 1; the change in l/d ratio was accomplished by reducing the length of the journal as indicated in figure 8. The second shaft was designed with two test journals of l/d of 1/2 and subsequently of 1/4 as indicated in figure 9. The double journal was decided upon for the extremely short bearing tests to increase stability and to permit the use of larger applied loads. Each of the bearings was lubricated from a single hole in the center of the bearing area in use. Drain oil holes were provided between the journals of the double journal in order to insure atmospheric pressure at each end of each journal and to guide the oil for collection.

A special boring bar, of the type developed by the Battelle Memorial Institute, was constructed to bore the bronze bearing to an accuracy of 50 millionths of an inch (0.000050 in.) as indicated by a special Federal hole gage. The journals were lapped to the same accuracy as indicated by a Pratt & Whitney supermicrometer. In order to insure a high accuracy

of roundness for the parts of the journal in contact with the levers measuring journal displacement, the entire length of the shaft was lapped before cutting the journals to length.

The diametral clearance at room temperature was measured prior to the installation of the test elements in the bearing machine. Although the determination of clearance as the difference of the individual measurements of bearing and journal was tried, it was found more accurate to measure clearance from the play between the parts. Clearance measurement in this manner is more direct than by the difference method. With the journal in the bearing, the ends of the shaft were securely clamped to V-blocks on a surface plate; the extreme displacements of the bearing allowed by the play clearance were measured with a 10-thousandths (0.0001 in.) dial indicator. The circles in figures 8 and 9 give the clearances measured in this manner at the radial and longitudinal locations indicated. Average clearances determined from the values shown are: 0.00264 inch for the single journals of l/d of 2 and 1 and 0.00232 inch for the double journals of l/d of 1/2 and 1/4.

Loading Mechanism

As shown in figure 10, the test bearing was loaded by a pressure capsule through a piston having an area of 15.02 square inches. The piston head was flush with and sealed by a 1/32-inch-thick neoprene sheet which permitted a steady pressure to be held in the capsule by an accumulator. An increase in load was obtained by allowing oil to enter the accumulator from a high pressure source, the motion of the piston being slight. A pressure gage connected to the capsule gave the magnitude of the load applied to the bearing. The load from the piston was transmitted to the test bearing through an oil-pressurized spherical seat. A flow of light oil forced between the surfaces of the spherical seat prevented metallic contact in order that the load could be transmitted without resistance to rotation of the bearing about its geometric axis. Freedom of rotation was necessary for the measurement of friction torque in the test bearing. The spherical seat was automatically stabilized by the use of four relieved areas, each with a separate source of oil flow.

Driving Mechanism

The test shaft was driven by a high-speed-aircraft, direct-current generator operating as a motor of about 10-horsepower capacity. Current was supplied from a similar unit which was part of a motor-generator set. By varying the field excitation of both direct-current units, a speed range of 500 to 10,000 rpm was attainable. Tachometers of the centrifugal type and the 3-second counting type indicated the rotative speed of the shaft.

Journal Displacement Measurement

The coordinate displacements of the journal with respect to the bearing during running were measured by the mechanical arrangement shown in figures 11 and 12. Horizontal and vertical motions of the shaft at stations beyond the ends of the bearing were transmitted by the bronze riders on levers or bell cranks through vertical rods to four dial indicators having 0.0001-inch divisions. The rods were held against the ball ends on the bell cranks by flat springs attached to the mast of the bearing hub. In order to eliminate large dial readings due to thermal expansion of the rods, a second set of similar parallel rods, intended for temperature compensation, moved the dial cases approximately the same amount the dial stems were moved by thermal expansion. The compensating rods were also held by flat springs against small ball ends fixed to the bearing hub. The dial cases were mounted on a set of flat springs cantilevered from the mast to permit the displacement caused by the temperature-compensation rods.

All experiments in which displacements were measured were made under conditions of varying load at constant speed. This was done to keep temperature changes during the tests to a minimum since it was found that varying load caused smaller changes of temperature than varying the journal speed.

During preliminary trial runs at speeds of 5000 rpm, difficulty arose because of considerable wearing of the bronze riders. By providing an oil-fed felt wiper against the shaft, a boundary oil film between the surfaces of contact reduced the wear to a satisfactory value at speeds as high as 6000 rpm, and no further trouble occurred. The method of using the data as an average of the change of position rather than as absolute values largely eliminated the possibility of slow wear affecting the accuracy of the readings.

As shown in figures 7 and 12, a second system was available for the measurement of displacement. This system, developed by Phelan (reference 5), is a photoelectric method particularly suited to indicate dynamic displacements. The glass plates shown attached to the displacement and temperature-compensating rods were photographically marked with parallel black lines. When displaced by the rods, the glass plates acted as a variable shutter so that the amount of light passing through them and impinging on the photoelectric cell was variable. The response of a pair of cells, for horizontal and vertical displacements, was transmitted to the two axes of an oscilloscope. The spot on the screen gave the coordinate displacements of the journal to a magnified scale. Two oscilloscopes were necessary to give the journal displacements of the two ends of the bearing A range of magnifications might be achieved by this method. The method was useful in the study of rapid or vibratory motions.

While the dial gages were originally intended as a method of calibrating the electronic system, all of the data taken during these experiments were obtained from the dial indicators; the photoelectric method was used only in trouble shooting to eliminate vibration.

Friction Torquemeter

Friction torque was measured by the torquemeter shown in figure 10. The torquemeter consisted of two 1/2-inch pistons which were connected to the mast extending from the test bearing so that the piston forces opposed each other. A flow of light oil was forced into the space at the head of each piston and was discharged through ports partially covered by the pistons. The friction torque of the test bearing applied a force to each of the pistons to cause a slight change in discharge-port area, resulting in a pressure differential on the two pistons to balance the applied force. The ports were adjusted to be open only a few thousandths of an inch so that the change in position of the mast in operation was a maximum of about $1/5^{\circ}$. The torquemeter pistons were supported in their bores by a pressurizing system of relieved areas, thus eliminating frictional contact.

The difference in pressure on the two pistons was indicated by a mercury manometer and was proportional to the torque on the test bearing. The test bearing and connected parts were balanced by adjustable weights so that the manometer readings in opposite directions of rotation of the journal were nearly equal. Friction-torque readings are in opposite sense for opposite rotations while unbalance is in the same sense so that the remaining unbalance is eliminated by averaging results in both directions of rotation.

Manometer readings were converted to friction torque by direct calibration. For a fixed set of operating conditions, known increments of moment were applied to the bearing hub by weights giving corresponding changes in manometer readings. A plot of these values as in figure 14 yields a straight line, the slope of which is the friction calibration factor.

Oil Flow Measurements

As shown in figure 10, the oil used to lubricate the support bearings was kept separate from the oil used in the test bearing by slingers on the shaft; the oil to the spherical seat was also separated from the test oil by baffles. As it issued from the ends of the test bearing, the test oil flowed down the walls of the bearing hub into the housing of the bearing machine. A hole in the bottom of the housing allowed the oil to be collected in a pan which could be removed for weighing on a balance graduated in hundredths of a pound.

In the experiments at l/d of 2, jet engine oil AN-09-1010 was used. Because of the high vaporization of this oil resulting in an uncomfortable atmosphere in the test room and causing slow changes in viscosity, the test oil was changed to SAE 10 oil for experiments at l/d of 1, 1/2, and 1/4. Air gusts from attempts to ventilate the room had been found to affect the torquemeter. Viscosity characteristics of these oils taken after test are given in figure 15. Low-viscosity oils were chosen to obtain high values of eccentricity ratio under reasonable loads and speeds. The use of the viscosity of the oil at running temperature in plotting the results tended to reduce the effect of the type of oil used.

The circulating system for the test oil consisted of a sump, a small pump with relief valve, a micronic-type oil filter, and a thermostatic heater. Control of the pressure of the oil entering the bearing was effected by a combination of adjusting the relief valve and adjusting a bypass valve. A pressure gage in the feed line gave the inlet oil pressure.

The thermostat of the heater was set at 140° F for all testing; there was, however, considerable heat loss in the oil lines as indicated by a thermocouple at the entrance to the bearing hub. The temperature of the test bearing near the oil film registered from 110° to 160° F, depending chiefly on rotative speed.

Bearing Temperature Measurements

As shown in figure 13, thermocouples were placed at 14 locations in the hub to give bearing temperatures near the oil film. Iron-constantan thermocouples were inserted in 0.094-inch-diameter holes to within 1/16 inch of the bearing surface.

A Leeds & Northrup potentiometer, with automatic cold-junction compensation and Fahrenheit temperature scale, was used to measure thermocouple temperatures. Thermocouple 9 gave the temperature of the bearing hub at a point 2 inches from the oil film in order to give some measure of the temperature gradient in the bearing wall.

TEST PROCEDURE

For each l/d condition two series of experiments were conducted. In the first series, displacements of the journal were measured by the dial-indicator equipment shown in figure 11. Friction torque and oil flow rate were measured in the second series of tests. Friction measurements were made in runs separate from displacement tests because it was

necessary to disconnect the dial indicators to eliminate any friction torque due to the riders. Also, oil flow tests could not be made during the displacement tests because the small oil flow, used to lubricate the riders, mixed with the oil flowing from the test bearing.

Prior to the experiments mentioned above, a series of speed runs to incipient seizure was conducted to determine the effect of temperature on the running clearance in the bearing. Because of the fundamental importance of clearance values in the calculation of capacity number and other nondimensional performance numbers, a series of experiments was made to determine the effect of differential thermal expansion of the bearing and journal on the bearing clearance. This was done by first measuring the diametral clearance at room temperature and then after running the journal at slowly increasing speeds without load to incipient seizure.

The low torque and inertia of the driving armature permitted a frictional increase or stoppage without any apparent effect on the bearing or journal surfaces. The bearing temperatures at incipient seizure were recorded as indicative of the temperature rise sufficient to cause a clearance change equal to the clearance at room temperature. By successively lapping the journal to give larger clearances, a series of three seizure runs yielded the clearance-temperature data given in figure 16. It was found that the difference in the bearing temperature near the oil film at thermocouple 4 and that at thermocouple 9, which is 2 inches from the oil film, is a linear function of the change in diametral clearance. As shown in figure 16, the three points from the seizure runs give a straight line passing through zero indicating that for zero gradient in the bearing wall there is no clearance change, both the bearing hub and the shaft being steel. It can also be said that, in effect, the temperature near the surface of the bearing has been used in lieu of the shaft temperature which was not measured.

Method Used for Locating Zero-Load Point

At first thought, it would appear to be a simple problem to relate the measured clearance of the bearing with the maximum change of the dial indicators and thus locate the position of the bearing center. In applying this on the test machine, these maximum readings of the dial indicators were obtained with the shaft stationary by applying up and down loads on the bearing. It was found that the clearance obtained in this way was less than the clearance measured at room temperature. In obtaining the clearance in the test machine, with the shaft stationary, the coordinate readings of the dial indicators, if plotted, indicate an arc-shaped line. The journal apparently was contacting the bearing several degrees each side of a theoretical vertical diameter of the clearance circle.

It might also appear desirable to set the dial gages at zero when the journal was in metallic contact with the bearing in order to increase the accuracy of the data near the point of metallic contact. This scheme was also made impracticable by the arc effect already mentioned. Thus, it was necessary to develop a technique for obtaining the location of the zero eccentricity.

The method actually used to locate the datum point at zero load at the center position of the bearing was as follows: Alternate up and down loads were applied to the bearing with the shaft stationary and coordinate dial readings at both ends of the shaft were noted. These positions located points in an arc a few degrees each side of the ends of a vertical diameter. The dial-indicator faces were then adjusted to approximately equal plus and minus readings and the process repeated for three alternate up and down loads, these readings being recorded.

The machine was then warmed up to operating conditions and, with the shaft running with an inlet oil pressure of 2 to 4 pounds per square inch, a small capsule pressure was found by repeated trials which made the average of dial readings for two directions of rotation closely equal to the average of the three up and down stationary readings. This small capsule pressure was of the order of 4 pounds per square inch and closely checked the capsule pressure needed to counteract the tare weight of the bearing assembly. The dial-gage reading was also checked against the average of horizontal displacement possible with the shaft stationary. The machine was then ready to run. The net load was calculated by using the difference between the capsule pressure under load and the capsule pressure representing tare weight. The displacements were also differences between dial readings under load and at no load to cancel the fact that the true center was not exactly at zero on the dial. After a varying-load test, the location of the datum point at zero load was rechecked in two directions of rotation to permit averaging out any small change during the test. Wear of the lever rubbing surfaces or riders was imperceptible during individual tests but would have been canceled by this method.

This method has the advantage that the change in load is plotted against change in displacement, using an experimentally determined zero-load position.

It was discovered that when running at zero load the bearing required nearly zero oil flow; the dials showed that the journal maintained its position steadily when the inlet oil pressure was reduced to 2 pounds per square inch and the flow was a few drops per minute. Increasing the inlet pressure caused the journal to displace as though a load had been applied. This effect was more marked as the inlet pressure was further increased, and the oil flow increased to a continuous stream. The position of zero eccentricity was achieved by adjusting the

loading capsule to balance the tare weight to give zero load and by using an inlet pressure of 2 to 4 pounds per square inch.

Displacement Experiments

Variations in displacement were obtained by varying the load at constant speed and constant inlet oil pressure. It was found that by holding a constant speed the variations in temperature were less than 5° F during an increasing-load run. A nearly constant temperature of the apparatus at thermal equilibrium assured a minimum thermal effect in the measurements of displacement. Prior to taking data, the test elements and measuring apparatus were brought to equilibrium temperature by running at constant speed and zero load for a period of 20 to 30 minutes.

After setting the dials and determining the datum position of the journal, the oil inlet pressure was raised to the value to be used in the remainder of the test. Displacement data as read from the four dials were then recorded for various increments of load. The load was increased in 10 to 15 increments and then decreased in the same increments to permit averaging of data. As shown in the sample log sheet of table I, the following data were recorded: Journal displacements, capsule pressure, bearing temperatures at critical locations, inlet oil pressure, speed, direction of rotation, time, inlet oil temperature, room temperature, and oil temperature after the heater. The same procedure was followed in the opposite direction of rotation so that the data could be averaged for the two rotations.

For each l/d value there were experimental runs in each direction of rotation at combinations of constant speed and constant inlet oil pressure, as given in figures 17 to 24. The speeds were 500, 1000, 2000, 2500, 4000, 5000, and 6000 rpm, and the inlet oil pressures were 4, 40, and 100 pounds per square inch. The maximum load on projected area was 760 pounds per square inch, and the maximum oil film temperature was 160° F.

Control of Whirl

At journal speeds of 500 and 1000 rpm, there was little difficulty with vibration even at zero load. However, at zero load at the higher speeds from 2000 to 6000 rpm a vibration, or whirl, in a rotating misalinement mode, would build up, preventing the reading of displacements. The vibration could be stopped by the application of load, but it was necessary to prevent vibration at zero load in order to use the routine procedure to obtain the position of zero eccentricity. By snubbing the top of the mast and the arm extending laterally from the bearing hub with

foam rubber, the vibrations were successfully eliminated. The foam rubber was placed to snub motion in misalinement directions only, using small snubbing forces perpendicular to the load. By temporarily removing the snubbers at loads where no vibration would occur, it was found that the snubbers had no effect on the dial-indicator readings.

Friction and Oil Flow Experiments

Friction torque and oil flow rate were measured simultaneously, with the displacement-measuring apparatus temporarily disconnected in order to eliminate the friction of the riders and the oil flow to them. Changes in friction and oil flow were made by varying the applied load and maintaining the journal speed and inlet oil pressure constant. Before beginning a test, a period of running of approximately 20 to 30 minutes at constant speed was allowed to reach thermal equilibrium. About 10 to 15 increments of increasing load were then applied. At each load, after the oil flow stabilized, the flow rate was determined by collecting the oil in a pan for periods of 1 to 4 minutes and recording the net weight of oil.

As given in the sample log sheet of table II, the following data were recorded at each condition of load: Friction torque as given by the manometer, weight of oil flow from the test bearing, time of oil flow, capsule pressure, bearing temperatures at critical locations, inlet oil pressure, speed, direction of rotation, time, inlet oil temperature, room temperature, and oil temperature after the heater. The same procedure was followed for the opposite direction of rotation so that data could be averaged for the two rotations.

Several runs at combinations of constant speed and constant inlet oil pressure were made in each rotational direction for each l/d ratio. The speeds were 500, 1000, 2000, 2500, 4000, 5000, and 6000 rpm, and the inlet oil pressures were 4, 40, and 100 pounds per square inch. The combinations of speed and oil pressure are given in figures 25 to 32. The maximum load on projected area was 900 pounds per square inch, and the maximum oil film temperature was 161° F.

The foam-rubber snubbers used to eliminate vibration in the displacement experiments were removed because they offered restraint to the motion of the bearing about its axis and interfered with the functioning of the torquemeter. At speeds above 1000 rpm, vibrations were stopped by the application of a small load. Since the condition of zero load is not of great importance in friction and oil flow measurements, data were taken only at loads where no vibration occurred.

At numerous times during the experiments, calibrations of the torquemeter were made as a check on operating accuracy. A small known

weight was applied to the arms extending from the front and rear of the bearing hub as shown in figure 10, giving a known turning moment of 1.71 inch-pounds. Manometer differences corresponding with the known moments, first to the front and then to the rear, are given in the sample log sheet of table II and are shown plotted in figure 14. More extensive tests with several weights had proven that the result was a straight line.

PRECISION

The specially constructed measuring equipment such as the torquemeter and the purchased laboratory instruments such as pressure gages, dial indicators, and tachometers were checked for reliability and accuracy. In most cases, an accuracy of 1 to 2 percent was considered satisfactory.

Torquemeter Calibration

In every run of the friction experiments, the torquemeter was calibrated as previously described. The 0.107-pound weight used to apply known moments to the bearing hub was measured to the nearest one-thousandths of a pound and the moment arms of 16 inches were measured to within 1/32 inch. From the many calibrations made, a mean value of the calibration factor was 0.485 inch-pound of torque per inch of manometer difference. The greatest deviation from the mean was 0.010 or 2 percent.

For reliable functioning of the torquemeter it was necessary to bleed air from the oil lines leading to the manometer at the beginning of each run. Because the torquemeter is sensitive enough to measure aerodynamic forces on the bearing hub, it was necessary to rid the test room of air gusts.

The torque measured by the torquemeter includes a small tare torque acting constantly in one direction which may be eliminated by averaging torques measured under the same conditions in opposite directions of rotation. The tare torque consists of two parts, the first part due to the remaining unbalance of the bearing hub for a given setting of the balance weights. The second part is proportional to load and is due to the remaining error in locating the center line of the spherical loading seat, shown in figure 10, on the center line of the bearing bore. By making test runs at the same load in each direction of rotation, the total tare torque adds in one sense and subtracts in the other, and the average yields only the bearing friction torque.

All pressure gages of both the laboratory and commerical grades were calibrated in a dead-weight tester with a capacity of 500 pounds per square inch. Pressure readings were corrected according to calibration curves in cases where a gage did not meet the satisfactory accuracy.

Loading-Capsule Calibration

The gross load on the test bearing was taken as the product of the loading-capsule pressure and the area of the piston which was 15.02 square inches. By suspending two calibrated 50-pound weights from the lateral arms of the bearing hub, the corresponding increase in capsule pressure showed that the calculation of loading in the low range was of satisfactory accuracy.

A pressure gage with a capacity of 120 pounds per square inch was used in experiments at l/d values of 2, 1, and 1/2; and one with a capacity of 30 pounds per square inch, in experiments at an l/d of 1/4. It was found that the pressure gages did not accurately read the capsule pressure due to the tare weight of the test bearing hub unless they were placed at the same level as the loading capsule.

Displacement Measurements

In making and locating the bell cranks, or levers, care was taken that the arms of the levers were in a ratio of 1:1. Wearing of the bronze riders on the levers was kept to a minimum to prevent displacements which might be caused by tangential movements of the journal on the rider face. No direct calibration of the displacement-measuring lever system was made.

The four dial indicators used to measure journal displacements are of laboratory test grade and are graduated in 0.0001-inch divisions. A direct calibration of the indicators was made and in the maximum range during tests of about 13 divisions they are accurate to within one-half division. In some cases, readings were made to the nearest tenth of a division although the accuracy in reading was probably within two-tenths of a division. As the load was increased and then decreased, it was found that there was a discrepancy of as much as one-half division in displacement for the same load. By averaging the displacement data for increasing and decreasing loads, the influence of the lag on accuracy of measurement is minimized.

Two aircraft-type tachometers were used, one of which is a centrifugal type having a scale range of 1000 to 10,000 rpm, and the other

was a 3-second counting type with a range of 0 to 1750 rpm. The centrifugal tachometer was checked under running conditions by timing the revolution counter of the tachometer. By connecting both tachometers to the test shaft simultaneously at speeds of 1000 to 1500 rpm, the two tachometers were checked against each other. A portable shop-type tachometer was used to check the lower range tachometer at 500 rpm. In all cases, the performances were of satisfactory accuracy.

The direct reading Fahrenheit scale of the Leeds & Northrup potentiometer used to measure bearing temperatures from thermocouples can be read to an accuracy of 1° to 2° F. A thermocouple attached to the bulb of a laboratory thermometer giving ambient temperature near the machine checked the thermometer temperature within 1° F. No direct calibration of the potentiometer was made.

The weighing scale used to measure oil flow was equipped with a scale of 2-pound capacity, graduated in hundredths of a pound which could be read to one-quarter of a division. Chemical balance weights were used to calibrate the scale which was found to be of satisfactory accuracy.

Two Saybolt viscosimeters having two viscosimeter tubes each were available for determining the viscosity of the test oils at various temperatures. Although no calibration of these instruments was made, the variations in running time from two tubes at a given temperature did not differ more than 1 second.

RESULTS

The results of this investigation are summarized in figures 1 to 5 and are shown separately for each l/d ratio in figures 17 to 32. Figures 1 to 5 include only data for l/d ratios of 1, 1/2, and 1/4. The data for l/d of 2 were not included in the summary figures because additional tests at this l/d value would be necessary to investigate further the deviation from the other data. The tests at l/d of 2 were the first group run, and only one speed of 500 rpm was used. Many improved techniques were developed after these curves for l/d of 2 were available for study.

Calculations of several nondimensional quantities are shown in the sample calculation sheets, tables III and IV. The necessary data for the calculations are given in the sample log sheets, tables I and II.

Capacity Number

The bearing variables of applied unit load, journal speed, oil film viscosity, clearance ratio, and l/d ratio are grouped quantitatively in the capacity number as given by the following expression:

$$C_n = \frac{\mu N'}{p}\left(\frac{d}{c_d}\right)^2\left(\frac{l}{d}\right)^2$$

For a given experimental run N', l, and d were constant. As shown in tables III and IV, the actual dimensions of the bearing were slightly different from the nominal values.

The gross load of the loading mechanism was determined as the product of the capsule pressure in pounds per square inch and the piston area of 15.02 square inches. The weight of the bearing and its attachments required a tare capsule pressure of 4.5 pounds per square inch in the displacement experiments and 3.5 pounds per square inch in the friction and oil flow experiments. The difference in the tare values was due to the weight of the displacement-measuring apparatus removed. Net load on the bearing was determined from the following expressions: In displacement runs,

$$P = 15.02\ (p_c - 4.5)$$

In friction and oil flow runs,

$$P = 15.02\ (p_c - 3.5)$$

Load on projected area was given for single journals by

$$p = \frac{P}{ld}$$

and, for double journals, by

$$p = \frac{P}{2ld}$$

As shown in tables I and II, the bearing temperatures increased up to 5° F as the load increased during a given run at constant speed. The temperature differences were 2° F or less at the same load when data were compared for increasing and decreasing loads and for opposite directions of rotation. Since the change in bearing clearance is relatively small for variation of 5° F, the clearance was taken as a constant value for the complete run at a given speed. On the other hand,

the change in viscosity with temperature is more rapid, so that it was desirable to compute a separate viscosity for each load.

Bearing clearance was determined by subtracting the change in clearance given by figure 16 from the clearance at room temperature. For the single journals (fig. 8), thermocouples 1 to 7 are in the loaded portion of the bearing. There was little variation between the temperature readings at these locations for a given load. Thermocouple 4 was taken as representative, and the difference of the averages of thermocouples 4 and 9 was determined for the complete run at a given speed. Using this average in figure 16 gives the change in clearance from that at room temperature. For the double journals where only the end thermocouples are in the loaded region, an average of thermocouples 1, 4, and 7 was compared with the average of thermocouple 9 to determine the bearing clearance.

Viscosity in the oil film was determined at each load from the average bearing temperature for the two directions of rotation and for increasing and decreasing load. In tests using the single journal, temperature data at thermocouple 4 were taken as representative of the oil film temperature. For the double journals, the average of thermocouples 1 and 7 was more nearly representative because of the location of these points in the narrow loaded area. These temperatures were used to determine viscosity in figure 15.

Eccentricity Ratio or Attitude

Referring to figure 6, the eccentricity ratio n is the ratio of the displacement of the journal axis to the radial clearance, and is given by the expression:

$$n = e/c_r$$

Coordinate vertical and horizontal displacements of the shaft were measured at the riders, which are located beyond the ends of the bearing $1\frac{11}{16}$ inches to the left and to the right of the center line of the load, as shown in figures 8 and 11. To determine the displacement of the test journal, calculations were made of the effect of shaft deflection on the vertical displacements measured at the riders.

As shown in the sample log sheet of table I, displacement data were taken as the load was increased and then decreased. These data are shown in the sample calculation sheet of table III, reduced to data values at the condition of zero load and an inlet oil pressure of 4 pounds per square inch, at which, as previously described, it was assumed that the journal and bearing axes were coincident. A plot of these data for the

two directions of rotation appears in figure 33(a). The bearing and journal are not ideally accurate cylinders, and there is a departure from symmetry of the displacements at the two ends.

Averages of displacements of the two ends are shown in figure 33(b). The displacements illustrated are typical for the case of a shaft with two journals. In order to determine the displacements of the centers of each journal, calculated values of shaft deflection were subtracted from the measured vertical displacements at the riders. Calculations of shaft deflection due to bending were based on uniformly distributed pressures on the journals and varying moments of inertia for the stepped shaft. The vertical and horizontal components of eccentricity ratio, n_v and n_h, were calculated by dividing the corrected journal displacements by the radial clearance. The plotting of n_v against n_h is shown on the polar diagram of figure 33(c) in terms of eccentricity ratio n and attitude angle ϕ. Eccentricity ratio n was calculated as the square root of the sum of the squares of the components.

In the case of single journals, the method of calculation of eccentricity ratio was similar. Because of the greater length of the single journals and the greater loads applied, shaft bending over the length of the journal was of considerable magnitude at high loads. Bent longitudinally in the shape of a fourth-degree parabola, the displacement and eccentricity ratio at the center of the journal were less than at its ends, as indicated in figures 34 and 35. To simulate the performance of a straight journal, the average eccentricity ratio of a parabolic elastic curve was calculated as representative of the eccentricity ratio of a straight journal (see fig. 35). Four-fifths of the height of the deflection curve within the journal was subtracted from the displacement at the ends.

Eccentricity ratios as a function of capacity number are shown in figures 1 and 17 to 20; as a function of attitude angle, they are shown in figures 2 and 21 to 24.

Bearing Friction Coefficient

Experimenters usually distinguish between friction measured on the journal and that measured on the bearing, since the friction torque measured on the bearing is evidently somewhat reduced by the couple resulting from the product of the load and the horizontal component of the displacement (fig. 6). The measured data in this report are the friction measured on the bearing and have been referred to as bearing friction variables.

Data on friction and shaft displacement were both available so that it was possible to compute the journal friction by adding the couple to the bearing friction. Referring to table IV in the column labeled friction variable f_v, the bearing friction and calculated journal friction for an l/d of 1 compare as follows:

Load, P (lb)	Bearing friction, $f_b\left(\frac{d}{c_d}\right)$	Couple, $f_c\left(\frac{d}{c_d}\right)$	Journal friction, $f_j\left(\frac{d}{c_d}\right)$	Ratio, f_j/f_b
0	0	0	0	-----
22.5	24.10	.10	24.20	1.002
60.1	9.13	.19	9.32	1.020
97.6	5.70	.27	5.97	1.048
135.1	4.23	.31	4.54	1.073
172.6	3.36	.33	3.69	1.099
248.0	2.36	.34	2.70	1.143
398.0	1.55	.36	1.91	1.230
623.0	1.06	.35	1.41	1.330
848.0	.83	.32	1.15	1.385

In the above table the couple is to be added to the bearing friction variable and is numerically equal to the horizontal displacement n_h as follows:

$$f_c\left(\frac{d}{c_d}\right) = \frac{Pe \sin \phi}{Pr}\left(\frac{r}{c_r}\right) = \frac{e}{c_r} \sin \phi = n \sin \phi = n_h$$

The values of n_h are those shown in figure 22 for the run at 1000 rpm and 40 pounds per square inch.

Manometer differences indicating bearing friction in inches of mercury for each load condition are shown in the sample log sheet of table II; they are of opposite sign for opposite directions of rotation. For a given load, the absolute values of the manometer differences for the two directions of rotation were averaged as indicated in the sample calculation sheet of table IV. Multiplication by the calibration factor F_c gave the friction torque M_t in inch-pounds. The friction coefficient f was determined from the following relationship:

$$f = \frac{M_t}{Pr}$$

Values of the friction variable f_v were calculated from the following expression:

$$f_v = f\left(\frac{d}{c_d}\right)\left(\frac{l}{d}\right)^2$$

The sample calibration-factor curves corresponding with the experimental data of the sample log sheet (table II) are shown in figure 14. Experimental values of bearing friction variable are shown plotted as a function of capacity number in figures 3 and 25 to 28.

Oil Flow

Two distinct methods of plotting oil flow are used in this report. The first method consists of plotting a nondimensional quantity called the oil flow number against the capacity number C_n. Separate curves for l/d of 2, 1, 1/2, and 1/4 are shown in figures 29 to 32. These curves present the data so that the individual runs are clearly distinguishable, but combining the curves for three of the l/d ratios on one sheet gives the result shown in figure 4.

The second method of plotting oil flow as shown in figure 5 uses an oil flow factor q as the ordinate which differs from the oil flow number q_n as follows:

$$q_n = \frac{Q}{\pi d l c_d \frac{N'}{2}}$$

where Q is experimental total oil flow

$$q = \frac{Q}{\pi d l c_d \frac{N'}{2} n}$$

$$\frac{q_n}{q} = n$$

The abscissa of figure 5 is also different from the capacity number C_n used in figure 4 and is called inlet-pressure capacity number C_{p_o}, derived as follows:

$$C_{p_o} = \frac{\mu N'}{p_o}\left(\frac{d}{c_d}\right)^2\left(\frac{l}{d}\right)^2$$

This expression differs from the capacity number C_n by having p_o the inlet oil pressure used in place of p, the unit load, in the denominator.

As shown in the sample calculation sheet (table IV), oil flow data for the two directions of rotation were averaged at each condition of load. Dividing the weight of oil by the time interval during which it was collected gave the rate of flow in pounds per minute Q'. Since Q in the oil flow number must be given in cubic inches per second, a conversion was made from the following expression:

$$Q = Q' \times \frac{1728}{62.4 \times \text{sp. gr.}} \times \frac{1}{60}$$

in which sp. gr. is the measured specific gravity of the oil at oil film temperature. Where double journals were concerned, half of the oil flow was used in calculations of oil flow numbers.

ANALYSIS AND DISCUSSION

Figures 1 to 5 include only the experimental data for bearings of l/d ratios of 1, 1/2, and 1/4 and represent the principal results of this investigation. All these data are in satisfactory agreement with the theoretical analysis of reference 2. The data for bearings of l/d of 2 are not included in figures 1 to 5 and are not in satisfactory agreement as shown in figures 17, 21, 25, and 29. One of the simplifying assumptions used in reference 2 limits the theoretical analysis to bearings of short length, and it would be expected that the most satisfactory agreement with experiment would be in the low l/d range.

However, the tests at l/d of 2 were the first group attempted and were the least satisfactory in the judgment of the experimenters. As shown in figures 17, 21, 25, and 29, a relatively small amount of

data were taken at l/d of 2, and these were limited to the single speed of 500 rpm. Also the experimental techniques were less satisfactory than those used in connection with subsequent experiments at smaller l/d ratios. The important techniques of determining the position of zero eccentricity, of taking data at increasing and decreasing increments of load, and of waiting for the condition of thermal equilibrium were developed after the curves for l/d of 2 were available for study and were used in tests at l/d of 1, 1/2, and 1/4. Conclusions in regard to an l/d of 2 should be witheld until more data are available.

Eccentricity Ratio

Although the data shown in figure 1 for journal eccentricity are considered to be in good agreement with theory, there is some discrepancy since the line through the experimental data lies slightly above the theoretical line. Three factors which may have contributed to this discrepancy are apparent.

First, the effect of inlet oil pressure is to raise the experimental curve at low values of n. In drawing the experimental line through the combined data in figure 1, the higher points at different oil pressure, as indicated in figures 17 to 20, were disregarded with the result that the effect of inlet oil pressure has to some extent been minimized in locating the experimental line. However, on the higher speed runs data were available at only the one oil pressure, 100 pounds per square inch. Since the effect of inlet oil pressure disappears with increasing load and the value of n is not critical for bearings with low load or large capacity numbers, the effect of inlet oil pressure is usually of minor importance.

Second, disregarding machining imperfections of the parts, the bending deflection of the shaft under load caused a departure from the ideal shape, especially in the long journals. At l/d of 2 and 1, the journal itself was deflected to a parabolic shape; in the case of the double journals of l/d of 1/2 and 1/4, the journals were too short to be greatly bent, but, because the journals were located to each side of the center of the load, their axes were tilted with respect to the bearing axis. The maximum difference between the end and center eccentricity ratios was about 12 percent of n at the highest load for the longest journals. The experimental eccentricity ratios given in the curves represent the average eccentricity ratios of a deflected or tilted journal in order to simulate the characteristics of a straight journal. Thus, the experimental curve represents the average location of a deflected journal for comparison with an ideal condition.

Third, the magnitude of the clearance both at room temperature and at elevated temperature is of major importance in calculating eccentricity ratio. An error of 0.0001 inch in the radial clearance would represent an error of nearly 10 percent of n, and is proportional to n. Although the method of measuring clearance by the play of the journal in the bearing is considered the most accurate method, it is the minimum clearance that is measured in this manner to the exclusion of the valleys which may exist in the bearing. The actual average clearance is evidently greater if the valleys are included. Measurements of accuracy comparable with the "play" method are difficult and are not available. However, the play clearance was slightly less than that expected from measurements by ordinary methods.

As shown in figure 36, the location of the experimental curve is very sensitive to an error in clearance. A 10-percent increase in clearance would lower the experimental line about 9 percent of n and also moves the value of the capacity number to the left by about 17 percent since the clearance term is squared. If the data were recalculated assuming a radial clearance 10 percent larger, the experimental line would fall almost exactly on the theoretical line. The recalculated line would then pass through the point $n = 1.00$ and $C_n = 0$.

Since n has already been assumed equal to zero when the load is zero, that is, at C_n equals infinity, the correction of a possible error in clearance is a rational method of making the curve pass through the two known points. Certainly the shaft touches the bearing when the load is high and the speed is zero, that is, n equals 1.00 when C_n equals zero. With a 10-percent increase in clearance, as shown in figure 36, the spread of the data in figure 1 would remain almost unchanged, but the maximum value of n reached by the data would fall from about 0.99 to 0.90. With the data ending at $n = 0.90$ the line could easily be faired through the point $n = 1.00$ at $C_n = 0$. It should also be noticed that a 5-percent increase in clearance would also permit fairing the curve across a similar gap between $n =$ about 0.95 to $n = 1.00$.

Friction

The experimental data for bearing friction variable are in good agreement with the theoretical curve of figure 3, showing a compactness of points about the theoretical curve, especially at the low capacity numbers. It is interesting to note that, although the analysis of reference 2 is concerned principally with the loaded 180° of the bearing, it arrives at the friction by an integration of the shearing stresses in the oil film over the full 360°. The experimental data indicate that such a view of the extent of the oil film is acceptable for estimating

friction. This also bears out the view of Cameron and Wood in reference 2 that the cavitated film on the unloaded side of the bearing behaves as an uncavitated film in laminar flow insofar as friction is concerned. There is a possibility of a compensating error which would explain the friction without proving that cavitation does not exist.

At near zero load, or very high capacity numbers not shown in the curves, high inlet pressure produced values of the friction variable which were considerably higher than the theoretical values. This may be associated with an internal load caused by high oil pressure.

Oil Flow

For purposes of analysis, the oil flow of a bearing can be divided into two parts, the part that is squeezed out of the 180° of the converging wedge and the part that issues from the diverging wedge. The part that is squeezed out of the converging wedge can be calculated quite simply and can be called the theoretically required flow. The flow of the complete bearing which can be measured experimentally is the sum of the two parts and can be called the total or experimental flow, Q. The diverging wedge is an area of low pressure in the oil film, and, if oil is present at the ends of the bearing, the flow may be inward. However, if the oil inlet pressure is sufficient, the flow from the 180° of the diverging wedge will be positive and can be called the surplus flow, whatever its sign.

The flow theoretically required by the 180° of the converging oil film can be computed as follows: The pressure in the oil film is low at the two ends of the wedge, and it may be properly assumed that at the ends the effect of the pressure on the velocity of the oil film is small, so that the average velocity of the oil film at the two ends is $\pi dN'/2$. The flow enters the converging wedge at the widest gap where the gap equals c_r plus e, some of the oil escapes from the sides of the wedge or the ends of the bearing, and the part that leaves through the small end, where the gap is c_r minus e, returns around the other side of the bearing. Thus the flow escaping from the ends of the 180° of the converging wedge is the difference between the amount entering where the gap is c_r plus e and that leaving where the gap is c_r minus e. The difference between c_r plus e and c_r minus e is $2e$, which equals nc_d. Multiplying by the length of the bearing gives the theoretically required flow as follows:

$$Q_{req} = \pi dlc_d \frac{N'}{2} n$$

The flow issuing from the ends of the bearing in the 180° of the converging film is equal to the difference between the amount of oil entering and that returning to circulate again. The difference also equals the amount of oil flow theoretically required to maintain the converging wedge full. This amount is only a part of the total flow of the bearing as measured experimentally, assuming the surplus flow is positive.

Two distinct nondimensional terms have been used for plotting the oil flow results, the oil flow number q_n and the oil flow factor q. Although the oil flow number used in figures 4 and 29 to 32 can be obtained from reference 2, a nondimensional number similar to this was suggested by Blok in the discussion of the paper by Cameron and Wood, reference 1. The two nondimensional terms used are

$$q_n = \frac{Q}{\pi d l c_d \frac{N'}{2}}$$

and

$$q = \frac{Q}{Q_{req}}$$

$$= \frac{Q}{\pi d l c_d \frac{N'}{2} n}$$

The oil flow number is a nondimensional quantity in which the total flow in cubic inches per second has been divided by the dimensions of the bearing in cubic inches per second. If the oil flow number is plotted against the capacity number C_n the experimental flow can be compared with the theoretically required flow from the converging film. The oil flow number representing the theoretically required flow $q_{n(req)}$ on such a plot is numerically equal to n, that is,

$$q_{n(req)} = \frac{Q_{req}}{\pi d l c_d \frac{N'}{2}} = n$$

Thus the theoretical oil flow can be represented by an n curve, similar to that of figure 1, for comparison with the total flow number.

The experimental oil flow number is the sum of the theoretical flow number plus the surplus flow number.

As shown in figures 4 and 29 to 32 there is considerable variation of the oil flow number, both above and below the line representing the theoretically required flow. The lines for individual test runs indicate the possibility of a useful ratio between the actual flow and the theoretical flow for a given test, but that the general location with respect to the axes is primarily dependent on the inlet oil pressure. Figure 4 indicates that the location is also dependent on journal speed and on l/d ratio. Speculating that the oil film viscosity and clearance ratio were also related variables, all of the variables affecting the total oil flow in these tests were grouped nondimensionally in a form similar to the capacity number C_n but having the inlet oil pressure p_o used in place of the unit bearing load p, as follows:

$$C_{p_o} = \frac{\mu N'}{p_o}\left(\frac{d}{c_d}\right)^2\left(\frac{l}{d}\right)^2$$

Figure 5 is the result of plotting the ratio of total oil flow to the theoretical flow, called oil flow factor q, against the inlet-pressure capacity number. While there is some spread of the points at the center of the curve, the grouping of the points, especially at the ends, is an invitation to draw a single line. It should not be overlooked that one of the points is nearly 100 percent off the single-line curve, but there is a possibility of experimental error in the more divergent points since the two worst points are from a single run. This curve permits the total flow to be predicted for any of the test runs.

The oil flow factor appears to vary primarily with the inlet-pressure capacity number C_{p_o} rather than with C_n or n. It is interesting to note that n is related to both the numerator and the denominator of the oil flow factor. This can be explained by considering that the oil flow factor minus 1 would be equal to the surplus flow over the theoretical flow. The height of the passage for the surplus flow, which is the film thickness on the unloaded side, would increase with n. The denominator is the theoretical flow which has already been shown to include n.

In passing, it may be of interest to note that the denominator of the ratio denoting the oil flow number has some physical significance. The denominator of the oil flow number is equal to the theoretical flow of a bearing for the special case when n equals 1, that is, when the journal is touching the bearing. In this case c_r plus e equals c_d, c_r minus e equals 0, and nc_d is equal to c_d.

The oil flow curves strictly apply only to the bearing under test, having a small oil inlet hole without grooves. Figure 5 particularly has the interesting possibility of applying to bearings of other diameters. To check this, the oil flow data given by McKee in a recent paper (reference 6) have been added to figure 5. These data are in excellent agreement for the single-oil-hole case and show the increase in oil flow obtained by an axial oil inlet groove. The McKee data were obtained at the National Bureau of Standards using a bearing 2.06 inches in diameter with SAE 20 oil at speeds of 2030 and 3040 rpm, loads of 1553 and 3008 pounds, and temperatures from 203° to 228° F.

Oil Flow Starvation

In figures 4, 29, and 30, some of the points representing the experimental oil flow fall below the theoretically required oil flow line. This is also shown in figure 5 by all points having an oil flow factor less than 1 or an inlet capacity number greater than 0.12. This amount of oil flow can have either of two meanings. First, a condition that can be called starvation is occurring if the flow entering the converging wedge is less than that theoretically required. The second possibility is that the surplus flow is negative, which would mean that oil is available around the ends of the bearing and is being drawn into the low-pressure area, thus adding to the supply of oil for the converging wedge. In some test machines a bead of oil can be seen around the ends of the bearing at low rotative speeds, while at higher speeds the bead of oil is thrown clear.

When starvation actually occurs, it would apparently mean that the film thickness at the entrance of the converging wedge is not completely filled over the full length of the bearing. As the oil flows around the wedge, it can be imagined as spreading out leaving the entering corners unfilled. These are in a low-pressure region of the oil film where the lack of oil would cause the least effect on the total load capacity. There is a possibility that this condition of oil starvation is fairly common at the higher rotative speeds if a single oil hole is used without oil grooves.

USE OF SUMMARY CURVES

The summary curves, figures 1 to 5, may be used as charts to facilitate rapid determination of the performance characteristics of a bearing if the various items in the capacity number are known. The bearing clearance should be corrected for thermal expansion, and upper and lower limits may be used to simulate production tolerances and wear. The viscosity desired is that of the oil film and was approximated in

these experiments from temperature readings of thermocouples embedded near the bearing surface in the loaded area. If possible, the oil flow should be measured to determine a factor to be applied to the values of figure 5 to allow for the effects of variations of oil grooving and bearing size, which have not been determined experimentally in this report.

If the operating temperature is known, the charts can be used to estimate the existing conditions and the effects of various changes on the bearing. Changes which affect the operating temperature, such as alteration of viscosity, oil flow, clearance, or speed, require an approximation of the new equilibrium temperature. The construction of a heat-balance graph as suggested in figure 37 is aided considerably if an operating temperature at a different set of conditions is already known, since some of the unknowns can then be determined.

The charts may be used on a new design, where the bearing operating temperature is unknown, to determine values at two or more arbitrary temperatures representing an allowable temperature range. A graph of the heat balance illustrated by figure 37 may be partially constructed, if desired, from the values calculated at these two temperatures. The line representing other heat losses will be unknown, and if the oil flow line is drawn it should be understood that so far it has only been shown to apply to two sizes of test bearings. If there are grounds for believing the other heat losses to be relatively small, the heat-balance graph could be used to build up experience over a period of time in evaluation of the maximum temperature indicated by the intersection point.

Heat-Balance Graph for Determining Other Heat Losses and Bearing Temperature

The temperature of a bearing will stabilize at a point where the heat generated balances the heat loss to the oil flow plus the heat lost by other means such as conduction, radiation, and convection. If calculations are made at two or more arbitrary temperatures, a graphical solution similar to figure 37 can then be made of heat generated and heat loss against assumed temperature. A few points on the line representing other heat losses will be needed, which can be obtained from similar graphs on the same application for conditions where the temperature is known. The equilibrium temperature of the bearing will be indicated by the point of intersection of the heat-generated and heat-dissipated lines on this graph as illustrated in figure 37. In high-speed, high-load applications where the ambient temperature is high, it may be acceptable to assume that a high percentage of the heat is being transferred to the oil. In this case, the interesection point represents a limiting or maximum temperature which will be reduced

slightly by additional cooling. The relative effect of various assumed changes can be related to the bearing temperature, and a useful approximation of bearing temperature can often be reached even if complete information is lacking.

Heat generated by friction and power loss.- As already discussed in the section "Bearing Friction Coefficient" the couple caused by the eccentricity of the load should theoretically be added to the bearing friction torque to give the journal friction torque. If the bearing is stationary, it is the journal friction torque which should be used in estimating the rate of heat generation and power loss. The data for computing the additional friction due to the horizontal eccentricity ratio n_h are given in figure 2.

Heat removed by oil flow.- The heat removed by the oil flow is equal to the temperature rise times the flow rate in pounds per minute times the specific heat of the oil. The oil flow estimated, using the flow factor from figure 5, would be increased if oil grooves were present. Some data on the increase are given by Clayton (reference 7). Some experimental data on the actual parts or parts of a similar character would be valuable.

Maximum Eccentricity Ratio at Ends of Bearing

After the operating temperature of a bearing has been determined by actual measurement, or by estimating it by means of the heat-balance graph, the eccentricity ratio of a theoretically straight shaft may be obtained from figure 1. Corrections may then be applied to estimate the maximum eccentricity ratio at the ends of the bearing under actual conditions.

In figure 1 either the experimental line or the theoretical line may be used for predicting values of n. The experimental line gives values of n which are about 10 percent higher than those of the theoretical line and which would be on the safe side. The higher values were based on clearance measured by the play method which reads the minimum clearance between the high spots on the shaft and the bearing. If clearances in production are measured by ring and plug gages, the effect might be more nearly comparable with the clearance by the play method. The following considerations should be included in estimating the eccentricity ratio in an actual bearing:

(1) The theoretical line in figure 1 may be used by deducting a value from the clearance to allow for hills and valleys or waviness in the surface. For example, if this inaccuracy is 0.0001 inch in a bearing having c_r = 0.001 inch, the allowance to be added is equivalent to an n value of 1/9 of n.

(2) The plotted data are based on the clearance at operating temperature which is often considerably altered from that at room temperature.

(3) If the bearing is to be operated at very light load the effect of inlet oil pressure becomes appreciable as shown in figures 17 to 20.

(4) The radius of curvature of the shaft should be estimated and the deflection at the ends of the bearing computed relative to the center. The deflection can then be converted to an n value by dividing by the radial clearance and the result added to the chart value of n. Two cases arise (see fig. 38.):

(a) If the bearing axis and the journal axis are parallel at the center of the bearing, four-fifths of the deflection should be converted to an n value and added to the chart value of n. Assuming that the deflection curve is a fourth-degree parabola, the eccentricity ratio will be decreased one-fifth at the center and increased four-fifths at the ends, which corresponds to the method used in obtaining the curves.

(b) If the journal axis is at an angle to the bearing axis at the bearing center, the slope of the deflection curve will give a change in displacement from the center to one end. The full value of this figure should be converted to an n value and added to the chart value of n to correspond to the method used in obtaining the charts.

(5) Similar methods of estimating the increase in eccentricity ratio at the ends of the bearing should be applied for misalinement caused by differences in thermal expansion of the bearing supports and for machining or assembly tolerances. If possible the bearing supports should be designed so that their deflection counteracts the deflection of the shaft, and a correction for this can be introduced.

The resulting estimated eccentricity ratio at the ends of the bearing is a point considerably above the chart value shown by figure 1. A series of similar points at different loads would give a line representing n at the ends of the bearing comparable with the theoretical curve. The difference in eccentricity ratio between the center and the ends of the bearing increases with bearing length and decreases with an increase in bearing clearance.

It should be noted that the above procedure for determining the eccentricity ratio at the end of a bearing constitutes a quantitative method for evaluation of the effect of misalinement on a bearing, if the angle is known.

Practical Limits of Eccentricity Ratio

The operating limit of a bearing is evidently determined by the maximum value of the eccentricity ratio at any point within the bearing, and, if the bearing and journal are true cylinders, this occurs at the ends of the bearing. Soft bearing materials will evidently wear-in or accommodate themselves to a stable running condition, the bearing surface then becoming a curved surface similar to the deflected journal surface. In this case it is the change in deflection with a sudden increase in load which becomes important rather than the total deflection. However, if the eccentricity at the ends allows a suitable reserve of n value for overload, grit in the oil, machining and thermal variations, and so forth, little difficulty or wear should occur during running. Practical values of n can best be determined by comparison with values from well-proven designs of a similar character.

It is probable, although it has not been investigated experimentally, that a correlation exists between the eccentricity at the ends of the bearing as predicted above and the operating conditions at the point of the hook in friction curves. It has already been found using an earlier babbitt bearing in the machine used in the present investigation that the hook point will progress toward more severe conditions with continued running, the first hook possibly being of a very short duration. This is an example of the ability of babbitt to conform to a deflected journal, a sudden change in deflection causing a temporary hook point.

Meaning of Capacity Number

The capacity number C_n can be written in several different forms by manipulating the arrangement of the terms. Canceling the diameter term in numerator and denominator gives one interesting expression, and substituting the total load P over ld for the unit load on projected area p produces other forms.

All of the following relations are limited to the range of l/d from 1/4 to 1 which have thus far been investigated experimentally. The range in which these relations are true is also considerably limited by the increased deflection of a smaller diameter. Perhaps the most important consideration neglected in these theoretical relations is the effect on viscosity that might result from a change in the bearing temperature.

$$C_n = \frac{\mu N'}{p}\left(\frac{d}{c_d}\right)^2\left(\frac{l}{d}\right)^2 = \frac{\mu N'}{p}\frac{l^2}{{c_d}^2} \qquad (1)$$

Equation (1) indicates that the capacity number and the eccentricity ratio of a given bearing are independent of bearing diameter, if the unit loading and the bearing clearance are held constant. This is to be interpreted to mean that, for a small increase in diameter, the bearing clearance must be constant if the increased bearing area at the same unit bearing loading is to be taken advantage of. Large increases in diameter usually require some increase in bearing clearance for thermal expansion or contraction.

$$C_n = \frac{\mu N'}{P}\left(\frac{d}{c_d^2}\right)l^3 = \frac{\mu N'}{P}\left(\frac{\sqrt{d}}{c_d}\right)^2 l^3 \tag{2}$$

Equation (2) indicates that the capacity number and the eccentricity ratio of a bearing are independent of the diameter if the bearing clearance is made proportional to the square root of the diameter, the total load being constant. This rate of increase in clearance may approximate manufacturing requirements in some instances.

$$P = \frac{\mu N'}{C_n}\left(\frac{d}{c_d}\right)^2 \frac{l^3}{d} \tag{3}$$

$$P = \frac{\mu N'}{C_n}\left(\frac{d}{c_d}\right)\frac{l^3}{c_d} \tag{4}$$

Equation (3) indicates that, if a constant ratio of diameter to clearance is maintained, the total load is inversely proportional to the diameter, if the capacity number and other variables are constant.

Equation (4) indicates that if a constant ratio of diameter to clearance is maintained, the total load is inversely proportional to the clearance, if the capacity number and other variables are constant.

The verbal statements for both equations (3) and (4) are identical except for the interchange of the underlined words, where diameter is exchanged for clearance. It is to be noted that a proportionality has been assumed to exist between the two factors.

It may be hard to believe that the total load varies inversely as the diameter, at a constant clearance ratio, but the area can be considered to increase as the first power of the diameter in the numerator, while the l/d term changes as the second power of the diameter in the denominator. Holding the capacity number and n constant, with

increasing diameter, may be unnecessarily severe, since this results in an increase in minimum oil film thickness, if the clearance ratio is constant.

Equations (1) and (2) indicate that the unit load is proportional to l^2 and the total load, to l^3, for a given capacity number, if other variables are constant.

CONCLUSIONS

The following conclusions may be drawn from the results of this investigation:

1. After correction for shaft-deflection and bearing-clearance changes at running temperature, the experimental data obtained at length-diameter ratios of 1, 1/2, and 1/4 on a $1\frac{3}{8}$- inch-diameter bearing are in good agreement with the short-bearing theory. Conclusions in regard to a length-diameter ratio of 2 should be withheld until additional data are available.

2. The elastic deflection of the shaft has a considerable effect on the eccentricity ratio at high loads and increases the eccentricity ratio at the ends of the bearing.

3. The method of predicting eccentricity ratio at the ends of a bearing constitutes a method for quantitative evaluation of the effect of angular misalinement and elastic deflection on full journal bearings.

4. The experimental curves establish the use of the theoretical capacity number C_n, which is the Sommerfeld number times the square of the length-diameter ratio, for length-diameter ratios equal to or less than 1.

5. The form of the capacity number indicates that, in the range of length-diameter ratios of 1 or less and neglecting deflection and temperature changes:

(a) The eccentricity ratio is independent of diameter if the running clearance varies as the square root of the diameter, the total load being constant

(b) The eccentricity ratio is independent of diameter if the unit load and the running clearance are constant

(c) The total load capacity varies inversely with either the diameter or the clearance if the diameter clearance ratio and the eccentricity ratio are constant

(d) The unit load varies as the length squared and the total load, as the length cubed, for constant values of capacity number and other variables.

6. The semiempirical method of plotting oil flow reduces the experimental oil flow of the bearing tested to a single line.

Cornell University
Ithaca, N. Y., November 13, 1951

REFERENCES

1. Cameron, A., and Wood, W. L.: The Full Journal Bearing. Proc. Institution Mech. Eng. (London), vol. 161, W.E.P. Nos. 47-54, 1949, pp. 59-72.

2. Ocvirk, F. W.: Short-Bearing Approximation for Full Journal Bearings. NACA TN 2808, 1952.

3. Michell, A. G. M.: Progress in Fluid-Film Lubrication. Trans. A.S.M.E., MSP-51-21, vol. 51, 1929, pp. 153-163.

4. Cardullo, F. E.: Some Practical Deductions from Theory of Lubrication of Short Cylindrical Bearings. Trans. A.S.M.E., MSP-52-12, vol. 52, 1930, pp. 143-153.

5. Phelan, R. M.: The Design and Development of a Machine for the Experimental Investigation of Dynamically Loaded Sleeve Bearings. M.M.E. Thesis, Cornell Univ., June 1950.

6. McKee, S. A.: Oil Flow in Plain Journal Bearings. Preprint, A.S.M.E. Paper No. 51-A-34, Nov. 1951.

7. Clayton, D.: An Exploratory Study of Oil Grooves. Proc. Institution Mech. Eng. (London), vol. 155, War Emergency Issue No. 14, 1946, pp. 41-49.

TABLE I

SAMPLE LOG SHEET FOR JOURNAL DISPLACEMENT RUN USING SAE 10 OIL WITH $l/d = 1/2$, $N = 5000$ RPM, AND $p_o = 100$ POUNDS PER SQUARE INCH

[Bearing diameter, $1\frac{3}{8}$ in.; length, $\frac{11}{16}$ in.; diametral clearance at room temperature, 0.00232 in.; bronze bearing; steel shaft with two journals; oil fed through one $\frac{1}{8}$-in.-diam. hole at each journal]

(a) Counterclockwise shaft rotation.

Time	Shaft rotation	Speed (rpm)	Capsule pressure (lb/sq in.)	Displacement by dials (in.)				Temperature (°F) at thermocouple in -																	Room temperature by thermometer (°F)	Test oil		
								Left bearing	Test bearing							Right bearing	Block	Test bearing				Inlet oil	Air					
									Loaded side									Loaded side				Unloaded side						
				Left vertical	Right vertical	Left horizontal	Right horizontal	0	1	2	3	4	5	6	7	8	9	10	11	12	13	14	15	16	24		Type	Temperature after heater (°F)	Inlet pressure (lb/sq in.)
4:13	CCW	5000	4.5	0.00021	-0.00020	-0.00006	-0.00009	152	158	156	153	153	156	157	160	150	146	149	158	151	156	156	156	133	85	85		138	4
	CCW	5000	4.5	0.00017	-0.00017	0.00003	0.00004																				100
	CCW	5000	7.5	0.00028	-0.00013	0.00012	0.00023																				100
	CCW	5000	10.0	0.00042	-0.00004	0.00018	0.00036																				100
	CCW	5000	12.5	0.00050	0.00009	0.00020	0.00040		158			153			157		148						152					136	100
	CCW	5000	15.0	0.00060	0.00017	0.00022	0.00040																				100
	CCW	5000	20.0	0.00075	0.00029	0.00022	0.00040																				100
	CCW	5000	25.0	0.00083	0.00039	0.00022	0.00040																				100
	CCW	5000	30.0	0.00091	0.00049	0.00021	0.00040		158			152			157		147						151					137	100
	CCW	5000	40.0	0.00105	0.00061	0.00020	0.00038																				100
	CCW	5000	50.0	0.00113	0.00072	0.00018	0.00035																				100
	CCW	5000	60.0	0.00121	0.00080	0.00015	0.00033		162			153			160		147						151						100
	CCW	5000	60.0	0.00122	0.00080	0.00016	0.00033																				100
	CCW	5000	50.0	0.00116	0.00070	0.00016	0.00034																				100
	CCW	5000	40.0	0.00106	0.00059	0.00016	0.00037																				100
	CCW	5000	30.0	0.00095	0.00049	0.00019	0.00040		158			152			158		146						150					137	100
	CCW	5000	25.0	0.00087	0.00038	0.00019	0.00040																				100
	CCW	5000	20.0	0.00074	0.00028	0.00019	0.00040																				100
	CCW	5000	15.0	0.00059	0.00016	0.00020	0.00040																				100
	CCW	5000	12.5	0.00049	0.00008	0.00020	0.00040		157			152			156		146						151						100
	CCW	5000	10.0	0.00042	-0.00005	0.00018	0.00037																				100
	CCW	5000	7.5	0.00027	-0.00018	0.00011	0.00023																				100
	CCW	5000	4.5	0.00017	-0.00017	0.00004	0.00007																				100
4:40	CCW	5000	4.5	0.00021	-0.00020	-0.00005	-0.00006		158			154			158		147						156						4

SAE 10

NACA

TABLE I - Concluded

SAMPLE LOG SHEET FOR JOURNAL DISPLACEMENT RUN USING SAE 10 OIL WITH $\ell/d = 1/2$, N = 5000 RPM, AND p_o = 100 POUNDS PER SQUARE INCH - Concluded

(b) Clockwise shaft rotation.

Time	Shaft rotation	Speed (rpm)	Capsule pressure (lb/sq in.)	Displacement by dials (in.)				Temperature (°F) at thermocouple in -																		Room temperature by thermometer (°F)	Test oil		
								Left bearing	Test bearing							Right bearing	Block	Test bearing						Inlet oil	Air		Type	Temperature after heater (°F)	Inlet pressure (lb/sq in.)
									Loaded side									Loaded side				Unloaded side							
				Left vertical	Right vertical	Left horizontal	Right horizontal	0	1	2	3	4	5	6	7	8	9	10	11	12	13	14	15	16	24				
3:05	CW	5000	4.5	0.00005	0.00010	-0.00003	-0.00003	158	159	156	152	152	155	156	159	144	145	148	157	150	157	156	156	129	84	84		138	4
	CW	5000	4.5	0.00002	0.00013	-0.00011	-0.00021																					100
	CW	5000	7.5	0.00012	0.00011	-0.00024	-0.00036																					100
	CW	5000	10.0	0.00028	0.00015	-0.00033	-0.00051																					100
	CW	5000	12.5	0.00041	0.00025	-0.00040	-0.00060		156			152			156		148						152						100
	CW	5000	15.0	0.00047	0.00038	-0.00041	-0.00062																					100
	CW	5000	20.0	0.00062	0.00052	-0.00045	-0.00062																					100
	CW	5000	25.0	0.00074	0.00065	-0.00045	-0.00062																					100
	CW	5000	30.0	0.00082	0.00070	-0.00044	-0.00060		156			151			156		146						151					136	100
	CW	5000	40.0	0.00094	0.00082	-0.00040	-0.00056																					100
	CW	5000	50.0	0.00106	0.00092	-0.00038	-0.00052																					100
	CW	5000	60.0	0.00112	0.00097	-0.00038	-0.00048		158			152			157		146						151				SAE 10	137	100
	CW	5000	60.0	0.00113	0.00096	-0.00037	-0.00048																					100
	CW	5000	50.0	0.00104	0.00088	-0.00038	-0.00051																					100
	CW	5000	40.0	0.00092	0.00080	-0.00041	-0.00057																					100
	CW	5000	30.0	0.00081	0.00070	-0.00042	-0.00061		156			150			156		145						150					136	100
	CW	5000	25.0	0.00074	0.00064	-0.00044	-0.00063																					100
	CW	5000	20.0	0.00064	0.00053	-0.00044	-0.00064																					100
	CW	5000	15.0	0.00046	0.00037	-0.00044	-0.00064		155			150			155		144						150					137	100
	CW	5000	12.5	0.00039	0.00025	-0.00043	-0.00063																					100
	CW	5000	10.0	0.00027	0.00015	-0.00037	-0.00057																					100
	CW	5000	7.5	0.00013	0.00012	-0.00026	-0.00042																					100
	CW	5000	4.5	0.00001	0.00012	-0.00016	-0.00025		158			154			160		146						156					137	100
3:40	CW	5000	4.5	0.00005	0.00009	-0.00004	-0.00010																					4

NACA

TABLE II

SAMPLE LOG SHEET FOR FRICTION AND OIL FLOW RUN USING SAE 10 OIL WITH $l/d = 1$, $N = 1000$ RPM, AND $p_o = 100$ POUNDS PER SQUARE INCH

[Bearing diameter, $1\frac{3}{8}$ in.; length, $1\frac{3}{8}$ in.; diametral clearance at room temperature, 0.00264 in.; bronze bearing; steel journal; oil fed through one $\frac{1}{8}$-in.-diam. hole]

Time	Shaft rotation	Speed (rpm)	Capsule pressure (lb/sq in.)	Manometer reading (in. of Hg)			Calibration torque (in-lb)	Temperature (°F) at thermocouple in -																				Room temperature by thermometer (°F)	Test oil			Oil flow	
								Left bearing	Test bearing, Loaded side							Right bearing	Block	Test bearing, Loaded side				Test bearing, Unloaded side		Inlet oil	Air							
				+	-	Difference		0	1	2	3	4	5	6	7	8	9	10	11	12	13	14	15	16	24		Type	Temperature after heater (°F)	Inlet pressure (lb/sq in.)	Weight (lb)	Time (min)
3:15	CCW	1000	3.0	11.00	11.72	-0.72		107	122	122	122	122	122	122	122	106	118	122	122	122	122	120	120	110	78	78	SAE 10	136	100	0.060	2
	CCW	1000	5.0	11.00	11.74	-0.74						122					119					120						100	0.068	2
	CCW	1000	7.5	11.00	11.88	-0.88						122					118					120					137	100	0.092	2
	CCW	1000	10.0	11.00	11.97	-0.97						122					118					120						100	0.127	2
	CCW	1000	10.0	[a]12.63 [b]9.00	[a]10.00 [b]13.43	[a]2.63 [b]-4.43	[a]1.71 [b]-1.71																					100		
	CCW	1000	10.0	11.00	11.88	-0.88						122					118					120						100		
	CCW	1000	12.5	11.00	12.02	-1.02						122					119					120						100	0.158	2
	CCW	1000	15.0	11.00	12.11	-1.11						122					118					121						100	0.180	2
	CCW	1000	20.0	11.00	12.22	-1.22						124					119					121						100	0.216	2
	CCW	1000	30.0	11.00	12.53	-1.53						124					119					122					136	100	0.268	2
	CCW	1000	30.0	[a]13.01 [b]10.00	[a]11.00 [b]15.08	[a]2.01 [b]-5.08	[a]1.71 [b]-1.71																					100		
	CCW	1000	30.0	11.00	12.53	-1.53						124					120					122						100		
	CCW	1000	45.0	11.00	12.93	-1.93						124					120					124						100	0.320	2
	CCW	1000	60.0	11.00	13.35	-2.35						126					120					124						100	0.350	2
4:00	CW	1000	3.0	13.12	11.00	2.12		112	123	123	123	123	123	123	123	109	120	122	122	122	122	122	122	113	80	80		136	100	0.064	2
	CW	1000	5.0	13.12	11.00	2.12						122					120					122						100	0.071	2
	CW	1000	7.5	13.02	11.00	2.02						122					119					121						100	0.095	2
	CW	1000	10.0	12.97	11.00	1.97						122					120					121						100	0.122	2
	CW	1000	10.0	[a]15.45 [b]12.00	[a]10.00 [b]13.53	[a]5.45 [b]-1.53	[a]1.71 [b]-1.71																					100		
	CW	1000	10.0	13.00	11.00	2.00						122					119					121						100		
	CW	1000	12.5	13.00	11.00	2.00						122					118					121						100	0.150	2
	CW	1000	15.0	12.95	11.00	1.95						122					118					122						100	0.172	2
	CW	1000	20.0	12.88	11.00	1.88						123					120					122						100	0.207	2
	CW	1000	30.0	12.73	11.00	1.73						124					119					123			79		136	100	0.255	2
	CW	1000	30.0	[a]15.26 [b]12.00	[a]10.00 [b]13.83	[a]5.26 [b]-1.83	[a]1.71 [b]-1.71																					100		
	CW	1000	30.0	12.72	11.00	1.72						124					120					123						100		
	CW	1000	45.0	12.55	11.00	1.55						124					120					124						100	0.302	2
	CW	1000	60.0	12.36	11.00	1.36						126					120					125						100	0.335	2

[a]At front of bearing hub.
[b]At rear of bearing hub.

NACA

TABLE III

SAMPLE CALCULATION SHEET FOR JOURNAL DISPLACEMENTS USING SHAFT WITH TWO JOURNALS AND SAE 10 OIL WITH $\frac{l}{d} = \frac{1}{2}$, N = 5000 RPM, AND p_o = 100 POUNDS PER SQUARE INCH

[Nominal bearing dimensions: $d = 1\frac{3}{8}$ in., $l = \frac{11}{16}$ in., and c_d = 0.00232 in. True bearing dimensions: d = 1.387 in., l = 0.688 in., $\frac{l}{d}$ = 0.496, $\left(\frac{l}{d}\right)^2$ = 0.246, $\left(T_1T_4T_7\right)_{Av} - T_9 = 9.5^\circ$ F, c_d = 0.002025 in., $\left(\frac{d}{c_d}\right) = 0.683 \times 10^3$, $\left(\frac{d}{c_d}\right)^2 = 0.465 \times 10^6$, and N' = 83.33 rps.]

Shaft rotation	Capsule pressure, p_c (lb/sq in.)	Load, P (lb) (a)	Bearing pressure, p (lb/sq in.) (b)	Inlet pressure, p_o (lb/sq in.)	Rider displacements (0.0001 in.)																Correction for shaft deflection, δ (0.0001 in.)	Journal displacement at bearing center line (0.0001 in.)		Eccentricity ratio			Bearing temperature, $(T_1,T_7)_{av}$ ($^\circ$F)	Oil viscosity, Z (centipoises)	Oil viscosity, μ (reyns) (c)	Capacity number, C_n
					Left vertical			Left horizontal			Right vertical			Right horizontal			Average of left and right		Average of CW and CCW											
					Load increasing	Load decreasing	Average	Load increasing	Load decreasing	Average	Load increasing	Load decreasing	Average	Load increasing	Load decreasing	Average	Vertical	Horizontal	Vertical	Horizontal		Vertical, e_v	Horizontal, e_h	Vertical, n_v	Horizontal, n_h	Radial, n				
CCW	4.5	0	0	4	d_o	d_o	0	$d_{-0.05}$	$d_{0.05}$	0	d_o	d_o	0	$d_{-0.15}$	$d_{0.15}$	0	0	0	0	0	0	0	0	0	0	0	159	8.8	1.275×10^{-6}	∞
CCW	4.5	0	0	100	-0.40	-0.40	-0.40	0.85	0.95	0.90	0.30	0.30	0.30	1.15	1.45	1.30	-0.05	1.10	-0.04	1.21	0	-0.04	1.21	-0.004	0.119	0.119	159	8.8	1.275	∞
CCW	7.5	45.0	23.6	100	0.70	0.60	0.65	1.75	1.65	1.70	0.70	0.20	0.45	3.05	3.05	3.05	0.55	2.38	0.51	2.54	0.09	0.42	2.54	0.0415	0.250	0.253	158	8.9	1.29	0.5200
CCW	10.0	82.5	43.1	100	2.10	2.10	2.10	2.35	2.35	2.35	1.60	1.50	1.55	4.35	4.45	4.40	1.83	3.38	1.49	3.66	0.17	1.32	3.66	0.132	0.360	0.384	157	9.0	1.305	0.2880
CCW	12.5	120.0	62.9	100	2.90	2.80	2.85	2.55	2.55	2.55	2.90	2.80	2.85	4.75	4.75	4.75	2.85	3.65	2.69	4.15	0.21	2.48	4.15	0.244	0.410	0.477	156.5	9.1	1.32	0.2000
CCW	15.0	157.5	82.5	100	3.90	3.80	3.85	2.75	2.55	2.63	3.70	3.60	3.65	4.75	4.75	4.75	3.75	3.70	3.61	4.24	0.27	3.34	4.24	0.329	0.417	0.531	156.5	9.1	1.32	0.1530
CCW	20.0	232.5	122.0	100	5.40	5.30	5.35	2.75	2.45	2.60	4.90	4.80	4.85	4.75	4.75	4.75	5.10	3.68	5.07	4.28	0.40	4.67	4.28	0.460	0.421	0.623	156.5	9.1	1.32	0.1030
CCW	25.0	307.5	161.0	100	6.20	6.60	6.40	2.75	2.45	2.60	5.90	5.80	5.85	4.75	4.75	4.75	6.13	3.68	6.16	4.26	0.53	5.63	4.26	0.555	0.420	0.695	157	9.0	1.305	0.0772
CCW	30.0	382.5	200.0	100	7.00	7.40	7.20	2.65	2.45	2.55	6.90	6.70	6.80	4.75	4.75	4.75	7.00	3.65	6.92	4.16	0.66	6.26	4.16	0.616	0.410	0.740	157	9.0	1.305	0.0621
CCW	40.0	532.5	279.0	100	8.40	8.50	8.45	2.55	2.15	2.35	8.10	7.90	8.00	4.55	4.45	4.50	8.23	3.43	8.10	3.89	0.91	7.19	3.89	0.708	0.383	0.805	157.5	9.0	1.305	0.0445
CCW	50.0	675.0	354.0	100	9.20	9.50	9.35	2.35	2.15	2.22	9.20	9.00	9.10	4.25	4.15	4.20	9.23	3.23	9.13	3.60	1.17	7.96	3.60	0.785	0.355	0.860	158.5	8.9	1.29	0.0347
CCW	60.0	832.5	435.0	100	10.05		10.05	2.10		2.10	10.00		10.00	4.05		4.05	10.03	3.08	9.88	3.43	1.43	8.45	3.43	0.832	0.338	0.897	159.5	8.8	1.275	0.0279
CW	4.5	0	0	4	0	0	0	0.05	-0.05	0	0.05	-0.05	0	0.35	-0.35	0	0	0												
CW	4.5	0	0	100	-0.30	-0.40	-0.35	-0.75	-1.25	-1.00	0.35	0.25	0.30	-1.45	-1.85	-1.65	-0.03	-1.33												
CW	7.5	45.0	23.6	100	0.70	0.80	0.75	-2.05	-2.25	-2.15	0.15	0.25	0.20	-2.95	-3.55	-3.24	0.48	-2.70												
CW	10.0	82.5	43.1	100	1.30	2.20	1.75	-2.95	-3.35	-3.15	0.55	0.55	0.55	-4.45	-5.05	-4.75	1.15	-3.95												
CW	12.5	120.0	62.9	100	3.60	3.40	3.50	-3.65	-3.95	-3.80	1.55	1.55	1.55	-5.35	-5.65	-5.50	2.53	-4.65												
CW	15.0	157.5	82.5	100	4.20	4.10	4.15	-3.75	-4.05	-3.90	2.85	2.75	2.80	-5.55	-5.75	-5.65	3.48	-4.78												
CW	20.0	232.5	122.0	100	5.70	5.90	5.80	-4.15	-4.05	-4.10	4.25	4.35	4.30	-5.55	-5.75	-5.65	5.05	-4.88												
CW	25.0	307.5	161.0	100	6.90	6.90	6.90	-4.15	-4.05	-4.10	5.55	5.45	5.50	-5.55	-5.65	-5.60	6.20	-4.85												
CW	30.0	382.5	200.0	100	7.70	7.60	7.65	-4.05	-3.85	-3.95	6.05	6.05	6.05	-5.35	-5.45	-5.40	6.85	-4.68												
CW	40.0	532.5	279.0	100	8.90	8.70	8.80	-3.65	-3.75	-3.70	7.25	7.05	7.15	-4.95	-5.05	-5.00	7.98	-4.35												
CW	50.0	675.0	354.0	100	10.10	9.90	10.00	-3.45	-3.45	-3.45	8.25	7.85	8.05	-4.55	-5.45	-4.50	9.03	-3.98												
CW	60.0	832.5	435.0	100	10.75		10.75	-3.40		-3.40	8.70		8.70	-4.15		-4.15	9.73	-3.78												

[a] Area of loading piston = 15.02 sq in.
$P = 15.02(P_c - 4.5)$.

[b] $p = \frac{P}{2ld}$.

[c] $c_\mu = \frac{Z}{6.9 \times 10^6}$.

[d] Dial readings from log sheet reduced to zero value at condition of zero load and inlet oil pressure of 4 lb/sq in. Journal is assumed to be in center of bearing at this condition.

TABLE IV

SAMPLE CALCULATION SHEET FOR FRICTION AND OIL FLOW USING SAE 10 OIL WITH $l/d = 1$, N = 1000 RPM, AND p_o = 100 POUNDS PER SQUARE INCH

[Nominal bearing dimensions: $d = 1\frac{3}{8}$ in., $l = 1\frac{3}{8}$ in., $\frac{l}{d} = 1$, and $c_d = 0.00264$ in. True bearing dimensions: $d = 1.387$ in., $l = 1.375$ in., $\frac{l}{d} = 0.99$, $\left(\frac{l}{d}\right)^2 = 0.98$, $\left(T_4 - T_9\right) = 4^\circ$ F, $c_d = 0.00251$ in., $\frac{d}{c_d} = 0.551 \times 10^3$, $\left(\frac{d}{c_d}\right)^2 = 0.303 \times 10^6$, N' = 16.67 rps, sp. gr. of oil = 0.855, and $F_c = 0.485$ in-lb/in. of Hg.]

Capsule pressure, p_c (lb/sq in.)	$p_c - 3.5$ (lb/sq in.)	Load, P (lb) (1)	Bearing pressure, p (lb/sq in.) (2)	Average manometer difference, ΔHg (in. of Hg)	Average frictional torque, M_t (in-lb) (3)	Friction variable, f_v (4)	Bearing temperature, T_4 (°F)	Oil viscosity, Z (centipoises)	Oil viscosity, μ (reyns) (5)	Capacity number, C_n	Average oil flow, Q_{av} (lb)	Oil flow time (min)	Oil flow, Q' (lb/min)	Oil flow, Q (cu in./sec) (6)	Oil flow number, q_n (7)
3.5	0	0	0	1.42	0.689	∞	122	17.5	2.54×10^{-6}	∞	0.0620	2.0	0.0310	0.0168	0.134
5.0	1.5	22.5	11.8	1.43	0.694	24.10	122	17.5	2.54	1.066	0.0695	2.0	0.0348	0.0188	0.150
7.5	4.0	60.1	31.5	1.45	0.703	9.13	122	17.5	2.54	0.400	0.0935	2.0	0.0468	0.0252	0.201
10.0	6.5	97.6	51.2	1.47	0.713	5.70	122	17.5	2.54	0.246	0.1245	2.0	0.0623	0.0336	0.268
12.5	9.0	135.1	70.7	1.51	0.732	4.23	122	17.5	2.54	0.178	0.1540	2.0	0.0770	0.0415	0.330
15.0	11.5	172.6	90.5	1.53	0.742	3.36	122	17.5	2.54	0.139	0.1760	2.0	0.0880	0.0475	0.378
20.0	16.5	248.0	130.0	1.55	0.751	2.36	124	16.5	2.39	0.091	0.2115	2.0	0.1058	0.0570	0.454
30.0	26.5	398.0	208.5	1.63	0.791	1.55	124	16.5	2.39	0.0566	0.2615	2.0	0.1308	0.0705	0.561
45.0	41.5	623.0	326.5	1.74	0.844	1.06	124	16.5	2.39	0.0363	0.3110	2.0	0.1555	0.0840	0.670
60.0	56.5	848.0	446.0	1.855	0.899	0.83	126	16.0	2.32	0.0258	0.3425	2.0	0.1713	0.0925	0.736

[1] Area of loading piston = 15.02 sq in.
$P = 15.02(p_c - 3.5)$.

[2] $p = \frac{P}{ld}$.

[3] $M_t = F_c \times \Delta Hg$.

[4] $f_v = f\left(\frac{d}{c_d}\right)\left(\frac{l}{d}\right)^2$

$= \frac{M_t}{Fr}\left(\frac{d}{c_d}\right)\left(\frac{l}{d}\right)^2$.

[5] $\mu = \frac{Z}{6.9 \times 10^6}$.

[6] $Q = Q' \times \frac{1728}{62.4 \times 0.855} \times \frac{1}{60}$

$= 0.54Q'$.

[7] $q_n = \frac{2Q}{\pi d l c_d N'}$

$= \frac{2Q}{\pi \times 1.375 \times 1.387 \times 0.00251 \times 16.67}$

$= 7.97Q$.

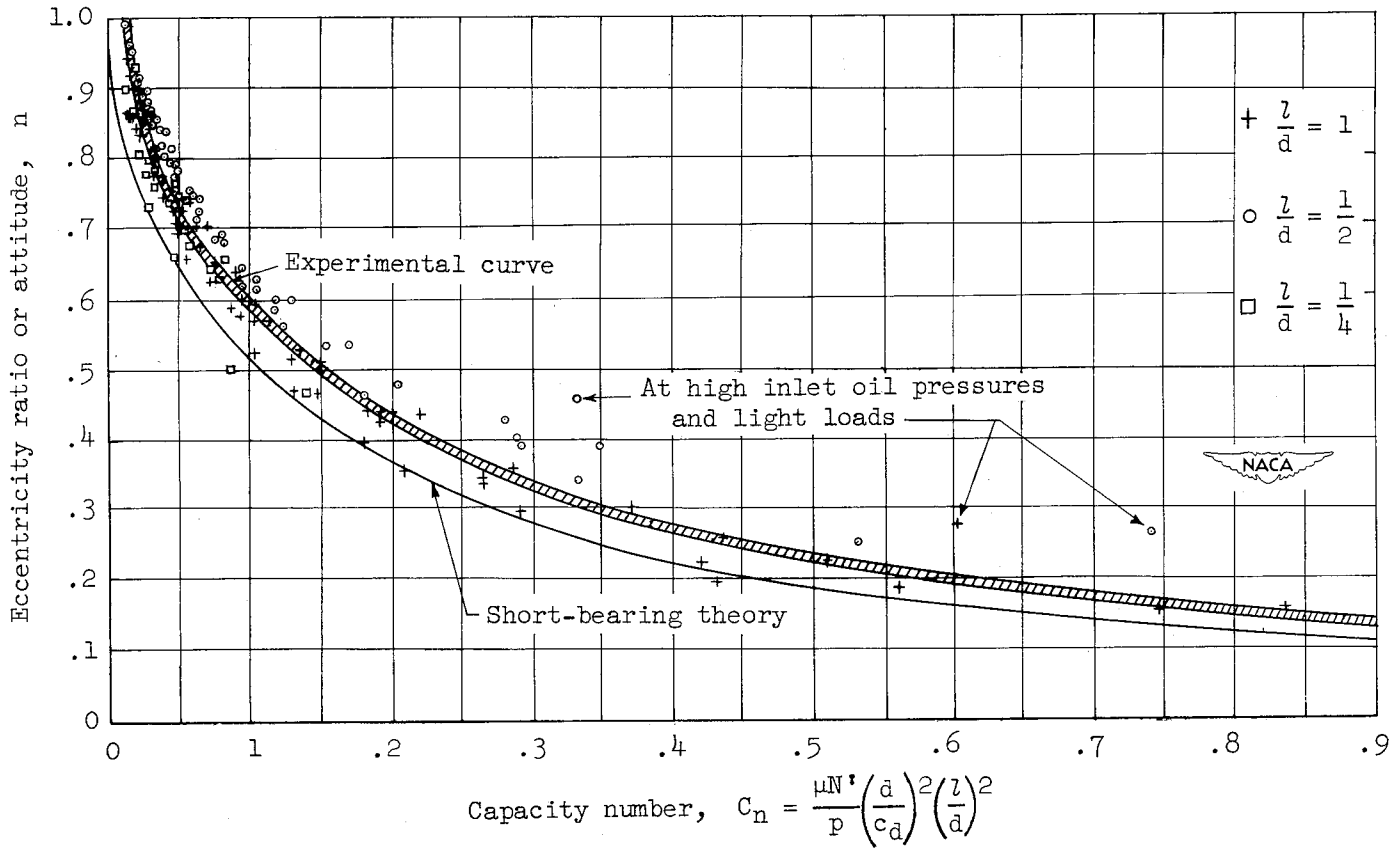

Figure 1.- Summary plot of eccentricity ratio against capacity number for comparison of experimental data for l/d of 1, 1/2, and 1/4 with theoretical curve. Experimental data: Bearing diameter, $1\frac{3}{8}$ inches; bearing, bronze; journal, steel; diametral clearance, 0.00232 and 0.00264 inch; inlet pressure of SAE 10 oil p_o fed through one 1/8-inch-diameter hole, 40 and 100 pounds per square inch; speed, 500 to 6000 rpm; load, 0 to 1450 pounds; bearing pressure, 0 to 760 pounds per square inch; average bearing temperature 1/16 inch from oil film T_{av}, 114° to 160° F.

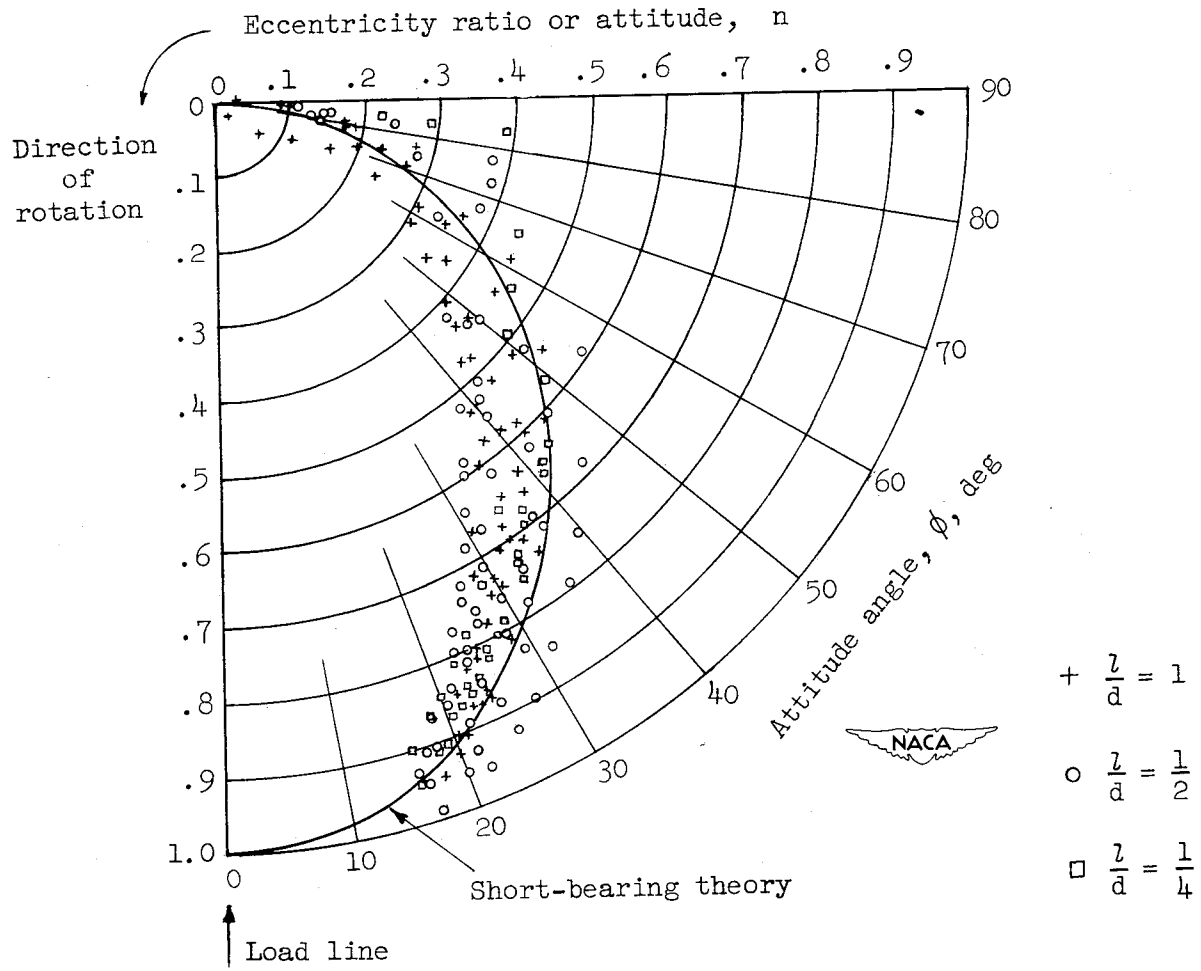

Figure 2.- Summary plot of eccentricity ratio against attitude angle for comparison of experimental data for l/d of 1, 1/2, and 1/4 with theoretical curve. Experimental data: Bearing diameter, $1\frac{3}{8}$ inches; bearing, bronze; journal, steel; diametral clearance, 0.00232 and 0.00264 inch; inlet pressure of SAE 10 oil p_o fed through one 1/8-inch-diameter hole, 40 and 100 pounds per square inch; speed, 500 to 6000 rpm; load, 0 to 1450 pounds; bearing pressure, 0 to 760 pounds per square inch; average bearing temperature 1/16 inch from oil film T_{av}, 114° to 160° F.

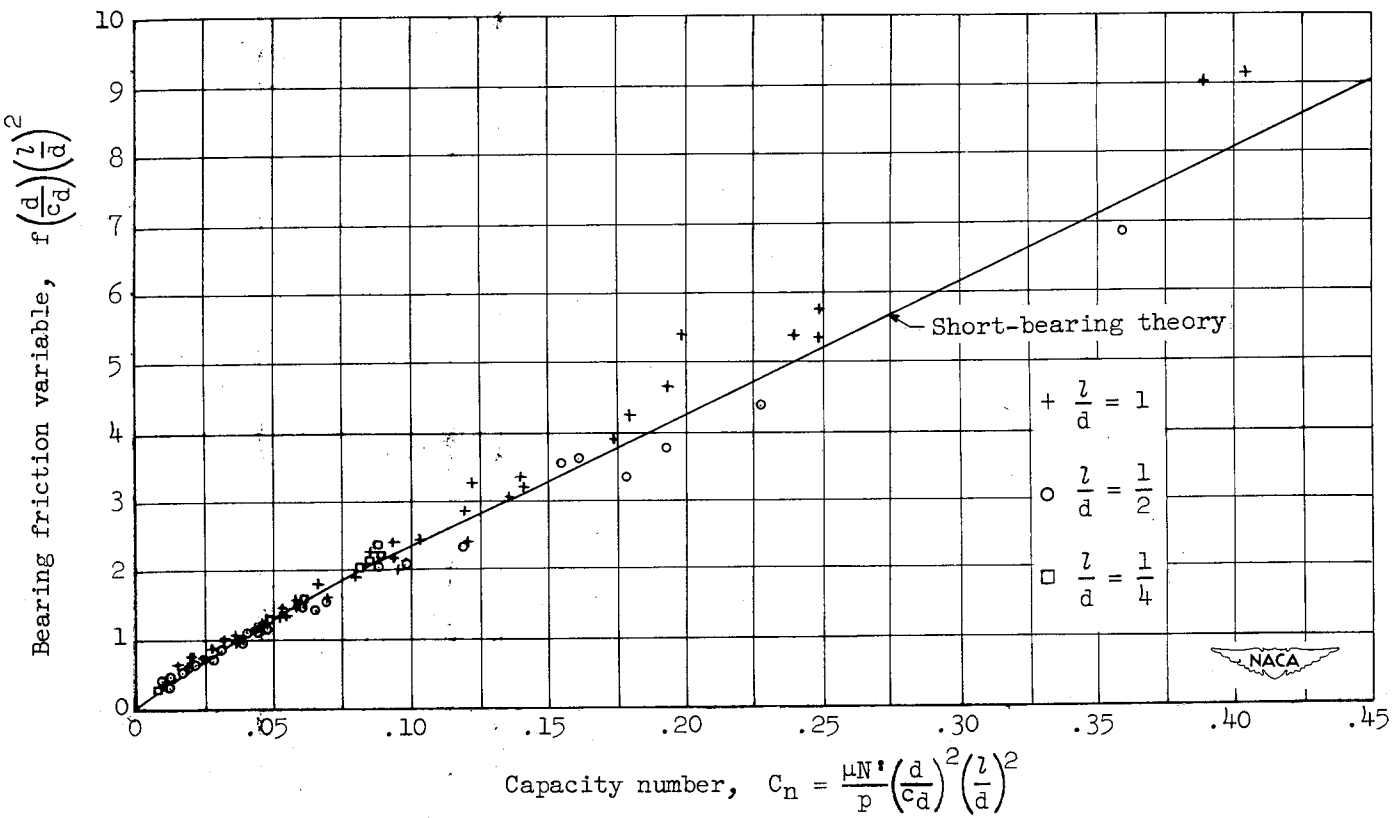

Figure 3.- Summary plot of bearing friction variable against capacity number for comparison of experimental data for l/d of 1, 1/2, and 1/4 with theoretical curve. Experimental data: Bearing diameter, $1\frac{3}{8}$ inches; bearing, bronze; journal, steel; diametral clearance, 0.00232 and 0.00264 inch; inlet pressure of SAE 10 oil p_o fed through one 1/8-inch-diameter hole, 40 and 100 pounds per square inch; speed, 500 to 6000 rpm; load, 0 to 1750 pounds; bearing pressure, 0 to 900 pounds per square inch; average bearing temperature 1/16 inch from oil film T_{av}, 115° to 161° F.

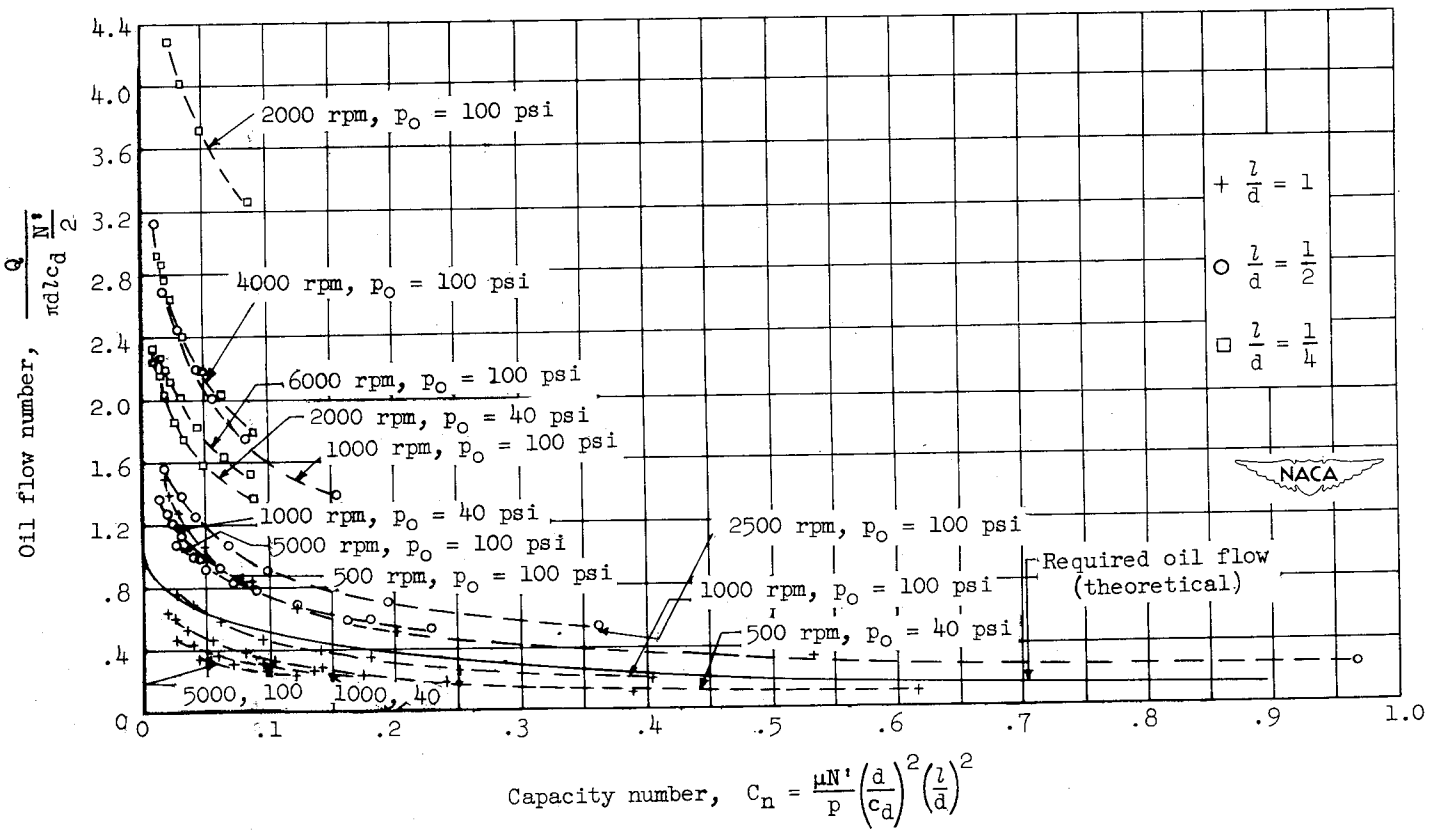

Figure 4.- Summary curves of oil flow number against capacity number for comparison of experimental total oil flow with theoretically required flow through loaded portion of oil film for l/d of 1, 1/2, and 1/4. Experimental data: Bearing diameter, $1\frac{3}{8}$ inches; bearing, bronze; journal, steel; diametral clearance, 0.00232 and 0.00264 inch; inlet pressure of SAE 10 oil p_o fed through one 1/8-inch-diameter hole, 40 and 100 pounds per square inch; speed, 500 to 6000 rpm; load, 0 to 1750 pounds; bearing pressure, 0 to 900 pounds per square inch; average bearing temperature 1/16 inch from oil film T_{av}, 115° to 161° F.

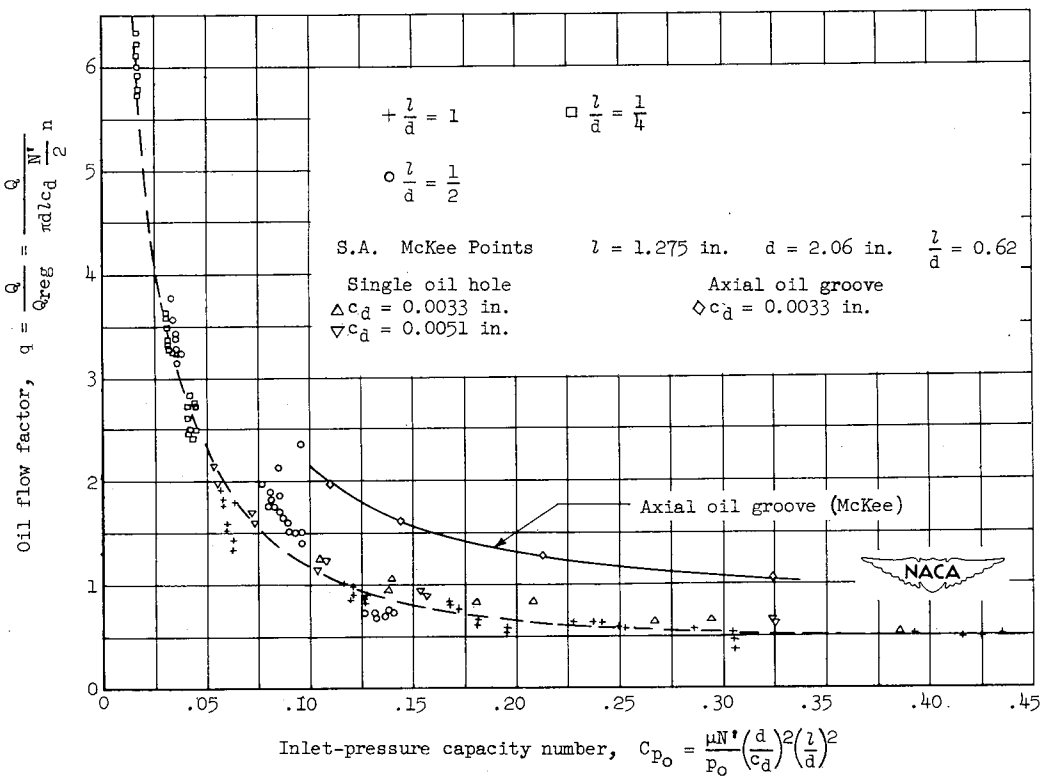

Figure 5.- Summary curve of oil flow factor against inlet-pressure capacity number. Experimental data are given for l/d of 1, 1/2, and 1/4. Oil flow factor is ratio of experimental total flow to flow required through loaded portion of oil film by short-bearing approximation. Experimental data: Bearing diameter, $1\frac{3}{8}$ inches; bearing, bronze; journal, steel; diametral clearance, 0.00232 and 0.00264 inch; inlet pressure of SAE 10 oil p_o fed through one 1/8-inch-diameter hole opposite the load line, 40 and 100 pounds per square inch; speed, 500 to 6000 rpm; load, 0 to 1750 pounds; bearing pressure, 0 to 900 pounds per square inch; average bearing temperature 1/16 inch from oil film T_{av}, 115° to 161° F. Experimental oil flow, $Q = q\left(\pi d l c_d \frac{N'}{2} n\right)$. McKee data are taken from reference 6.

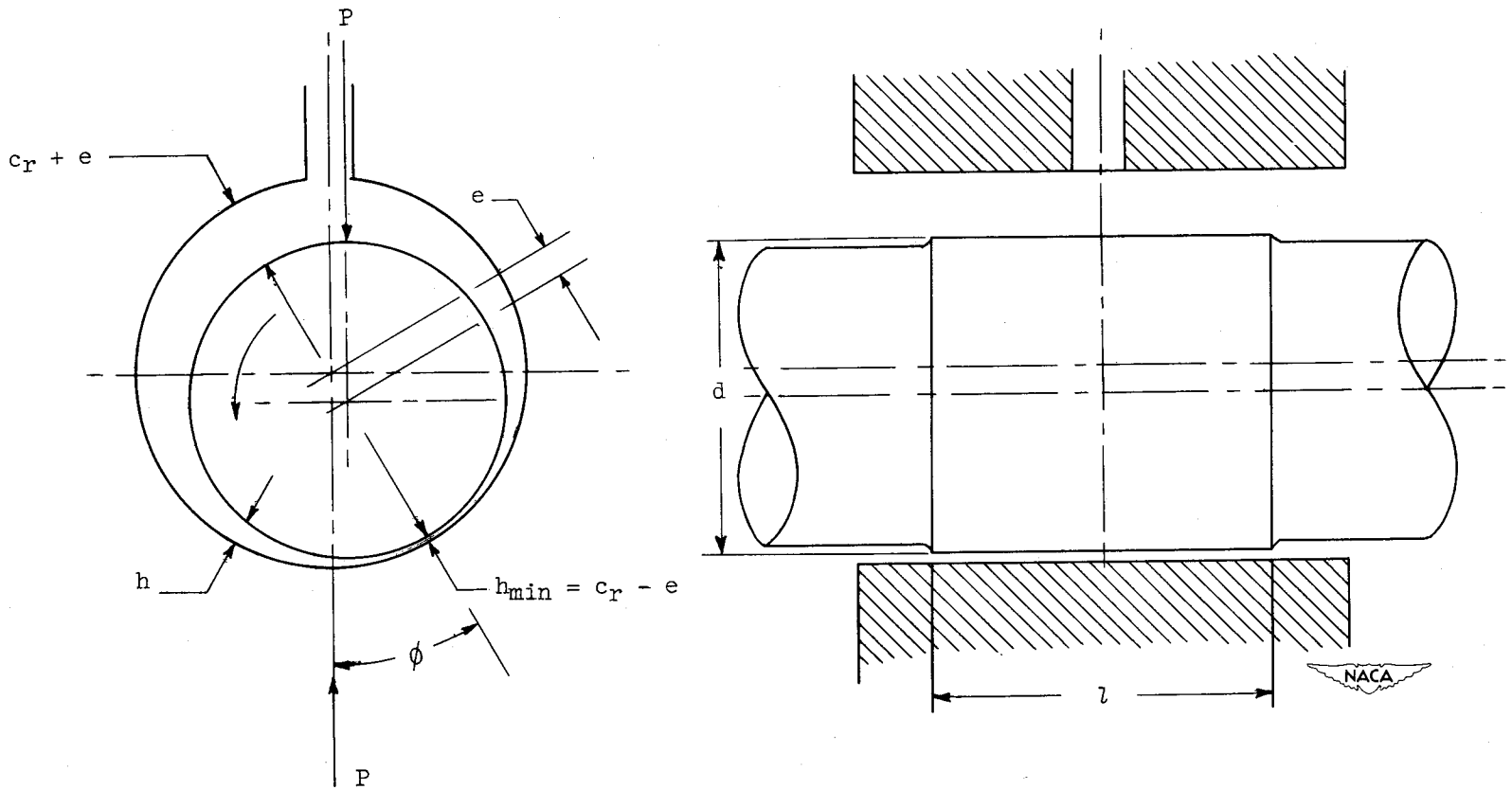

Figure 6.- Diagram of geometric relationship of journal and bearing.

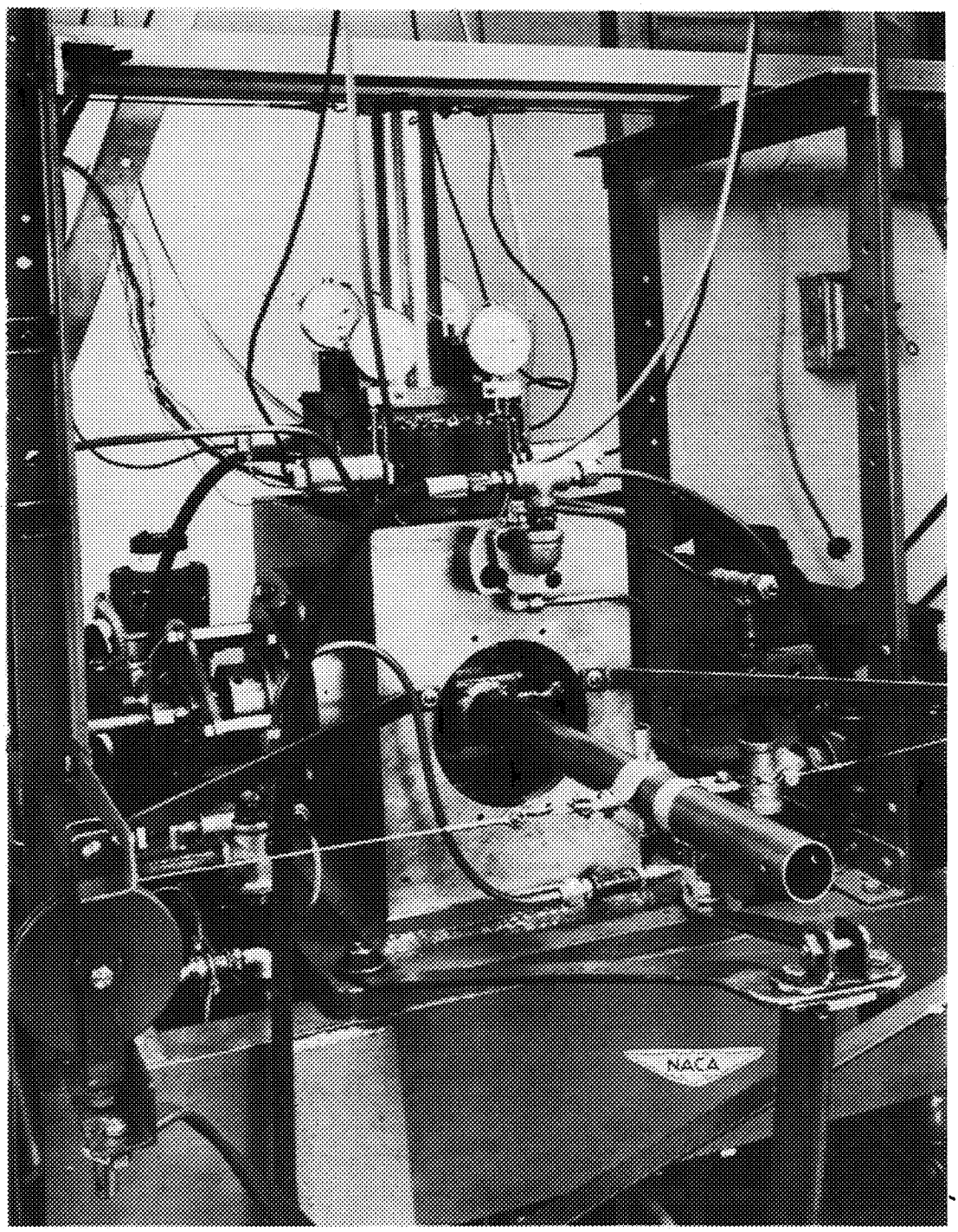

Figure 7.- Bearing testing machine used in experiments. Equipment includes variable speed electric drive to 10,000 rpm; direct hydraulic loading mechanism; misalining loading mechanism; and heater, filter, and pressure pump for lubricating oil. Measurements made include journal displacement, friction torque, oil flow, bearing temperatures, and, with accessories, oil film pressures.

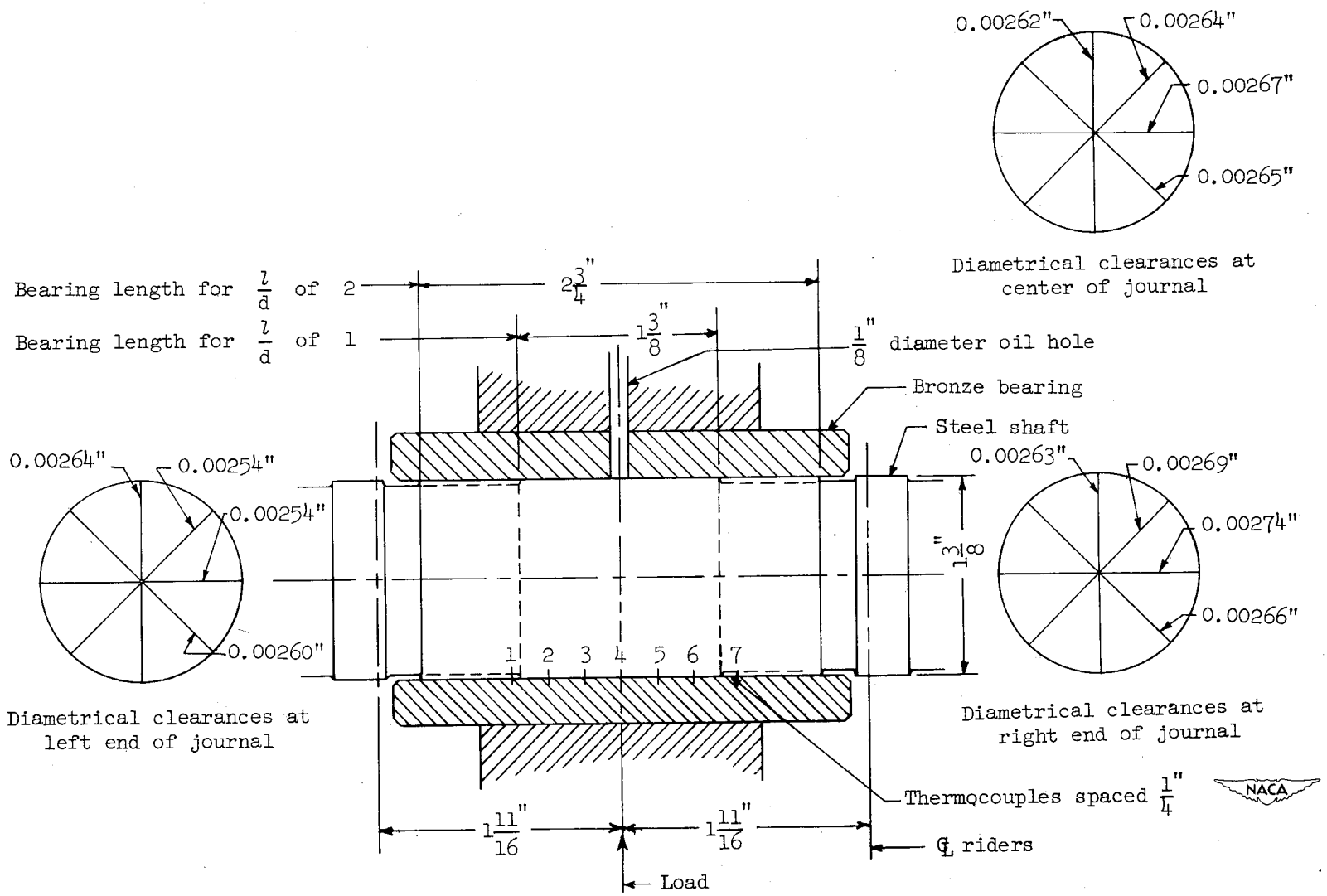

Figure 8.- Test shaft with single journal as used in experiments at l/d of 2 and 1. Average diametral clearance, 0.00264 inch.

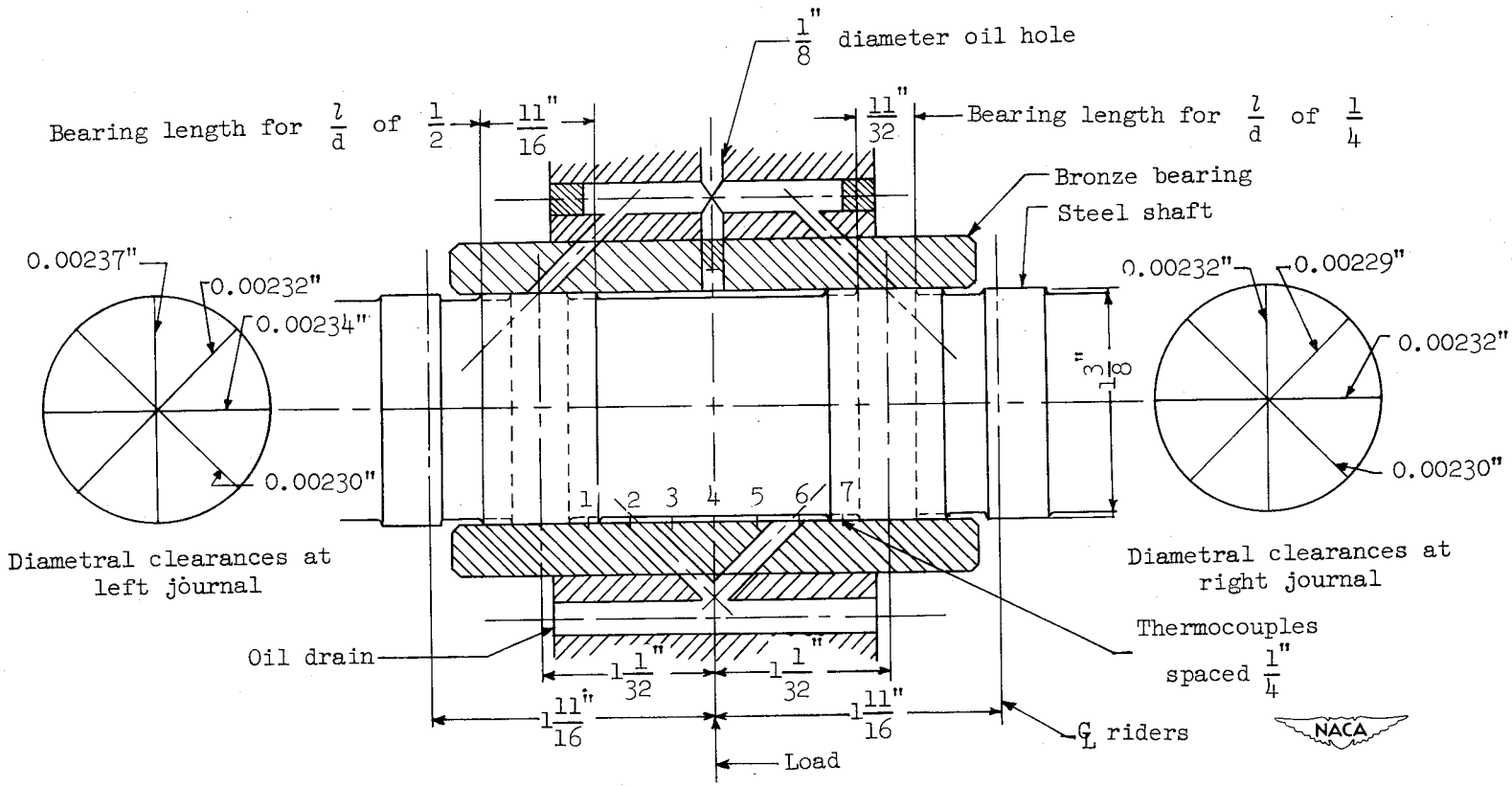

Figure 9.- Test shaft with two journals as used in experiments at l/d of 1/2 and 1/4. Average diametral clearance, 0.00232 inch.

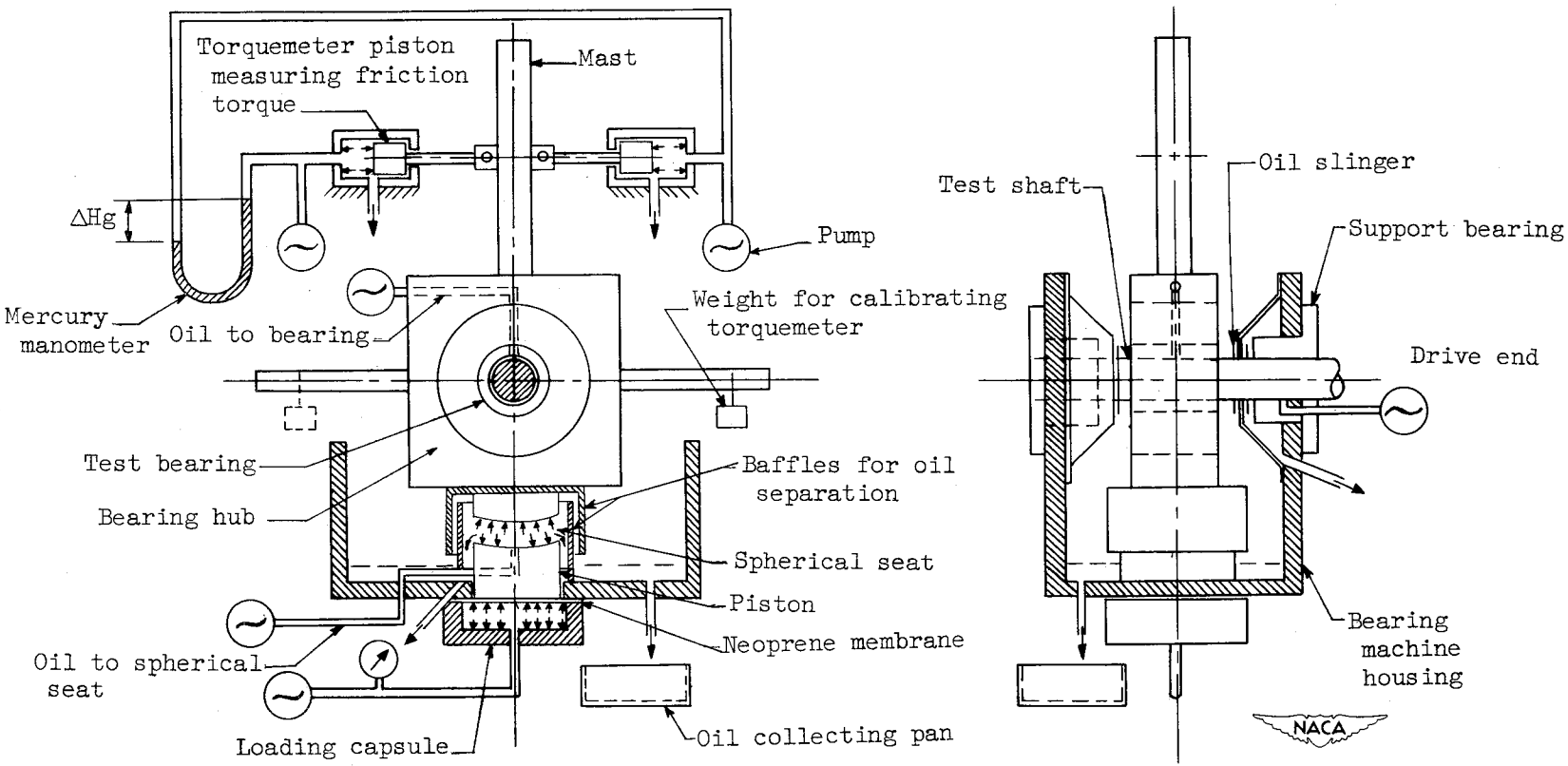

Figure 10.- Schematic diagram of apparatus for measuring friction torque on test bearing and oil flow through test bearing.

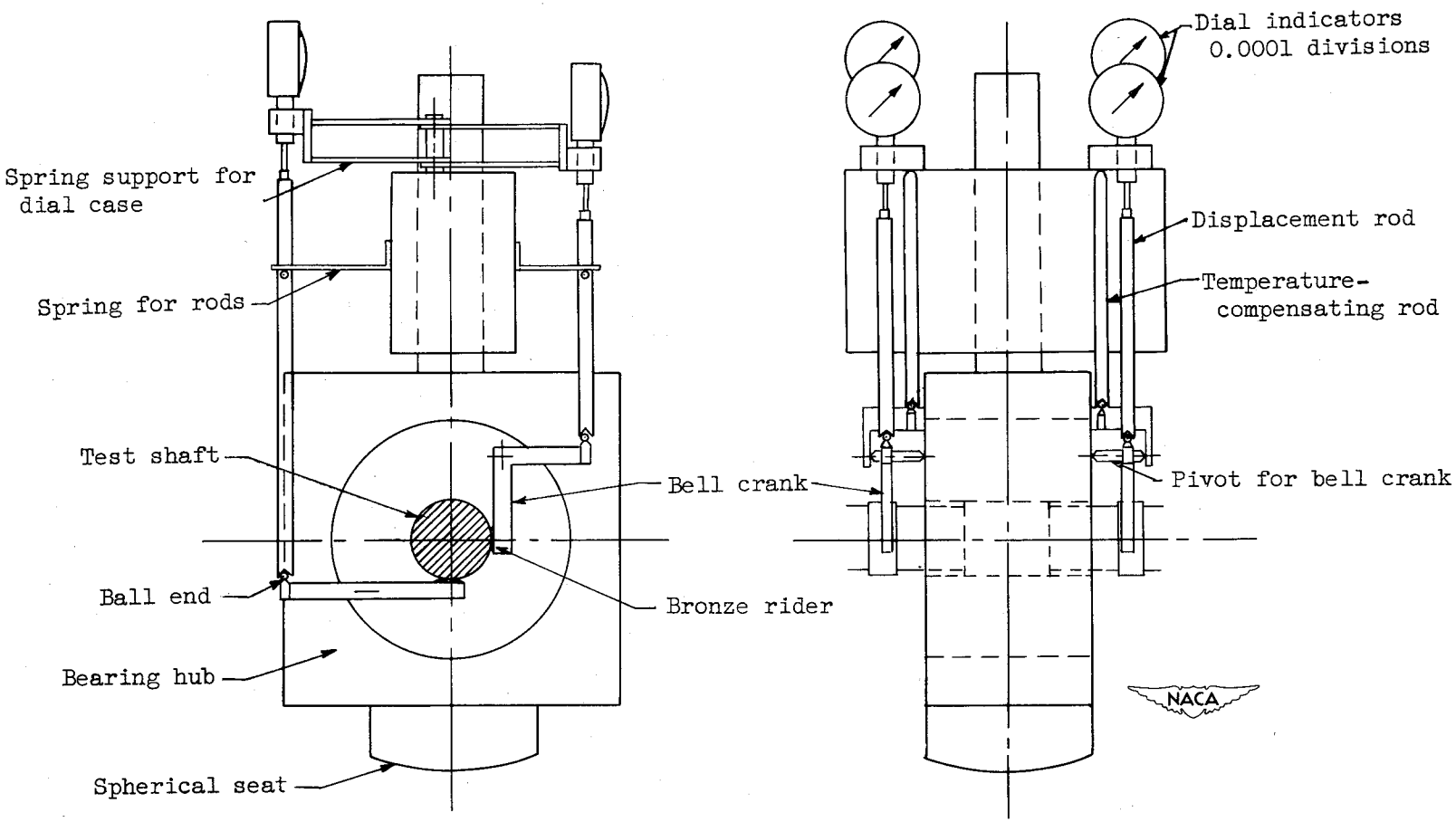

Figure 11.- Mechanical system for measuring displacement of journal with respect to bearing.

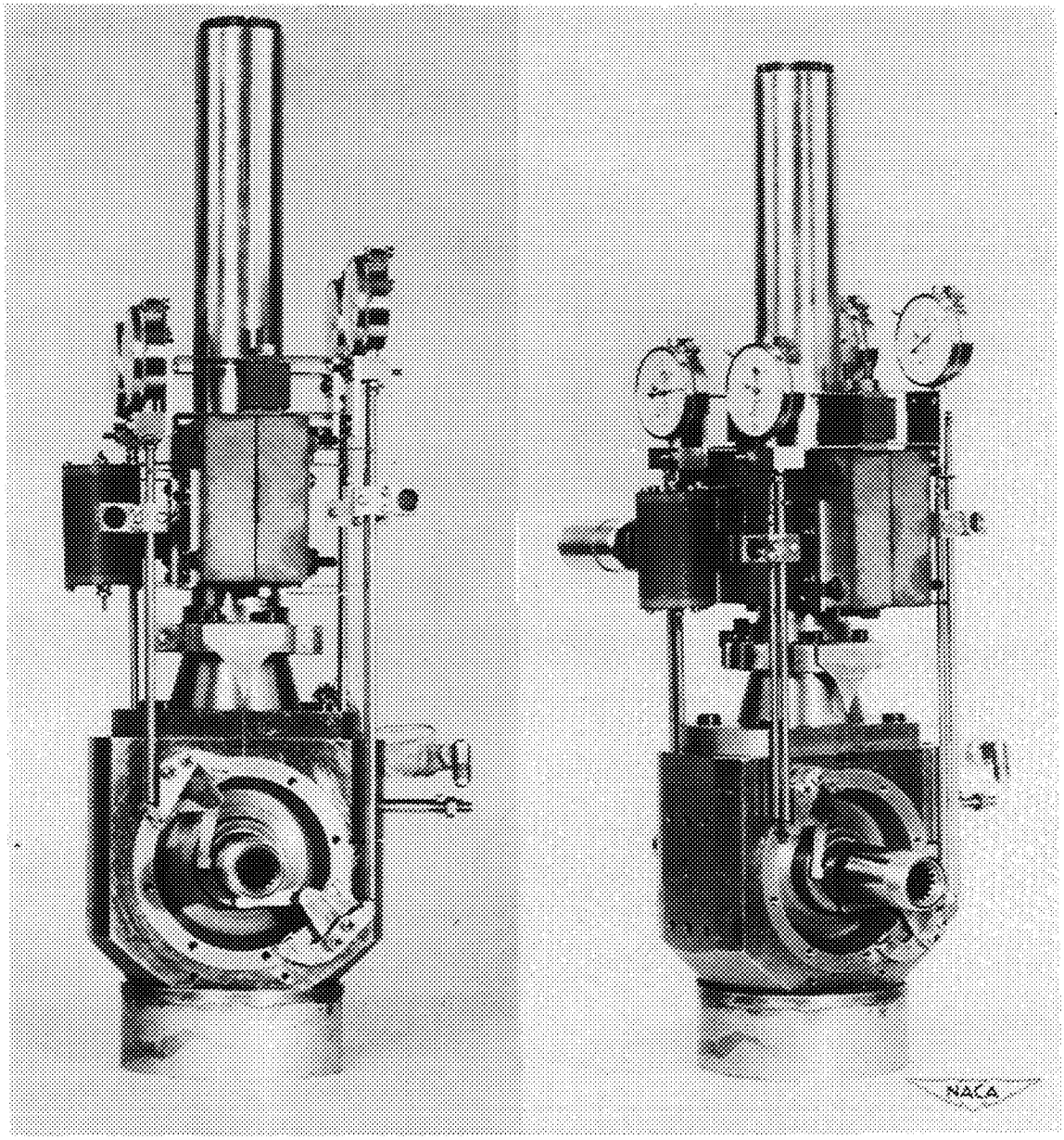

Figure 12.- Mechanical and photoelectric apparatus for measuring journal displacements with respect to bearing. Journal displacements are transmitted by levers and rods to dial indicators, which are used for steady-state conditions, and to photoelectric cells, for dynamic conditions.

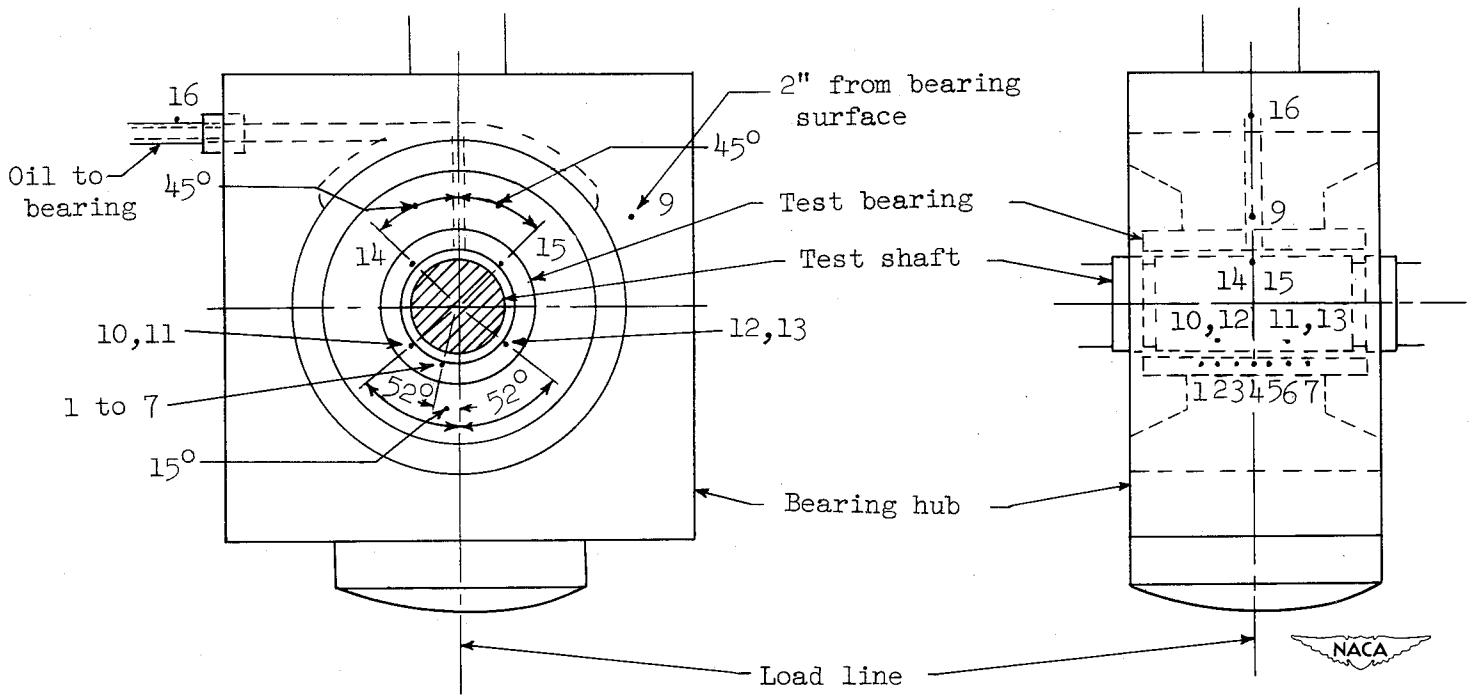

Figure 13.- Diagram of thermocouple locations. Bearing thermocouples are located 1/16 inch from bearing surface.

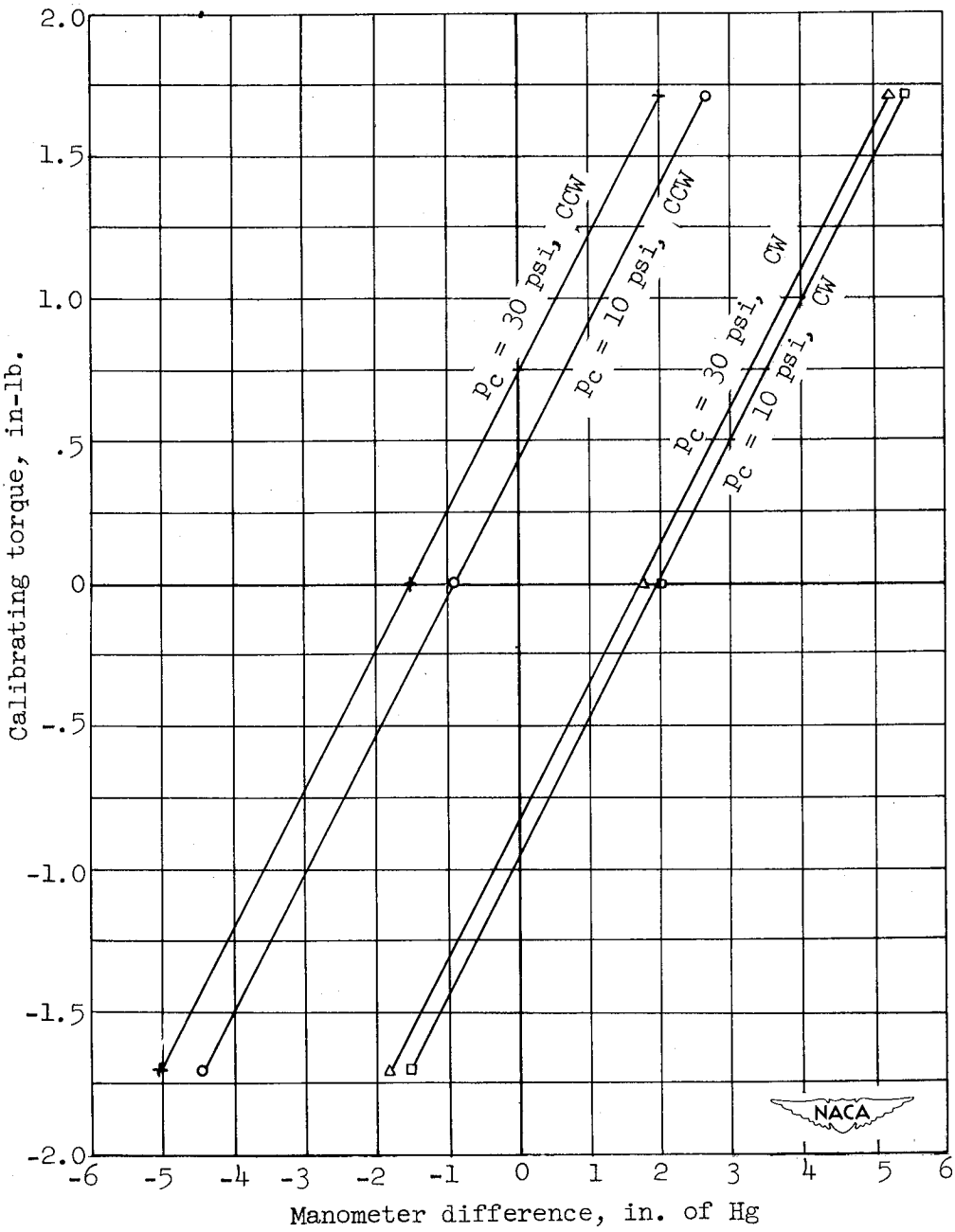

Figure 14.- Typical calibration curves for torquemeter used to measure friction torque on test bearing. Average slope of curves is calibration factor F_c giving friction torque per inch of difference in levels of mercury columns of manometer, $F_c = 0.485 \frac{\text{in-lb}}{\text{in. of Hg}}$. See table II for data.

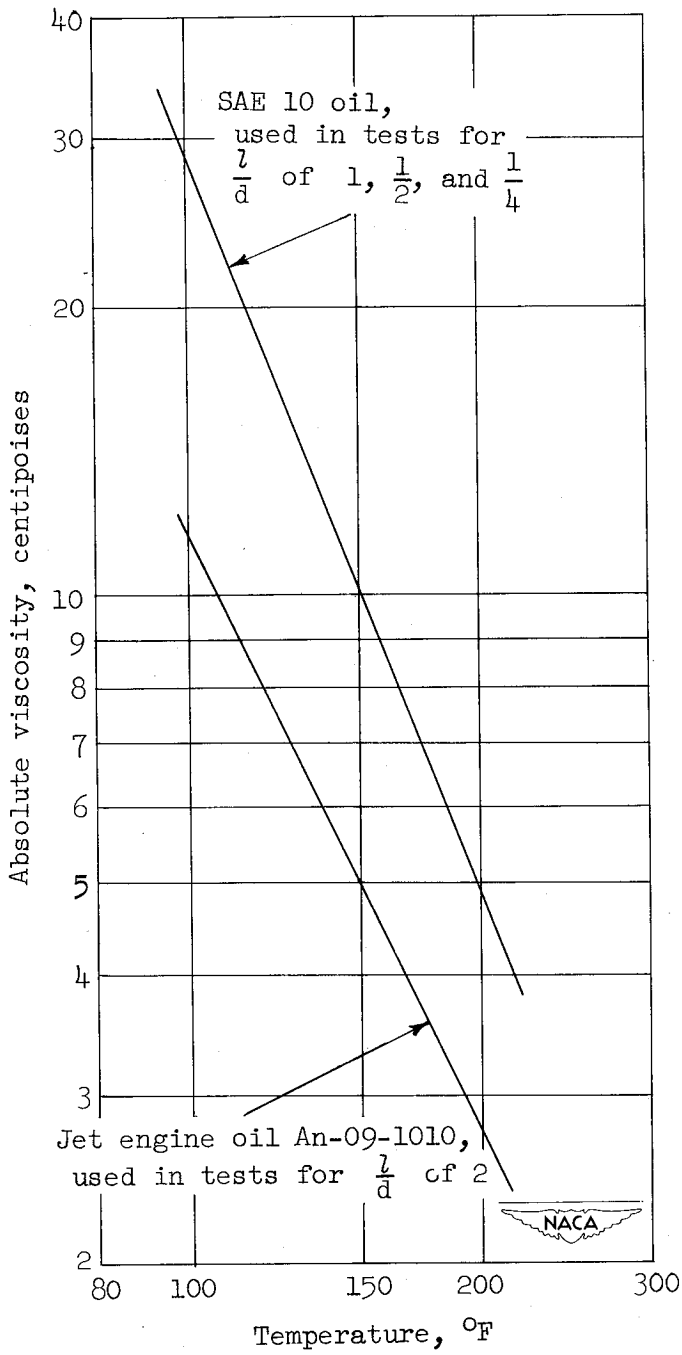

Figure 15.- Absolute-viscosity and temperature characteristics of lubricants used in experiments. Measurements of viscosity were made in a standard Saybolt viscosimeter.

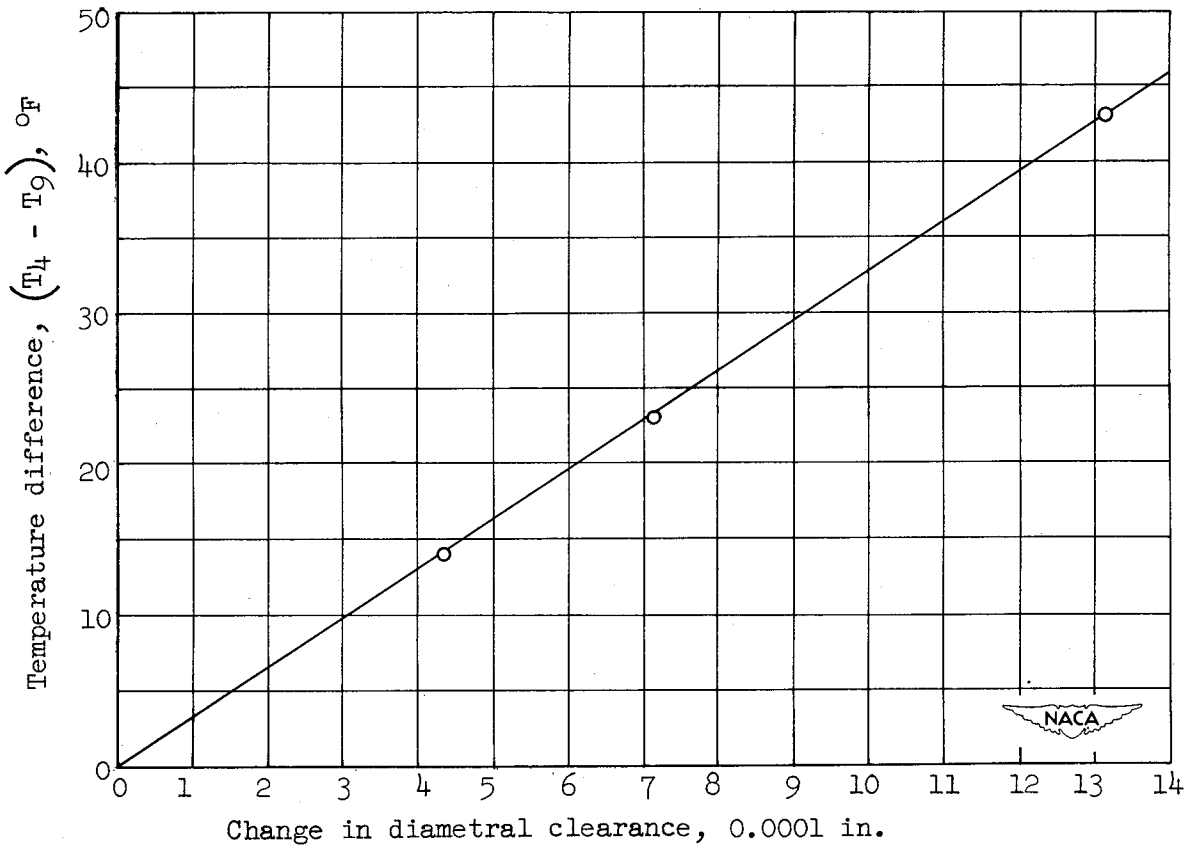

Figure 16.- Changes in diametral clearance as function of temperature difference of two points in test-bearing wall. T_4 and T_9 are bearing temperatures at 1/16 inch and 2 inches, respectively, from bearing surface. Running clearances of test bearing are determined by subtracting change in clearance from room-temperature clearance.

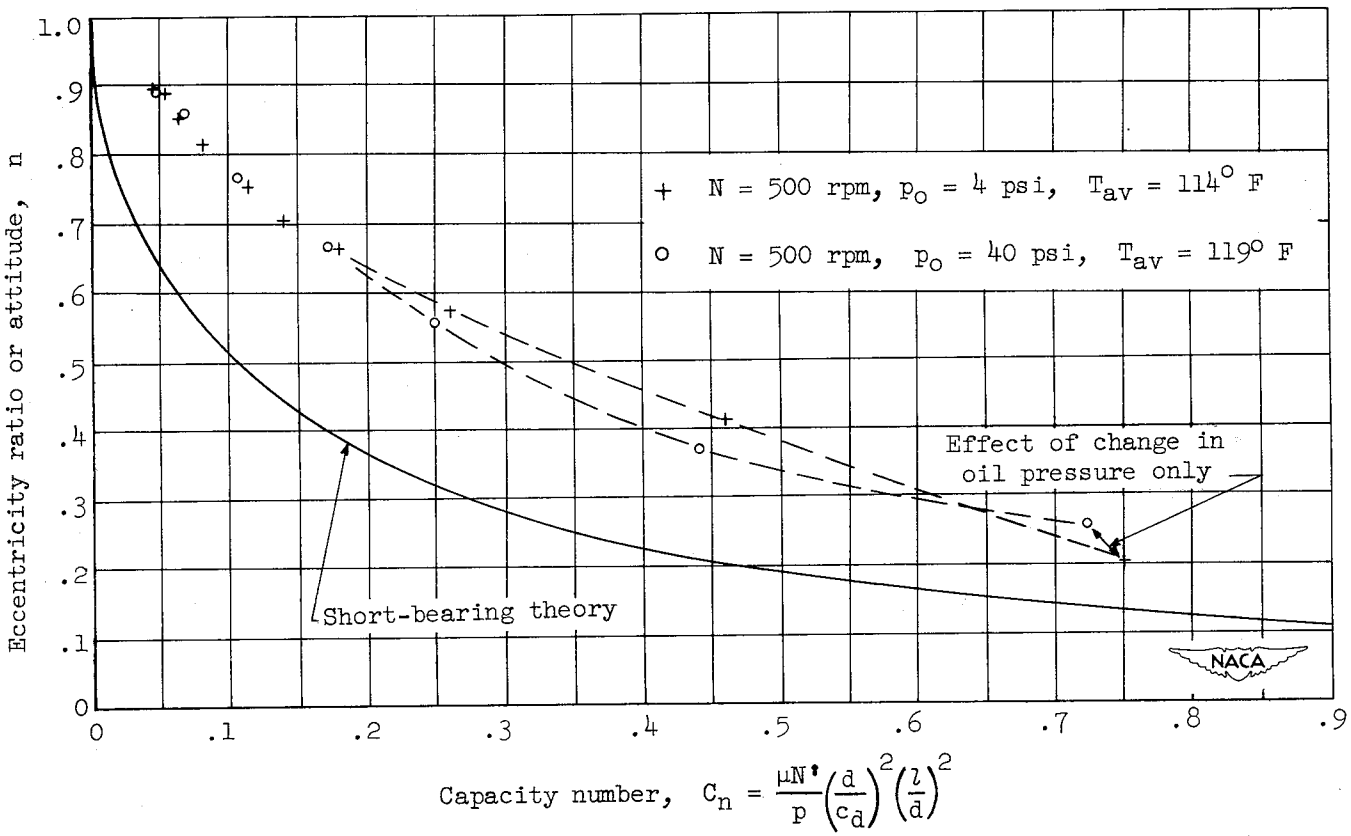

Figure 17.- Plot of eccentricity ratio against capacity number for comparison of experimental data for $l/d = 2$ with theoretical curve. Experimental data: Bearing diameter, $1\frac{3}{8}$ inches; bearing length, $2\frac{3}{4}$ inches; bearing, bronze; journal, steel; diametral clearance, 0.00264 inch; inlet pressure of jet engine oil AN-09-1010 p_o fed through one 1/8-inch-diameter hole, 4 and 40 pounds per square inch; speed, 500 rpm; load, 0 to 1000 pounds; bearing pressure, 0 to 260 pounds per square inch; average bearing temperature 1/16 inch from oil film T_{av}, 114° and 119° F.

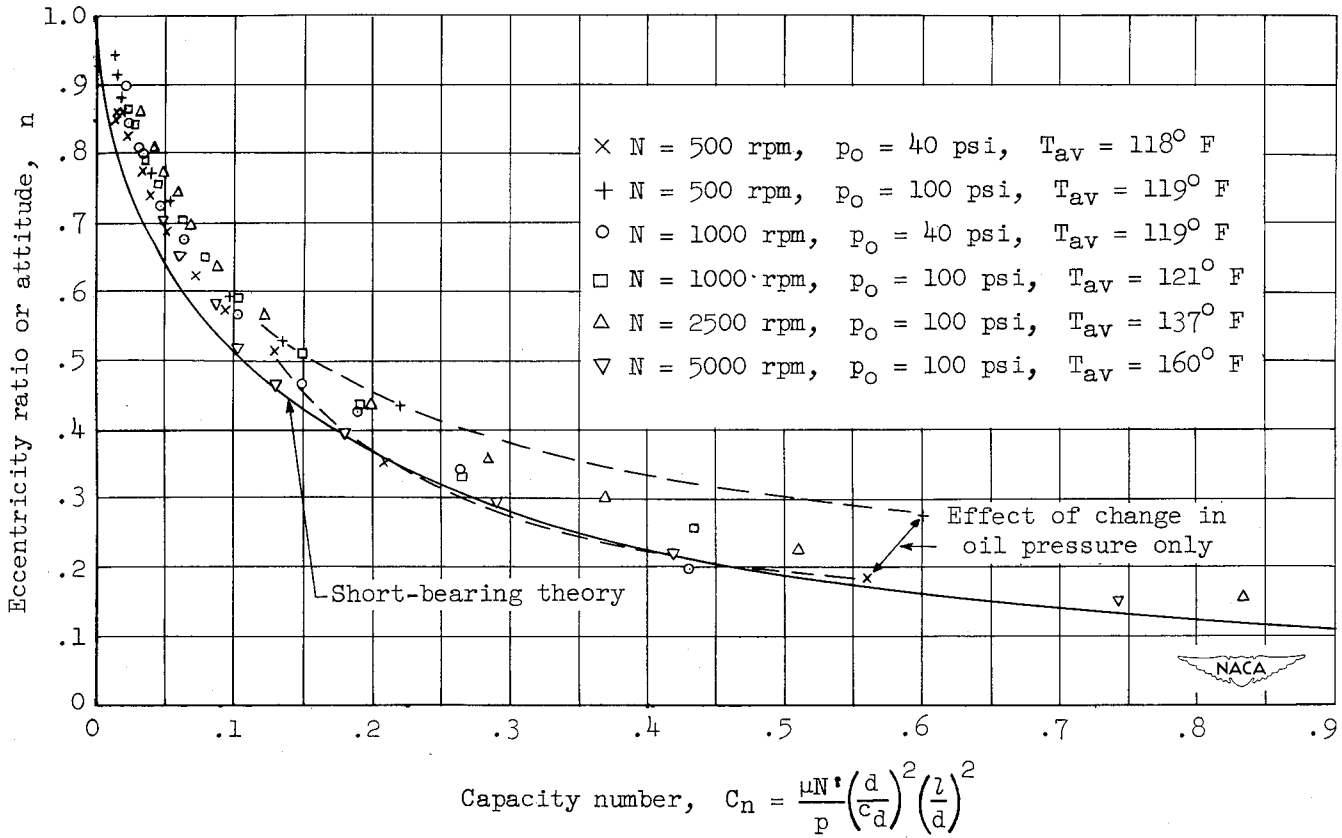

Figure 18.- Plot of eccentricity ratio against capacity number for comparison of experimental data for $l/d = 1$ with theoretical curve. Experimental data: Bearing diameter, $1\frac{3}{8}$ inches; bearing length, $1\frac{3}{8}$ inches; bearing, bronze; journal, steel; diametral clearance, 0.00264 inch; inlet pressure of SAE 10 oil p_o fed through one 1/8-inch-diameter hole, 40 and 100 pounds per square inch; speed, 500 to 5000 rpm; load, 0 to 1450 pounds; bearing pressure 0 to 760 pounds per square inch; average bearing temperature 1/16 inch from oil film T_{av}, 118° to 160° F.

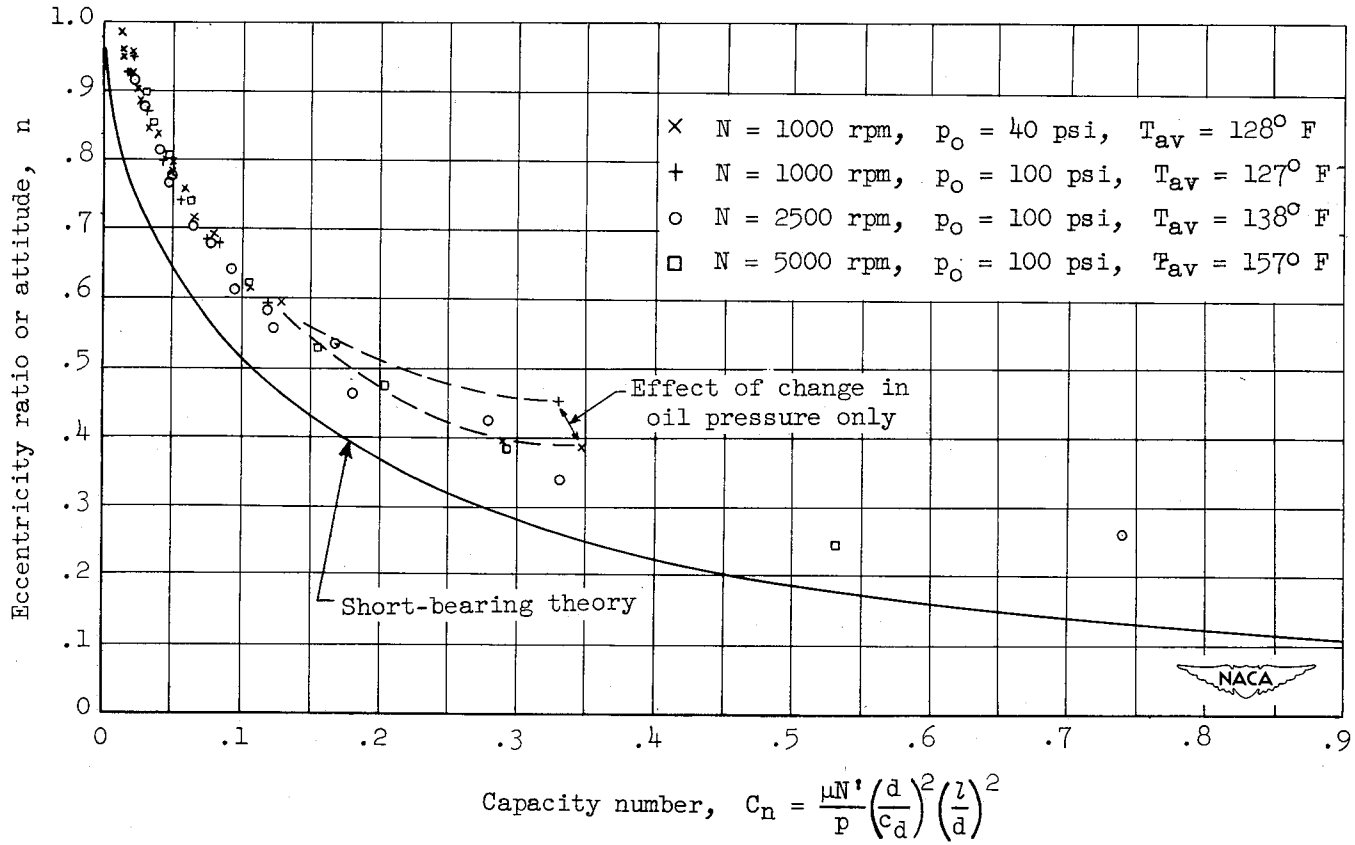

Figure 19.- Plot of eccentricity ratio against capacity number for comparison of experimental data for $l/d = 1/2$ with theoretical curve. Experimental data: Bearing diameter, $1\frac{3}{8}$ inches; bearing length, 11/16 inch; bearing, bronze; journal, steel; diametral clearance, 0.00232 inch; inlet pressure of SAE 10 oil p_o fed through one 1/8-inch-diameter hole, 40 and 100 pounds per square inch; speed, 1000 to 5000 rpm; load, 0 to 415 pounds; bearing pressure, 0 to 435 pounds per square inch; average bearing temperature 1/16 inch from oil film T_{av}, 127° to 157° F.

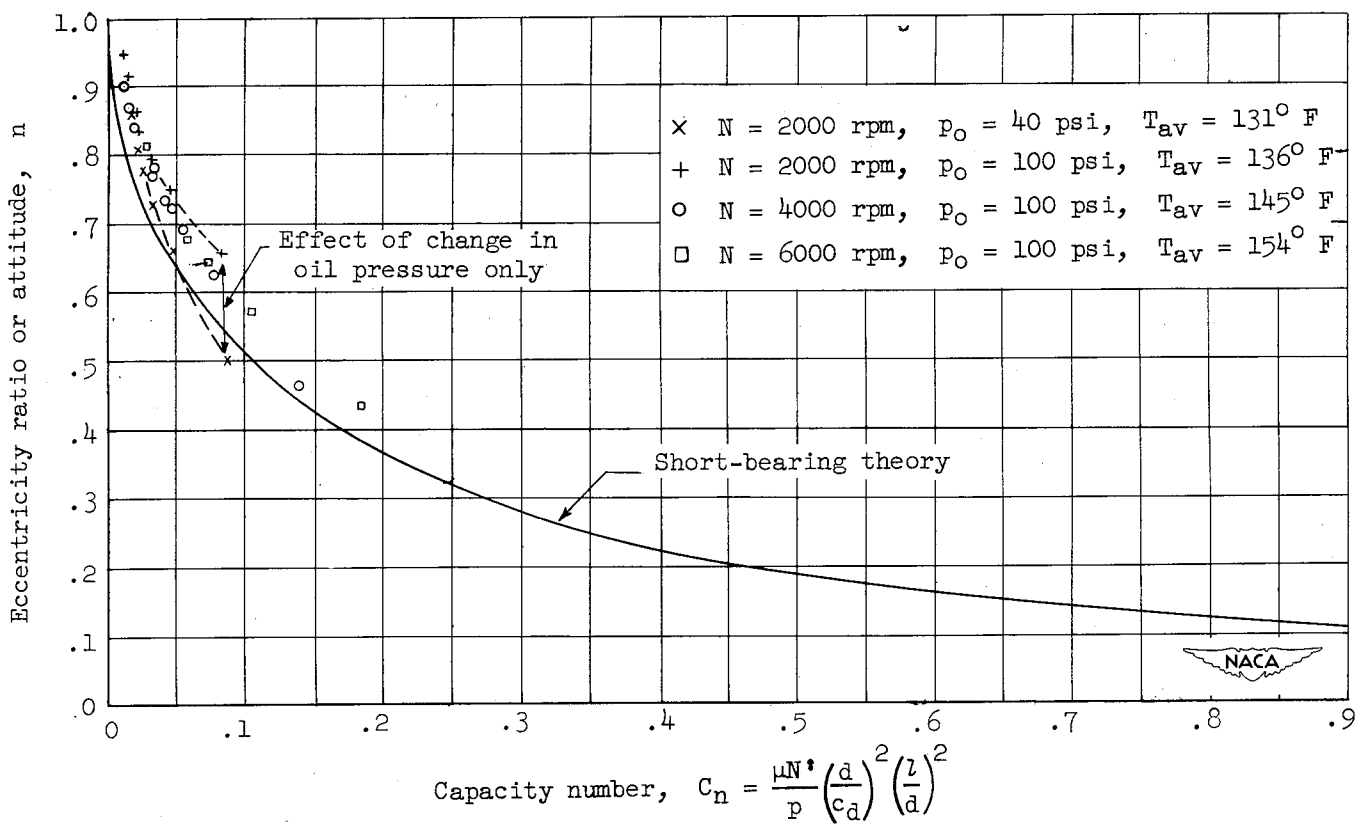

Figure 20.- Plot of eccentricity ratio against capacity number for comparison of experimental data for $l/d = 1/4$ with theoretical curve. Experimental data: Bearing diameter, $1\frac{3}{8}$ inches; bearing length, 11/32 inch; bearing, bronze; journal, steel; diametral clearance, 0.00232 inch; inlet pressure of SAE 10 oil p_o fed through one 1/8-inch-diameter hole, 40 and 100 pounds per square inch; speed, 2000 to 6000 rpm; load, 0 to 98 pounds; bearing pressure, 0 to 200 pounds per square inch; average bearing temperature 1/16 inch from oil film T_{av}, 131° to 154° F.

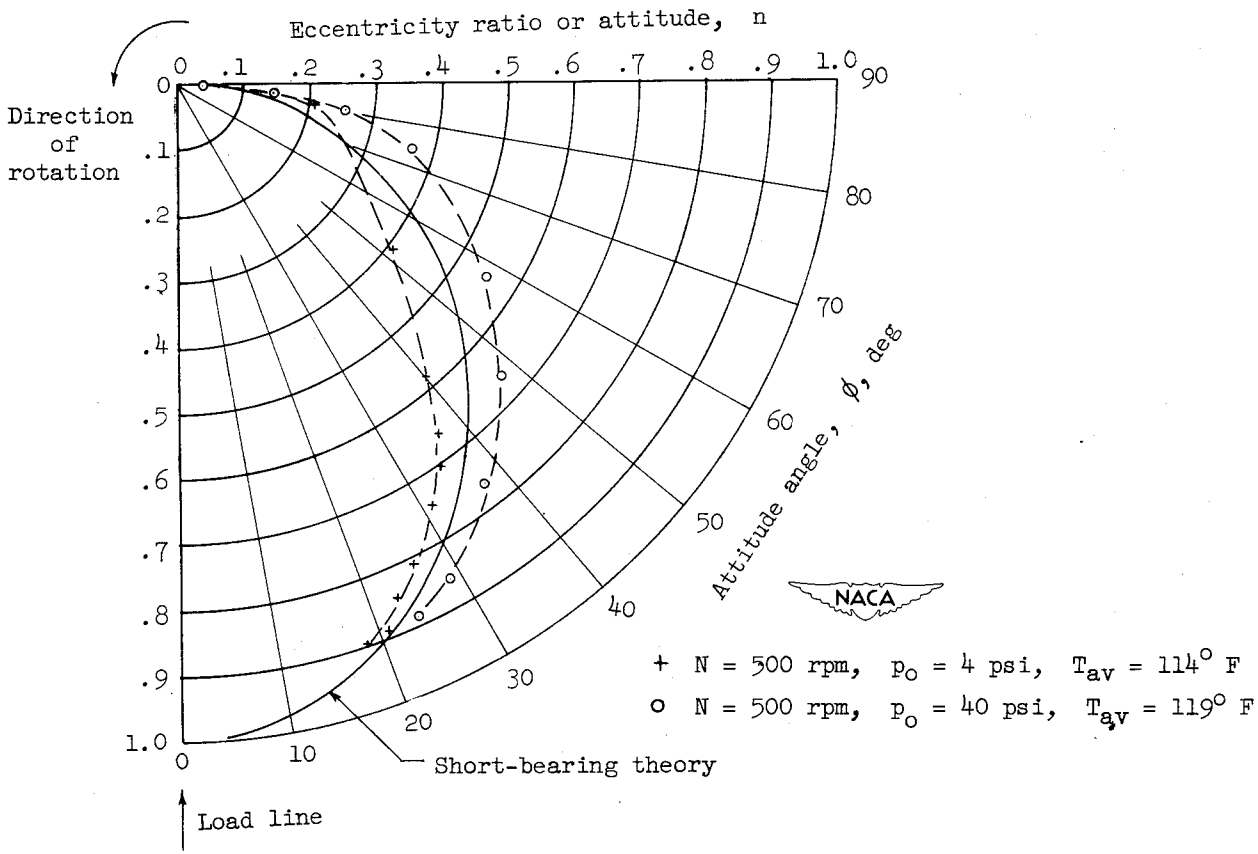

Figure 21.- Plot of eccentricity ratio against attitude angle for comparison of experimental data for $l/d = 2$ with theoretical curve. Experimental data: Bearing diameter, $1\frac{3}{8}$ inches; bearing length, $2\frac{3}{4}$ inches; bearing, bronze; journal, steel; diametral clearance, 0.00264 inch; inlet pressure of jet engine oil AN-09-1010 p_o fed through one 1/8-inch-diameter hole, 4 and 40 pounds per square inch; speed, 500 rpm; load, 0 to 1000 pounds; bearing pressure, 0 to 260 pounds per square inch; average bearing temperature 1/16 inch from oil film T_{av}, 114° and 119° F.

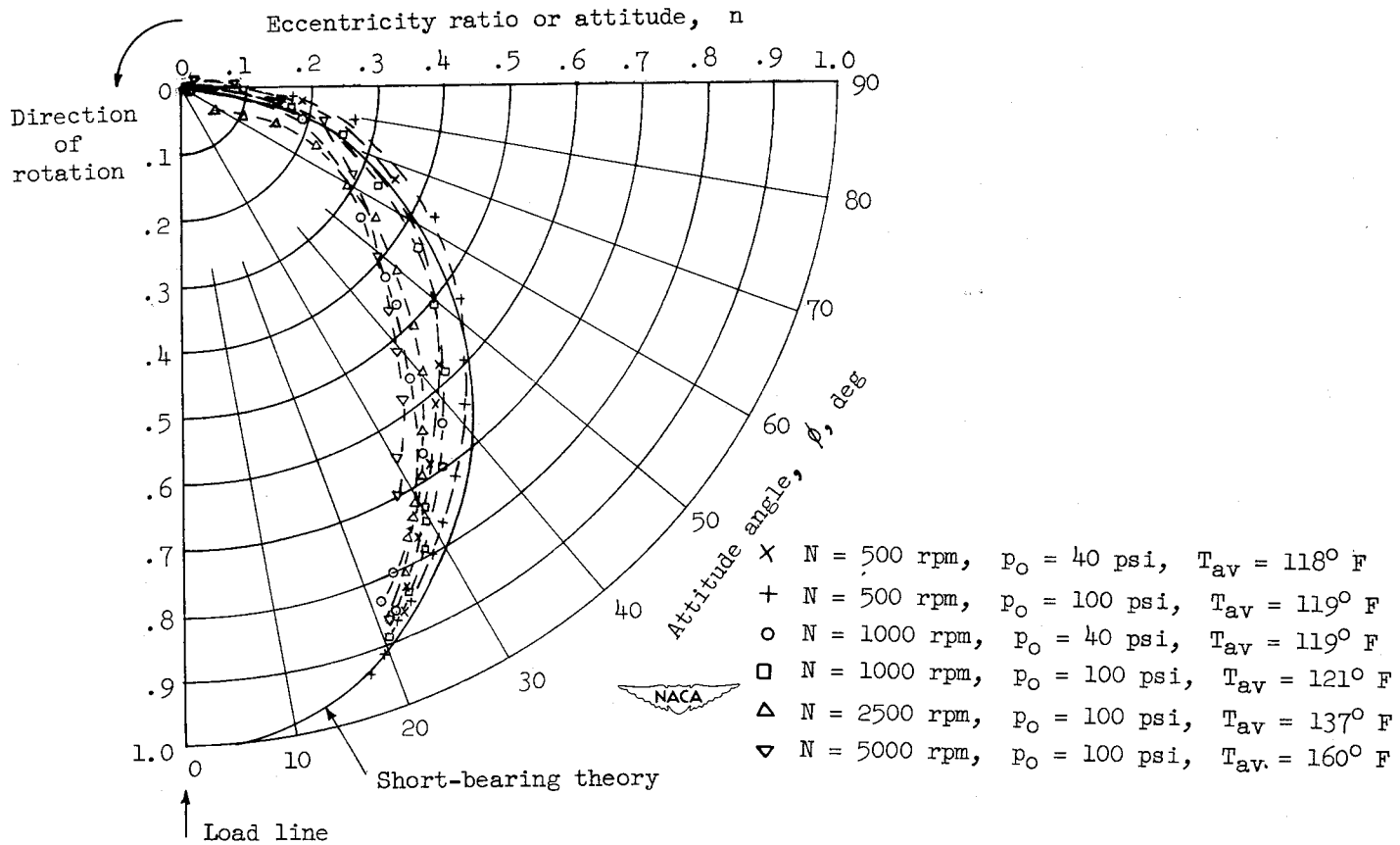

Figure 22.- Plot of eccentricity ratio against attitude angle for comparison of experimental data for $l/d = 1$ with theoretical curve. Experimental data: Bearing diameter, $1\frac{3}{8}$ inches; bearing length, $1\frac{3}{8}$ inches; bearing, bronze; journal, steel; diametral clearance, 0.00264 inch; inlet pressure of SAE 10 oil p_o fed through one 1/8-inch-diameter hole, 40 and 100 pounds per square inch; speed, 500 to 5000 rpm; load, 0 to 1450 pounds; bearing pressure, 0 to 760 pounds per square inch; average bearing temperature 1/16 inch from oil film T_{av}, 118° to 160° F.

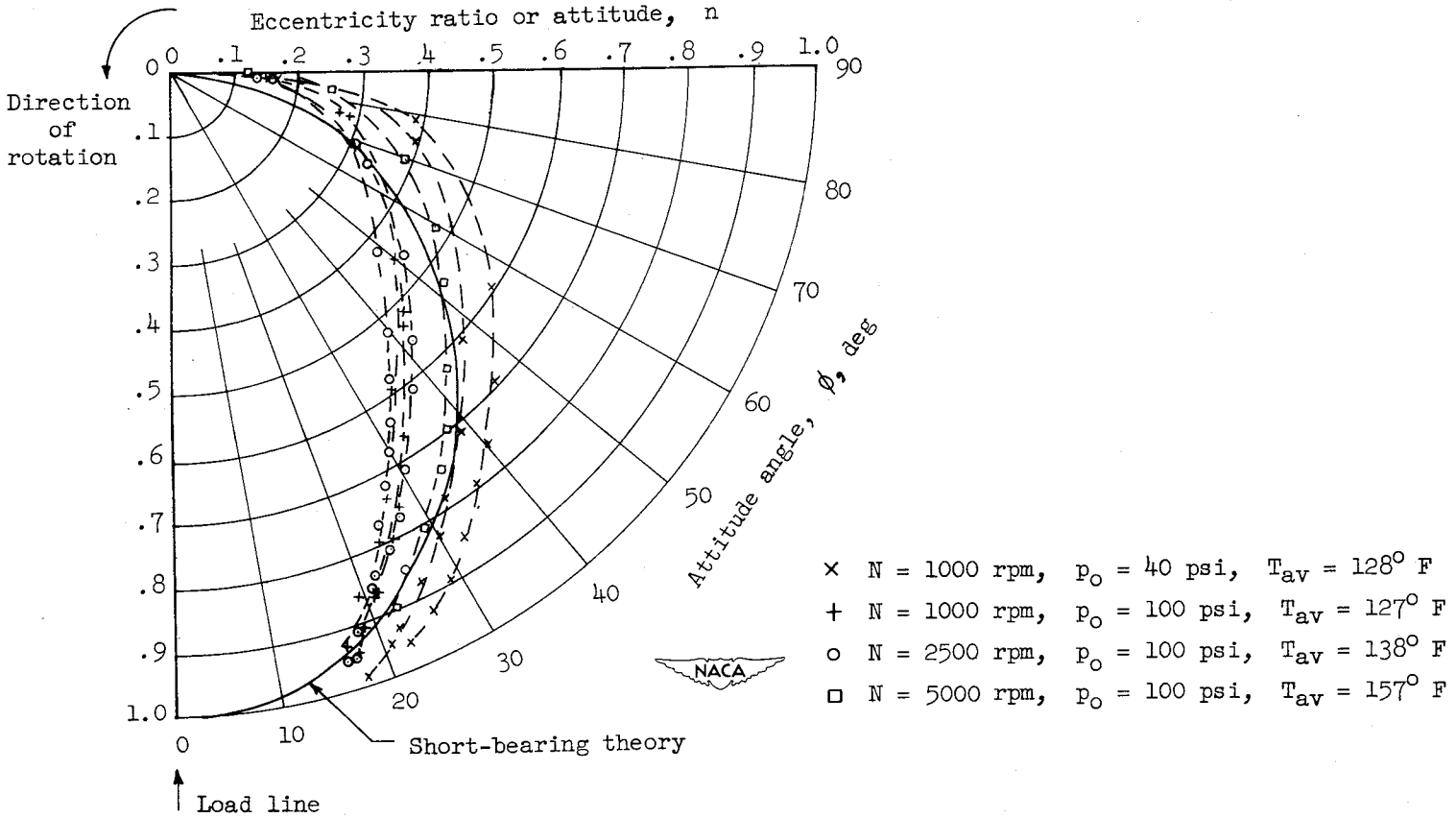

Figure 23.- Plot of eccentricity ratio against attitude angle for comparison of experimental data for $l/d = 1/2$ with theoretical curve. Experimental data: Bearing diameter, $1\frac{3}{8}$ inches; bearing length, 11/16 inch; bearing, bronze; journal, steel; diametral clearance, 0.00232 inch; inlet pressure of SAE 10 oil p_o fed through one 1/8-inch-diameter hole, 40 and 100 pounds per square inch; speed, 1000 to 5000 rpm; load, 0 to 415 pounds; bearing pressure, 0 to 435 pounds per square inch; average bearing temperature 1/16 inch from oil film T_{av}, 127° to 157° F.

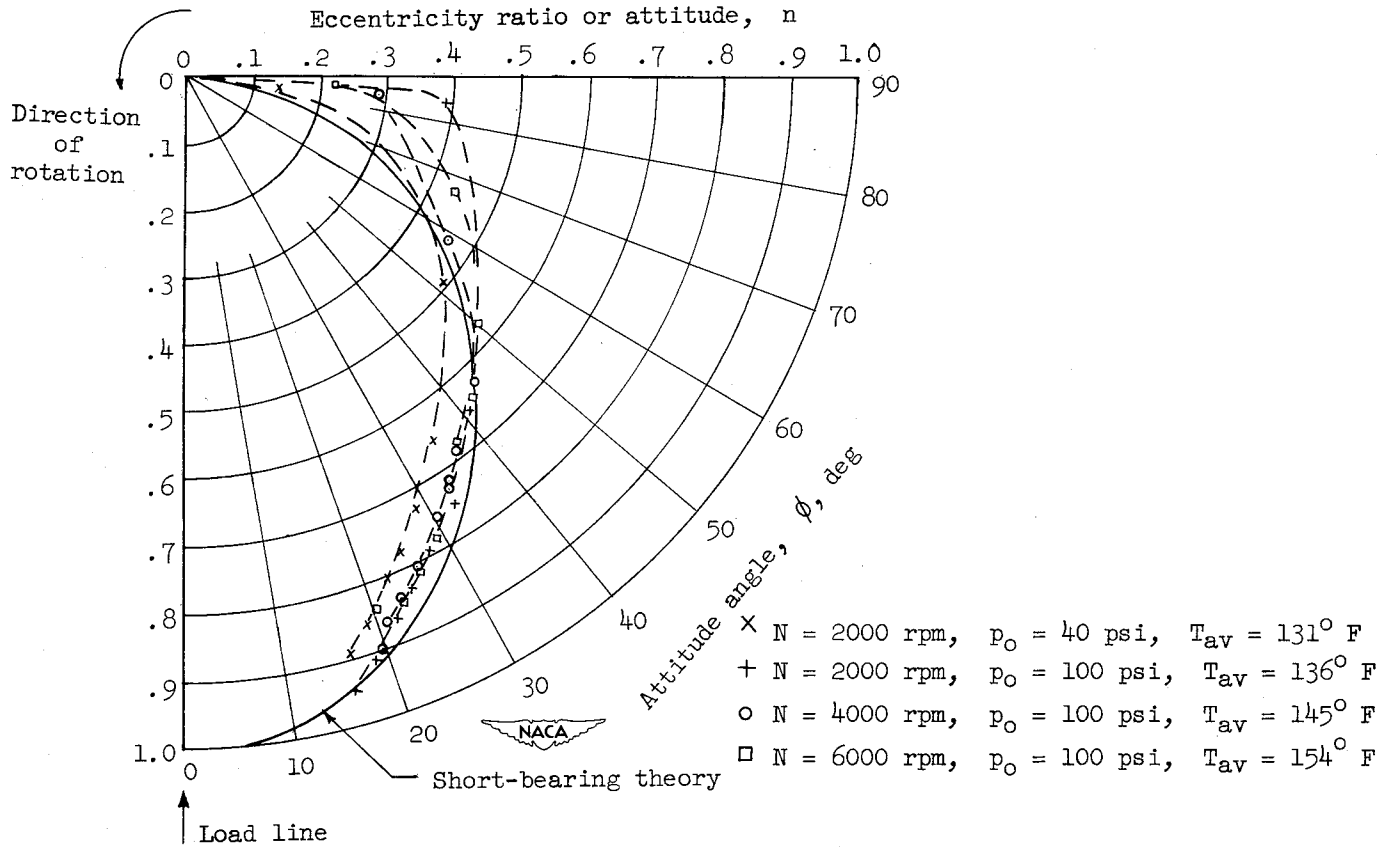

Figure 24.- Plot of eccentricity ratio against attitude angle for comparison of experimental data for $l/d = 1/4$ with theoretical curve. Experimental data: Bearing diameter, $1\frac{3}{8}$ inches; bearing length, 11/32 inch; bearing, bronze; journal, steel; diametral clearance, 0.00232 inch; inlet pressure of SAE 10 oil p_o fed through one 1/8-inch-diameter hole, 40 and 100 pounds per square inch; speed, 2000 to 6000 rpm; load, 0 to 98 pounds; bearing pressure, 0 to 200 pounds per square inch; average bearing temperature 1/16 inch from oil film T_{av}, 131° to 154° F.

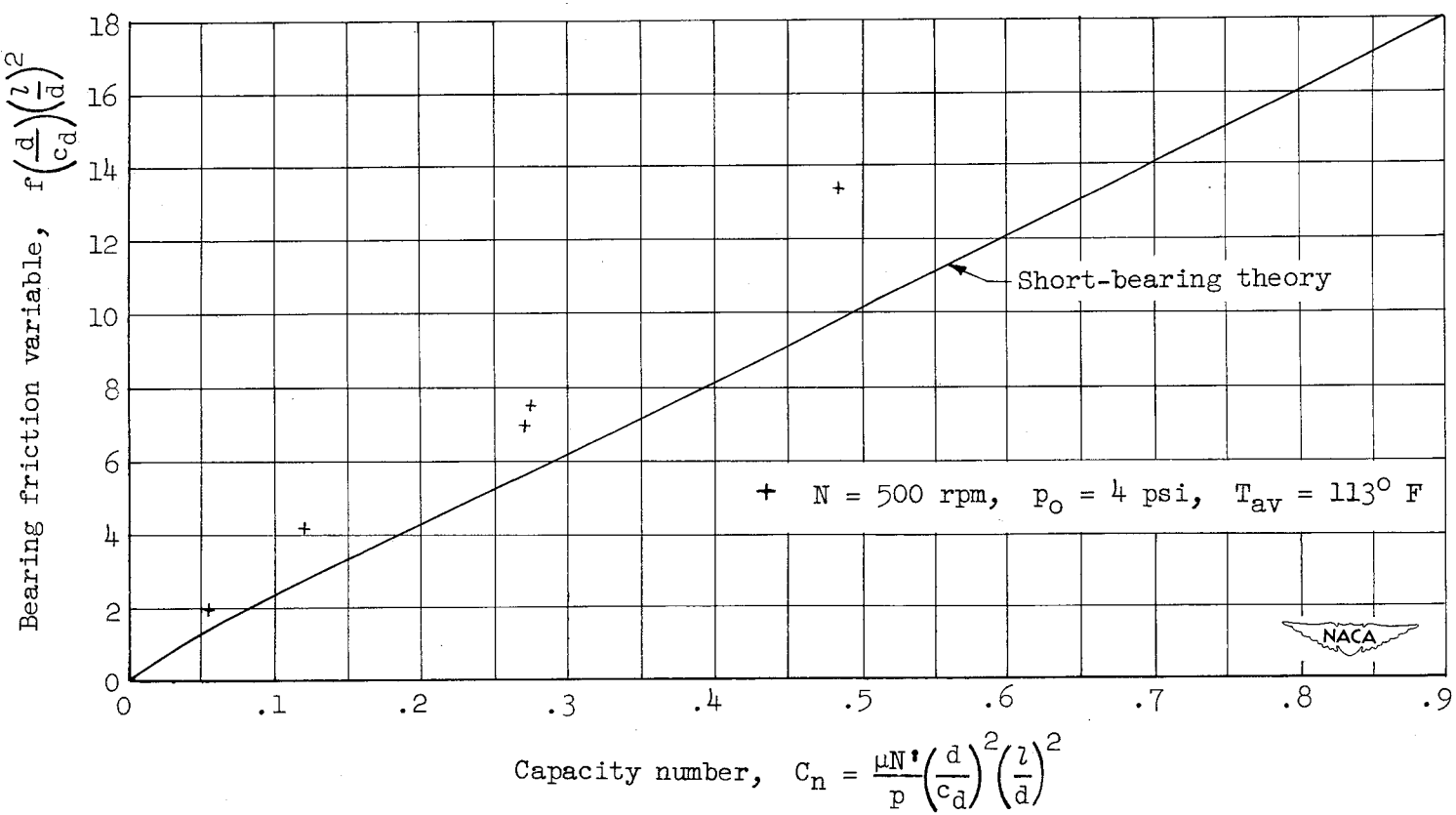

Figure 25.- Plot of bearing friction variable against capacity number for comparison of experimental data for $l/d = 2$ with theoretical curve. Experimental data: Bearing diameter, $1\frac{3}{8}$ inches; bearing length, $2\frac{3}{4}$ inches; bearing, bronze; journal, steel; diametral clearance, 0.00264 inch; inlet pressure of jet engine oil AN-09-1010 p_o fed through one 1/8-inch-diameter hole, 4 pounds per square inch; speed, 500 rpm; load, 0 to 850 pounds; bearing pressure,,0 to 220 pounds per square inch; average bearing temperature 1/16 inch from oil film T_{av}, 113° F.

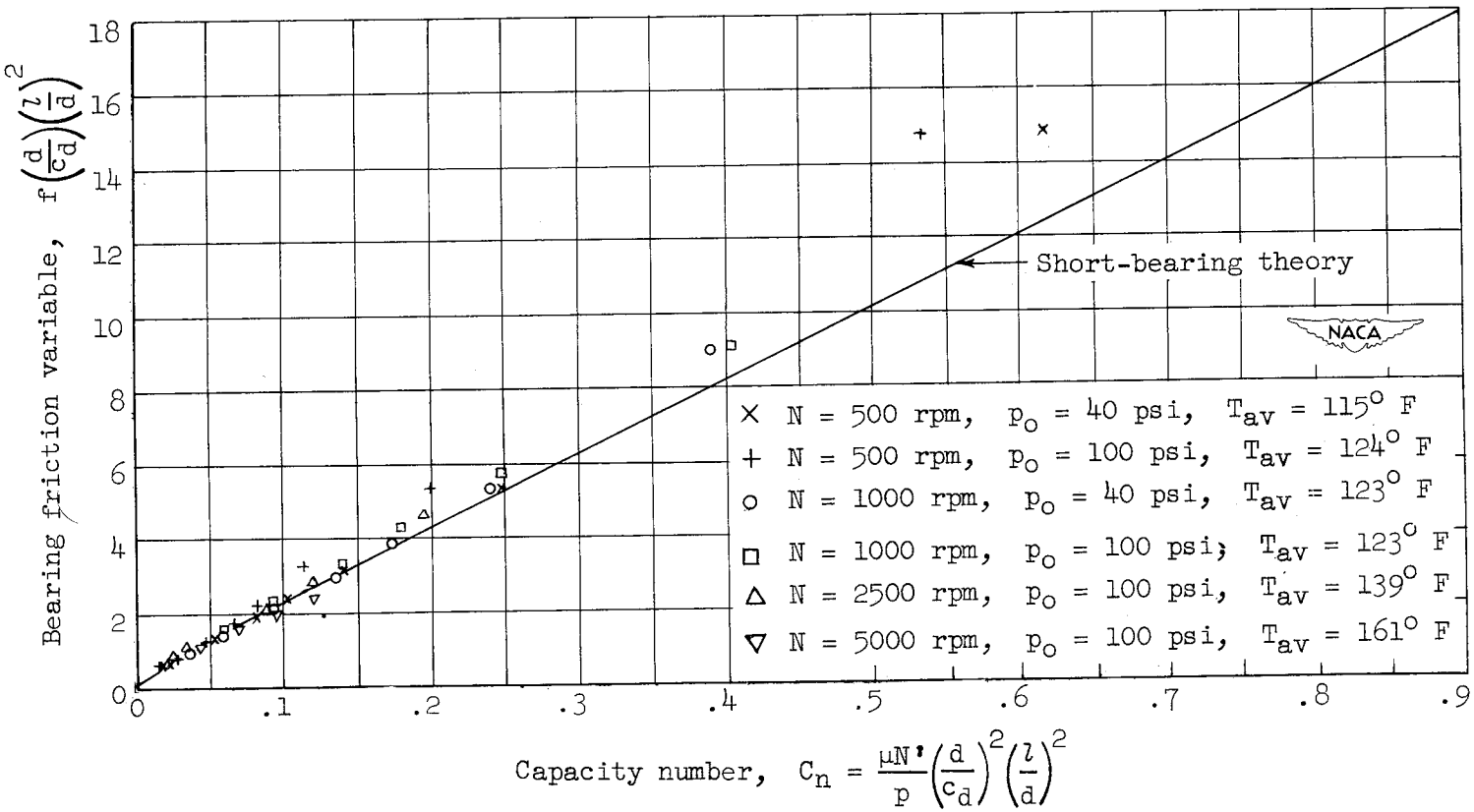

Figure 26.- Plot of bearing friction variable against capacity number for comparison of experimental data for $l/d = 1$ with theoretical curve. Experimental data: Bearing diameter, $1\frac{3}{8}$ inches; bearing length, $1\frac{3}{8}$ inches; bearing, bronze; journal, steel; diametral clearance, 0.00264 inch; inlet pressure of SAE 10 oil p_o fed through one 1/8-inch-diameter hole, 40 and 100 pounds per square inch; speed, 500 to 5000 rpm; load, 0 to 1750 pounds; bearing pressure, 0 to 900 pounds per square inch; average bearing temperature 1/16 inch from oil film T_{av}, 115° to 161° F.

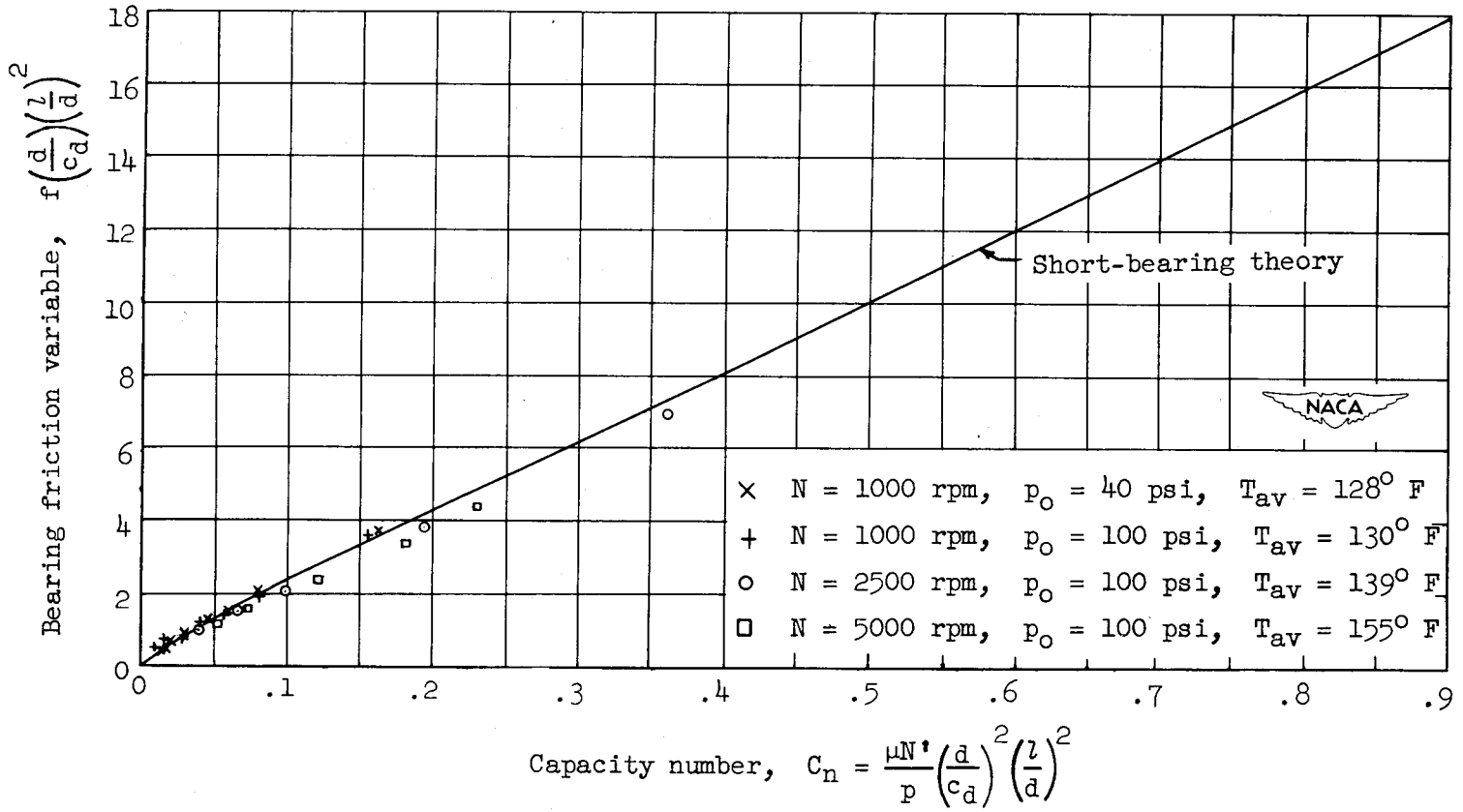

Figure 27.- Plot of bearing friction variable against capacity number for comparison of experimental data for $l/d = 1/2$ with theoretical curve. Experimental data: Bearing diameter, $1\frac{3}{8}$ inches; bearing length, 11/16 inch; bearing, bronze; journal, steel; diametral clearance, 0.00232 inch; inlet pressure of SAE 10 oil p_o fed through one 1/8-inch-diameter hole, 40 and 100 pounds per square inch; speed, 1000 to 5000 rpm; load, 0 to 490 pounds; bearing pressure, 0 to 515 pounds per square inch; average bearing temperature 1/16 inch from oil film T_{av}, 128° to 155° F.

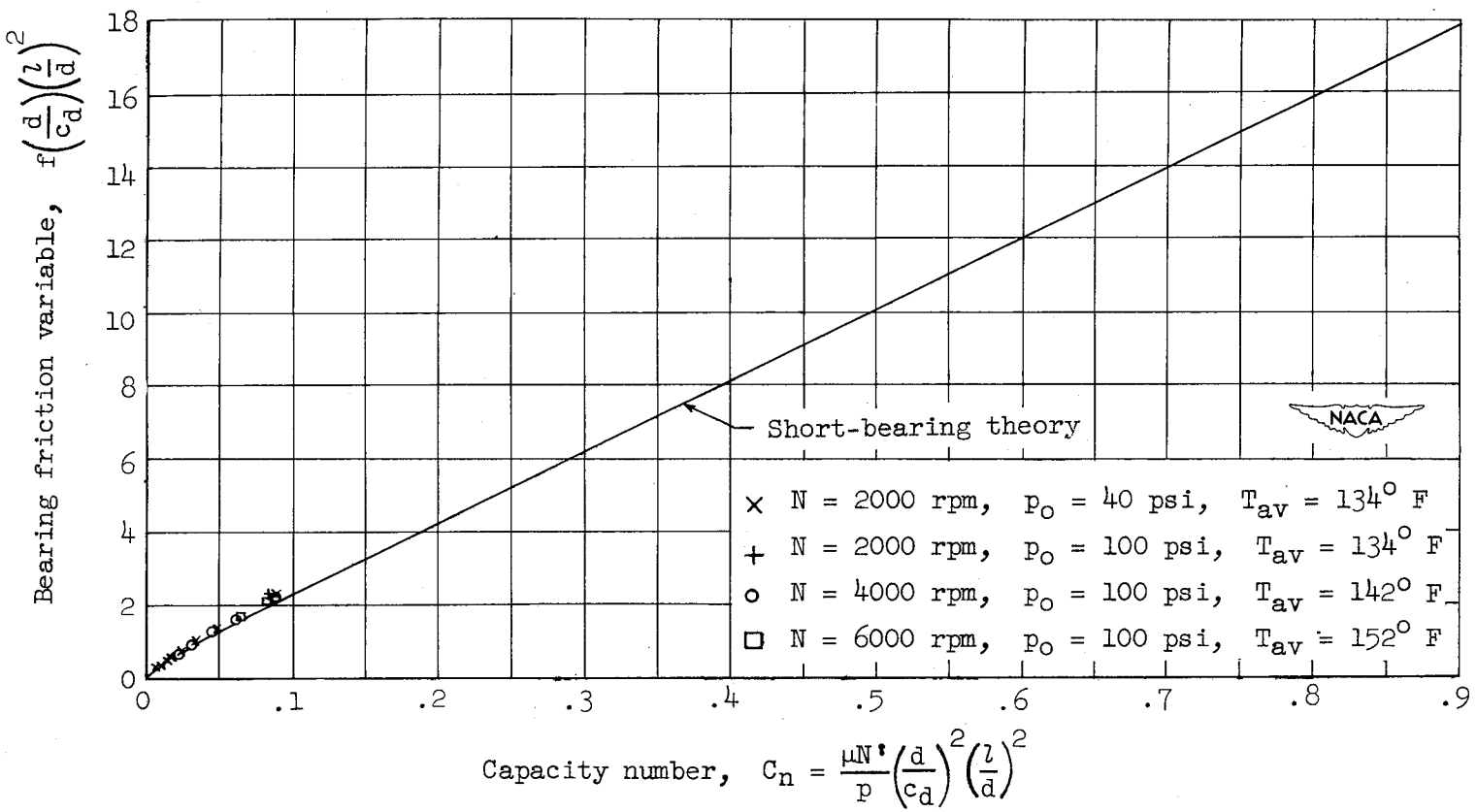

Figure 28.- Plot of bearing friction variable against capacity number for comparison of experimental data for $l/d = 1/4$ with theoretical curve. Experimental data: Bearing diameter, $1\frac{3}{8}$ inches; bearing length, 11/32 inch; bearing, bronze; journal, steel; diametral clearance, 0.00232 inch; inlet pressure of SAE 10 oil p_o fed through one 1/8-inch-diameter hole, 40 and 100 pounds per square inch; speed, 2000 to 6000 rpm; load, 0 to 135 pounds; bearing pressure, 0 to 285 pounds per square inch; average bearing temperature 1/16 inch from oil film T_{av}, 134° to 152° F.

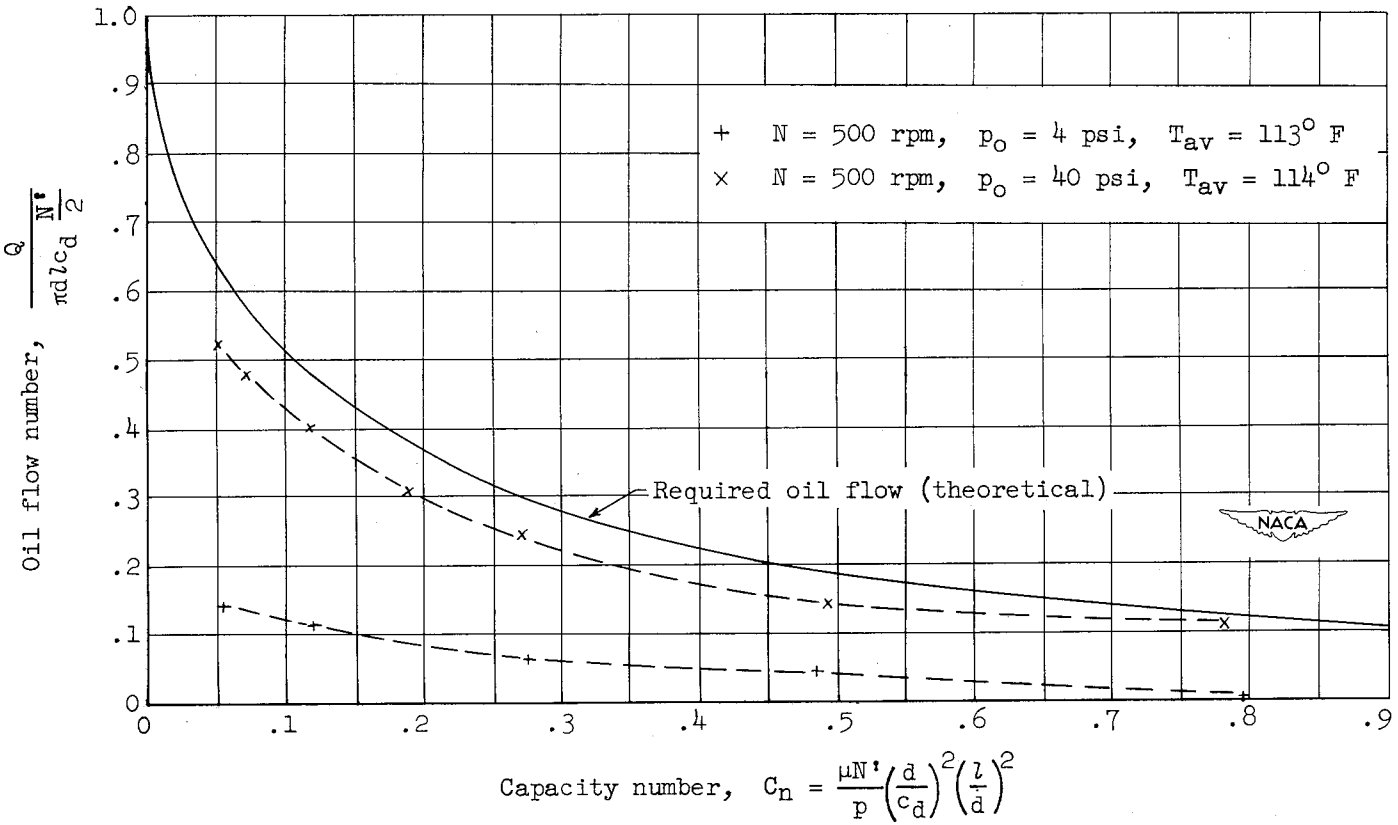

Figure 29.- Plot of oil flow number against capacity number for comparison of experimental total oil flow with theoretically required flow through loaded portion of oil film for $l/d = 2$.

Experimental data: Bearing diameter, $1\frac{3}{8}$ inches; bearing length, $2\frac{3}{4}$ inches; bearing, bronze; journal, steel; diametral clearance, 0.00264 inch; inlet pressure of jet engine oil AN-09-1010 p_o fed through one 1/8-inch-diameter hole, 4 and 40 pounds per square inch; speed, 500 rpm; load 0 to 850 pounds; bearing pressure, 0 to 220 pounds per square inch; average bearing temperature 1/16 inch from oil film T_{av}, 113° and 114° F.

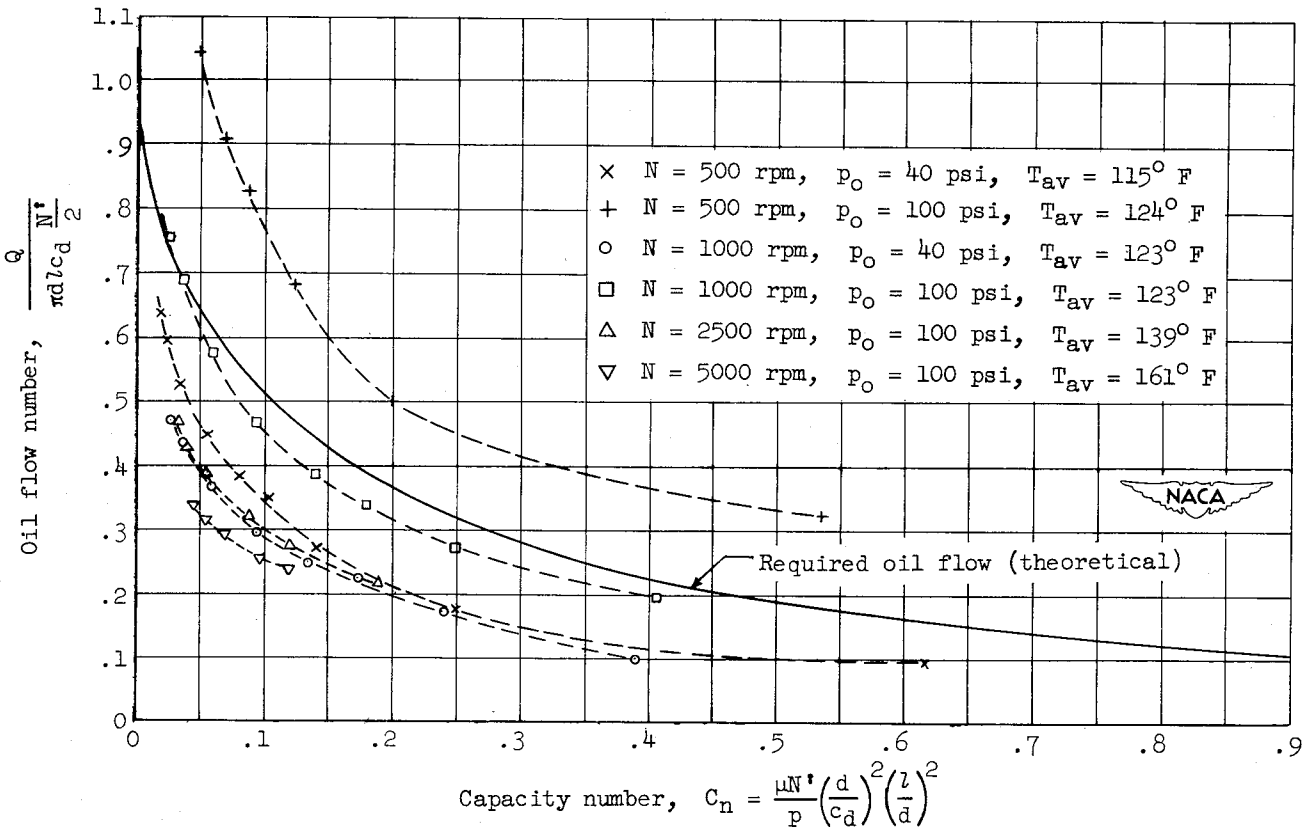

Figure 30.- Plot of oil flow number against capacity number for comparison of experimental total oil flow with theoretically required flow through loaded portion of oil film for $l/d = 1$. Experimental data: Bearing diameter, $1\frac{3}{8}$ inches; bearing length, $1\frac{3}{8}$ inches; bearing, bronze; journal, steel; diametral clearance, 0.00264 inch; inlet pressure of SAE 10 oil p_o fed through one 1/8-inch-diameter hole, 40 and 100 pounds per square inch; speed, 500 to 5000 rpm; load, 0 to 1750 pounds; bearing pressure, 0 to 900 pounds per square inch; average bearing temperature 1/16 inch from oil film T_{av}, 115° to 161° F.

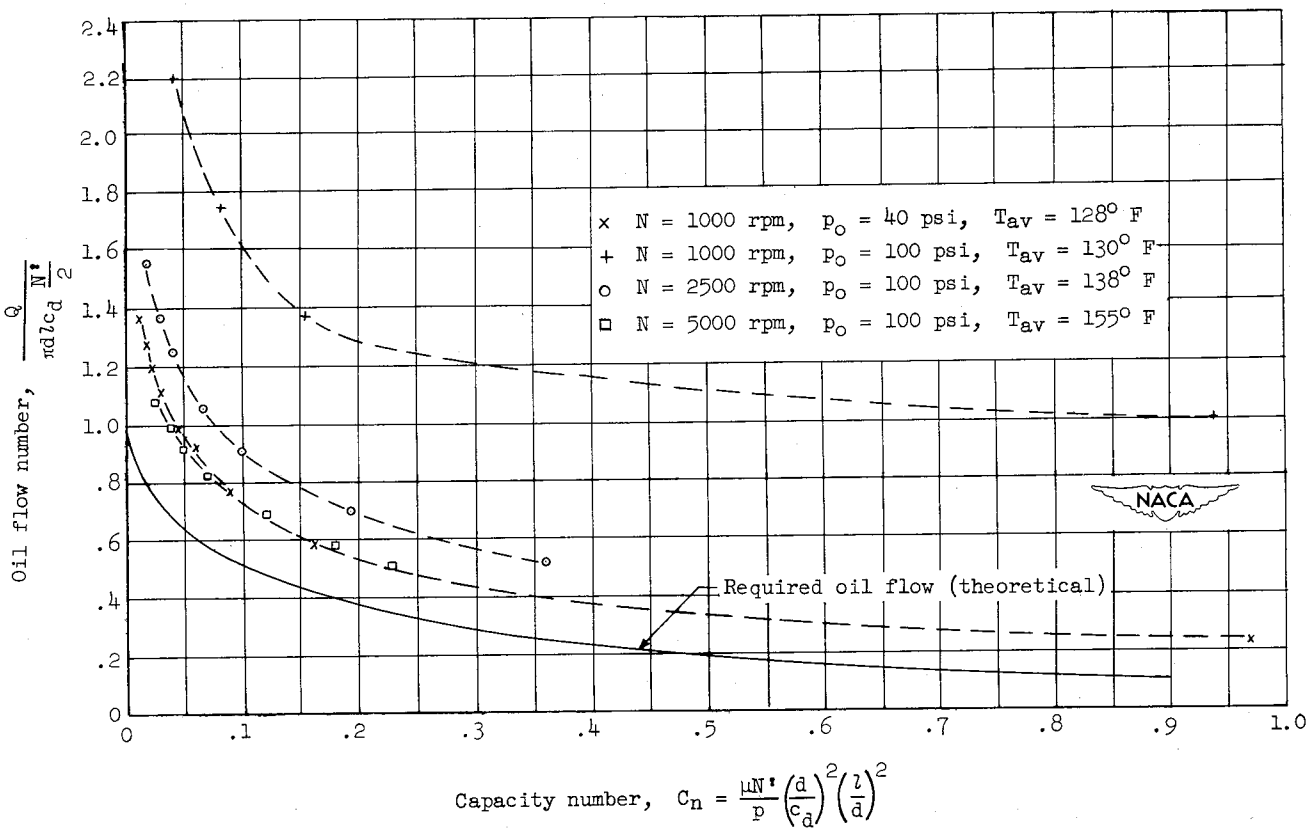

Figure 31.- Plot of oil flow number against capacity number for comparison of experimental total oil flow with theoretically required flow through loaded portion of oil film for $l/d = 1/2$.

Experimental data: Bearing diameter, $1\frac{3}{8}$ inches; bearing length, 11/16 inch; bearing, bronze; journal, steel; diametral clearance, 0.00232 inch; inlet pressure of SAE 10 oil p_o fed through one 1/8-inch-diameter hole, 40 and 100 pounds per square inch; speed, 1000 to 5000 rpm; load, 0 to 490 pounds; bearing pressure, 0 to 515 pounds per square inch; average bearing temperature 1/16 inch from oil film T_{av}, 128° to 155° F.

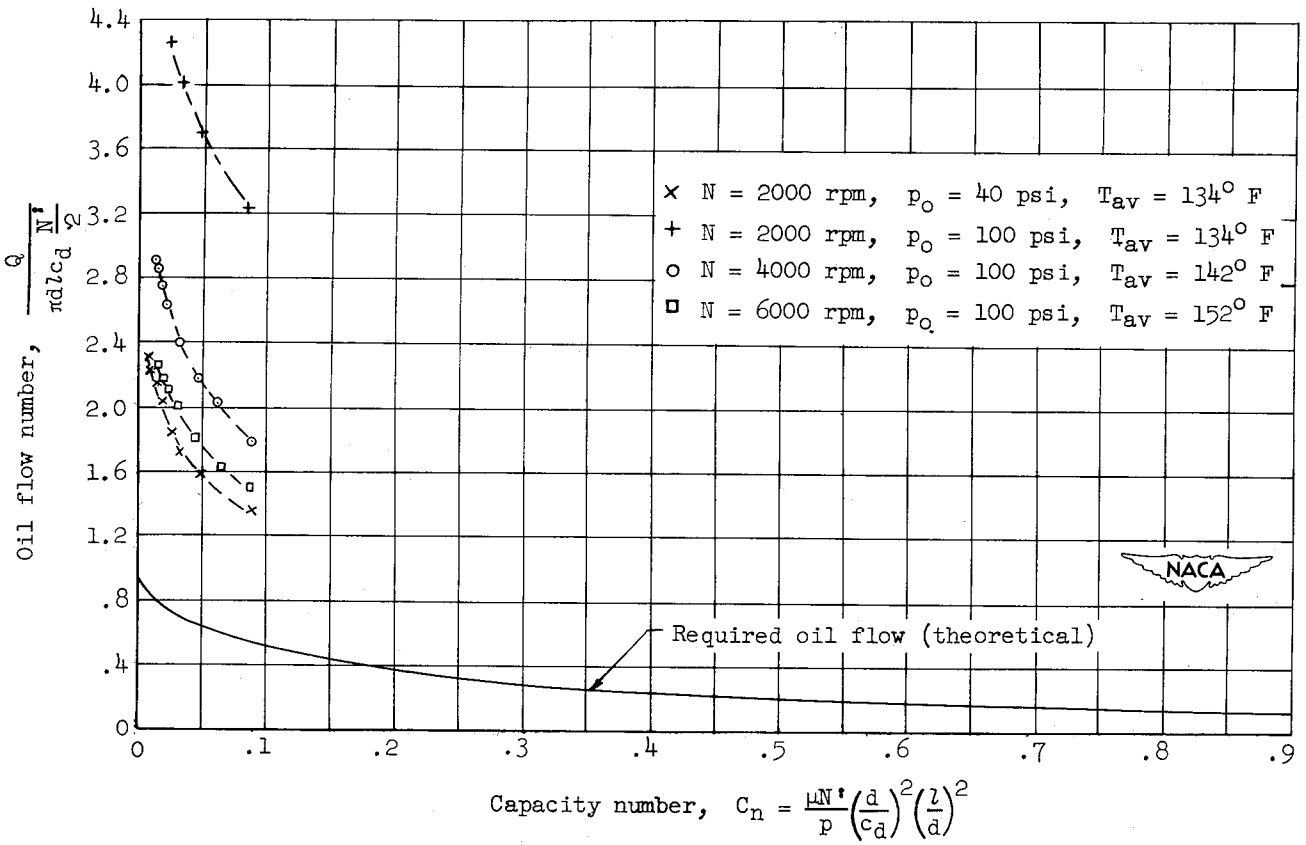

Figure 32.- Plot of oil flow number against capacity number for comparison of experimental total oil flow with theoretically required flow through loaded portion of oil film for $l/d = 1/4$. Experimental data: Bearing diameter, $1\frac{3}{8}$ inches; bearing length, 11/32 inch; bearing, bronze; journal, steel; diametral clearance, 0.00232 inch; inlet pressure of SAE 10 oil p_o fed through one 1/8-inch-diameter hole, 40 and 100 pounds per square inch; speed, 2000 to 6000 rpm; load, 0 to 135 pounds; bearing pressure, 0 to 285 pounds per square inch; average bearing temperature 1/16 inch from oil film T_{av}, 134° to 152° F.

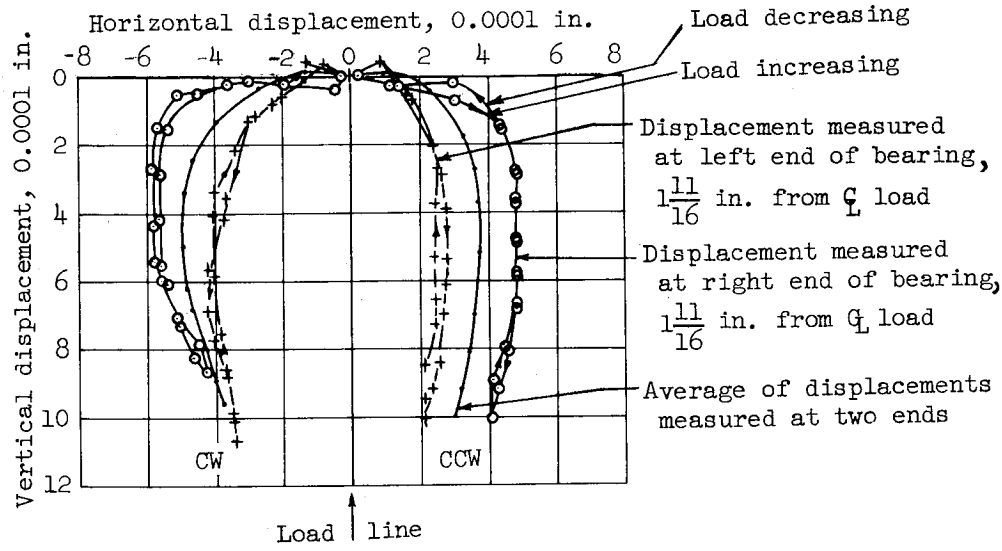

(a) Displacements of journal measured by riders beyond bearing ends.

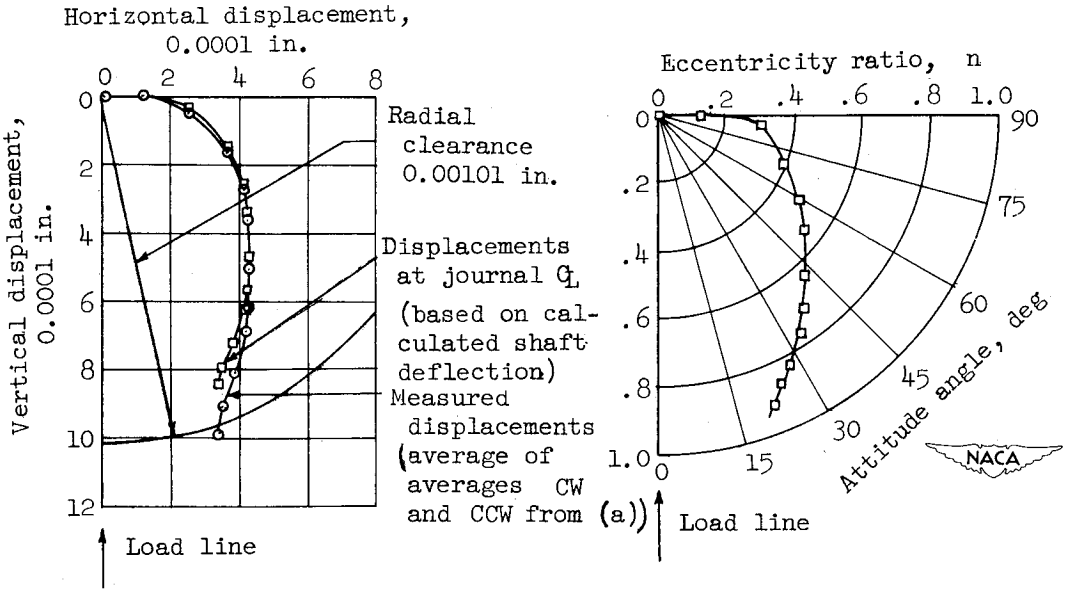

(b) Average journal displacements by riders and displacements at journal center line.

(c) Displacements at journal center line reduced to eccentricity ratios.

Figure 33.- Journal displacements with respect to bearing for shaft with two journals of l/d of 1/2. Steps shown illustrate typical method of determining average eccentricity ratios and attitude angles from displacement data measured beyond ends of bearing. See tables I and III for experimental data and calculations.

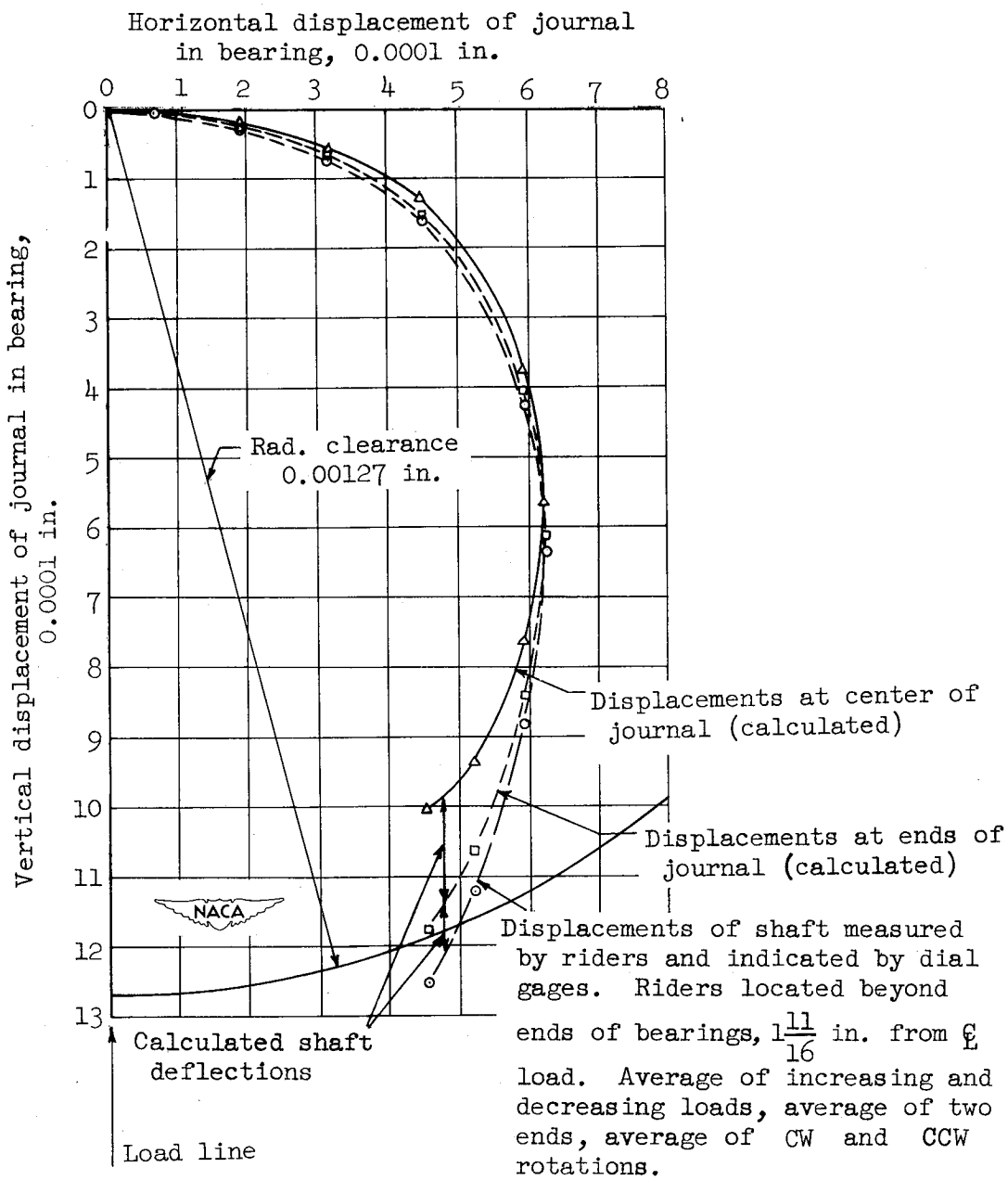

Figure 34.- Journal displacements with respect to bearing for shaft with single journal of l/d of 2. Displacements at ends and center of a bent journal are shown in comparison with displacements measured beyond ends of bearing. Average eccentricity ratios and attitude angles as determined from displacements are shown in figure 35.

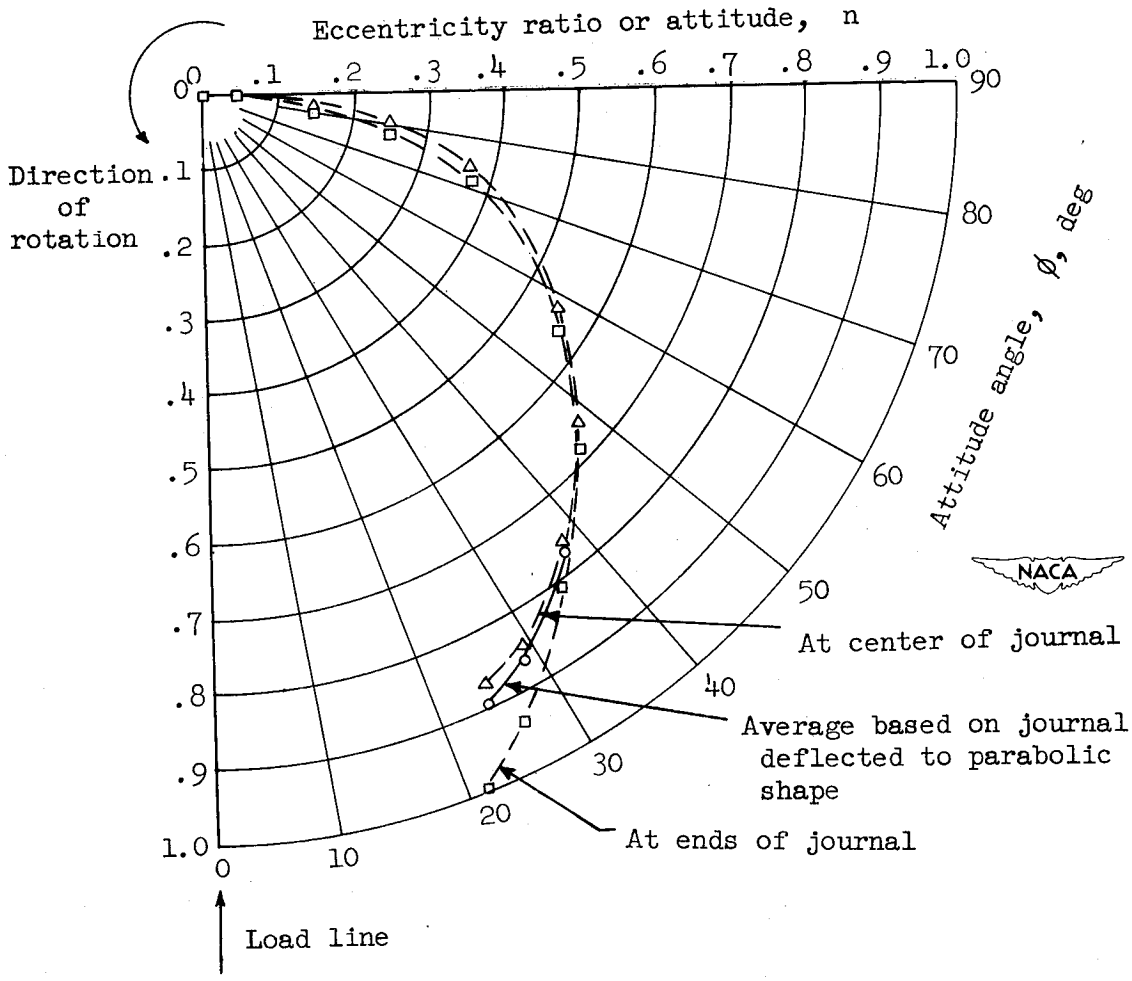

Figure 35.- Eccentricity ratios and attitude angles for shaft with single journal of l/d of 2 as determined from displacements shown in figure 34. The curve of average eccentricity ratios is shown in comparison with eccentricity ratios at ends and center of a bent journal. Experimental data: Speed, 500 rpm; inlet pressure p_o, 40 pounds per square inch; diametral clearance at room temperature, 0.00264 inch; diametral clearance at bearing temperature T_{av} of 119° F, 0.00254 inch; load, 0 to 855 pounds; bearing pressure, 0 to 245 pounds per square inch; AN-09-1010 jet engine oil fed through one 1/8-inch-diameter hole.

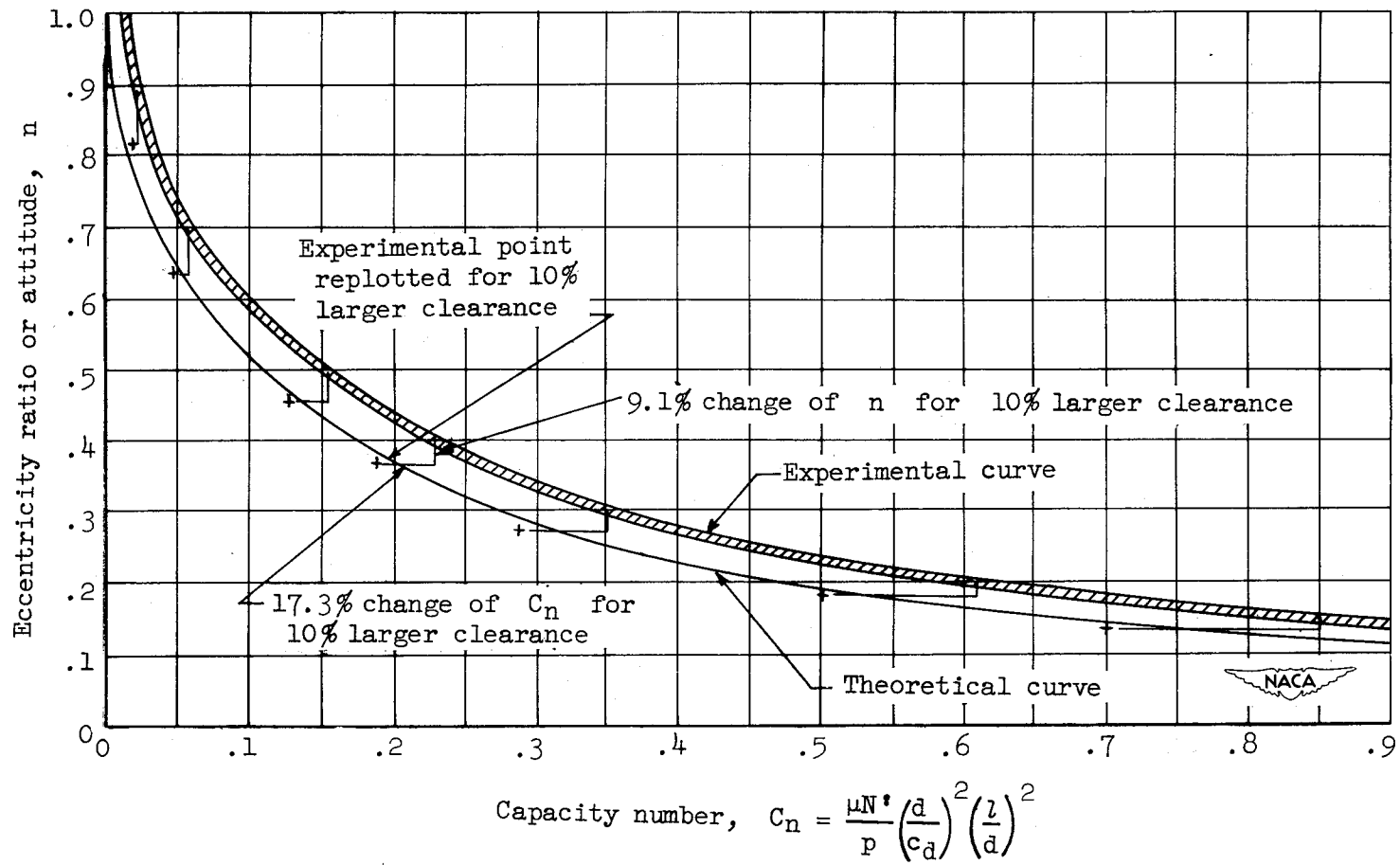

Figure 36.- Effect of error in bearing clearance measurement on eccentricity ratio and capacity number. Shown is amount which experimental curve changes based on assumption that actual clearance of bearing is 10 percent larger than clearance measured by "play" method.

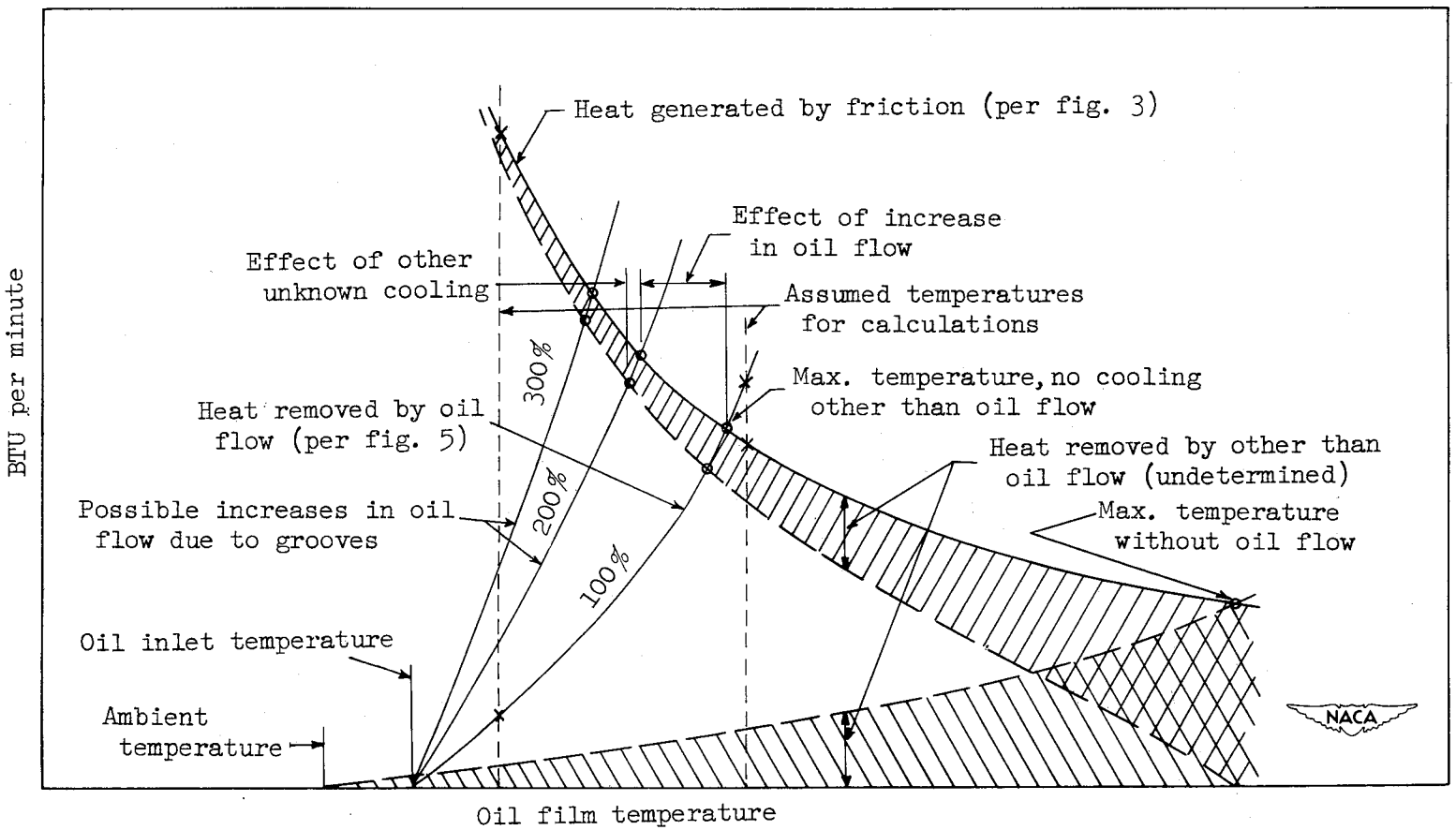

Figure 37.- Heat-balance curves for estimating equilibrium oil film temperature.

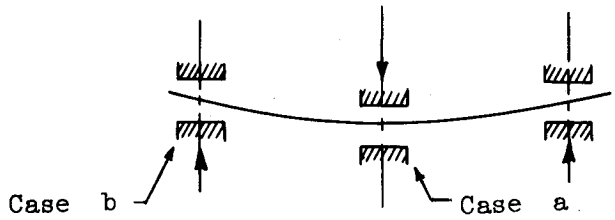

(a) Position of bearing in relation to journal for cases a and b.

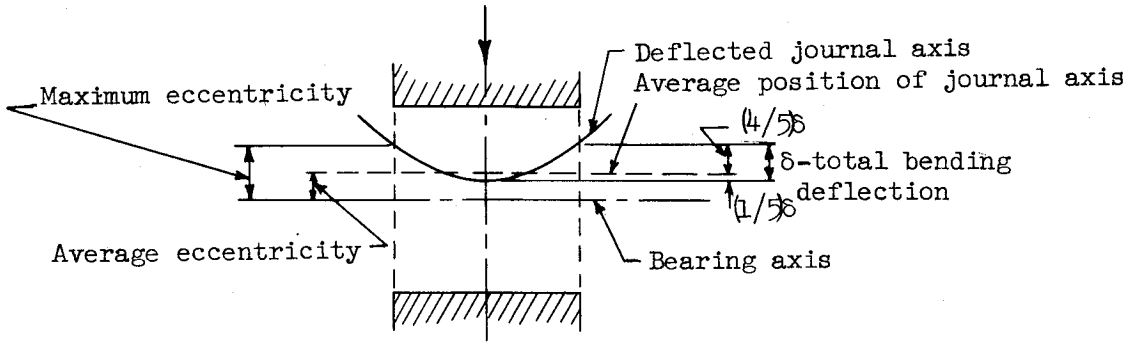

(b) Case a, journal axis parallel to bearing axis at center of bearing.

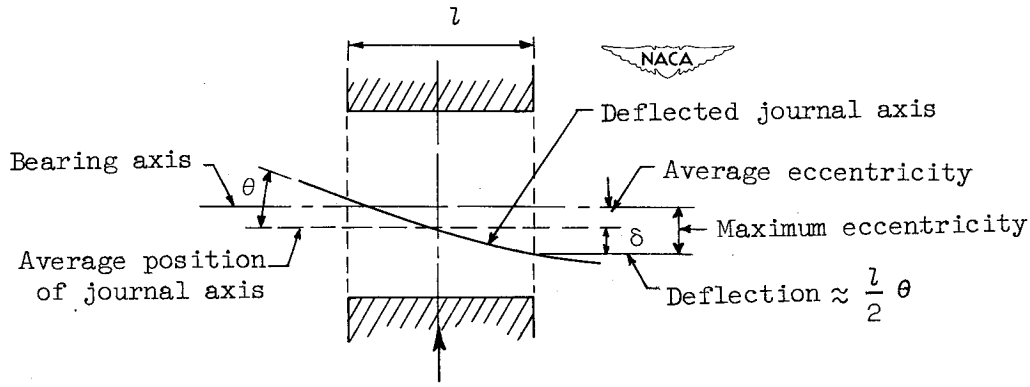

(c) Case b, journal axis inclined to bearing axis at center of bearing.

Figure 38.- Effect of deflection and misalinement on eccentricity at ends of bearing.

NACA-Langley - 11-12-52 - 1000

NACA TN 2809
National Advisory Committee for Aeronautics.
EXPERIMENTAL INVESTIGATION OF ECCENTRICITY RATIO, FRICTION, AND OIL FLOW OF SHORT JOURNAL BEARINGS. G. B. DuBois and F. W. Ocvirk, Cornell University. November 1952. 79p. diagrs., photos., 4 tabs. (NACA TN 2809)

An experimental investigation was conducted to obtain performance data on bearings of length-diameter ratios of 1, 1/2, and 1/4 for comparison with theoretical curves. A 1.375-inch-diameter bearing was tested at speeds up to 6000 rpm and with unit loads from 0 to 900 pounds per square inch. Experimental data for eccentricity ratio and friction followed single lines when plotted against a theoretically derived capacity number, which is equal to Sommerfeld number times the square of the length-diameter ratio. The form of the capacity number indicates that under certain conditions the eccentricity ratio is theoreti-

Copies obtainable from NACA, Washington (over)

1. Friction and Lubrication - Theory and Experiment (3.8.1)
2. Bearings, Sleeve (3.8.2.1)

I. DuBois, George B.
II. Ocvirk, F. W.
III. NACA TN 2809
IV. Cornell U.

NACA TN 2809
National Advisory Committee for Aeronautics.
EXPERIMENTAL INVESTIGATION OF ECCENTRICITY RATIO, FRICTION, AND OIL FLOW OF SHORT JOURNAL BEARINGS. G. B. DuBois and F. W. Ocvirk, Cornell University. November 1952. 79p. diagrs., photos., 4 tabs. (NACA TN 2809)

An experimental investigation was conducted to obtain performance data on bearings of length-diameter ratios of 1, 1/2, and 1/4 for comparison with theoretical curves. A 1.375-inch-diameter bearing was tested at speeds up to 6000 rpm and with unit loads from 0 to 900 pounds per square inch. Experimental data for eccentricity ratio and friction followed single lines when plotted against a theoretically derived capacity number, which is equal to Sommerfeld number times the square of the length-diameter ratio. The form of the capacity number indicates that under certain conditions the eccentricity ratio is theoreti-

Copies obtainable from NACA, Washington (over)

1. Friction and Lubrication - Theory and Experiment (3.8.1)
2. Bearings, Sleeve (3.8.2.1)

I. DuBois, George B.
II. Ocvirk, F. W.
III. NACA TN 2809
IV. Cornell U.

NACA TN 2809
National Advisory Committee for Aeronautics.
EXPERIMENTAL INVESTIGATION OF ECCENTRICITY RATIO, FRICTION, AND OIL FLOW OF SHORT JOURNAL BEARINGS. G. B. DuBois and F. W. Ocvirk, Cornell University. November 1952. 79p. diagrs., photos., 4 tabs. (NACA TN 2809)

An experimental investigation was conducted to obtain performance data on bearings of length-diameter ratios of 1, 1/2, and 1/4 for comparison with theoretical curves. A 1.375-inch-diameter bearing was tested at speeds up to 6000 rpm and with unit loads from 0 to 900 pounds per square inch. Experimental data for eccentricity ratio and friction followed single lines when plotted against a theoretically derived capacity number, which is equal to Sommerfeld number times the square of the length-diameter ratio. The form of the capacity number indicates that under certain conditions the eccentricity ratio is theoreti-

Copies obtainable from NACA, Washington (over)

1. Friction and Lubrication - Theory and Experiment (3.8.1)
2. Bearings, Sleeve (3.8.2.1)

I. DuBois, George B.
II. Ocvirk, F. W.
III. NACA TN 2809
IV. Cornell U.

NACA TN 2809
National Advisory Committee for Aeronautics.
EXPERIMENTAL INVESTIGATION OF ECCENTRICITY RATIO, FRICTION, AND OIL FLOW OF SHORT JOURNAL BEARINGS. G. B. DuBois and F. W. Ocvirk, Cornell University. November 1952. 79p. diagrs., photos., 4 tabs. (NACA TN 2809)

An experimental investigation was conducted to obtain performance data on bearings of length-diameter ratios of 1, 1/2, and 1/4 for comparison with theoretical curves. A 1.375-inch-diameter bearing was tested at speeds up to 6000 rpm and with unit loads from 0 to 900 pounds per square inch. Experimental data for eccentricity ratio and friction followed single lines when plotted against a theoretically derived capacity number, which is equal to Sommerfeld number times the square of the length-diameter ratio. The form of the capacity number indicates that under certain conditions the eccentricity ratio is theoreti-

Copies obtainable from NACA, Washington (over)

1. Friction and Lubrication - Theory and Experiment (3.8.1)
2. Bearings, Sleeve (3.8.2.1)

I. DuBois, George B.
II. Ocvirk, F. W.
III. NACA TN 2809
IV. Cornell U.

cally independent of bearing diameter. A method of plotting oil flow data as a single line is shown. Methods are also discussed for approximating a maximum bearing temperature and evaluating the effect of deflection or misalinement on the eccentricity ratio at the ends of the bearings.

NACA TN 2809

cally independent of bearing diameter. A method of plotting oil flow data as a single line is shown. Methods are also discussed for approximating a maximum bearing temperature and evaluating the effect of deflection or misalinement on the eccentricity ratio at the ends of the bearings.

Copies obtainable from NACA, Washington

NACA TN 2809

cally independent of bearing diameter. A method of plotting oil flow data as a single line is shown. Methods are also discussed for approximating a maximum bearing temperature and evaluating the effect of deflection or misalinement on the eccentricity ratio at the ends of the bearings.

Copies obtainable from NACA, Washington

NACA TN 2809

cally independent of bearing diameter. A method of plotting oil flow data as a single line is shown. Methods are also discussed for approximating a maximum bearing temperature and evaluating the effect of deflection or misalinement on the eccentricity ratio at the ends of the bearings.

Copies obtainable from NACA, Washington

NACA TN 2809
National Advisory Committee for Aeronautics.
EXPERIMENTAL INVESTIGATION OF ECCENTRICITY RATIO, FRICTION, AND OIL FLOW OF SHORT JOURNAL BEARINGS. G. B. DuBois and F. W. Ocvirk, Cornell University. November 1952. 79p. diagrs., photos., 4 tabs. (NACA TN 2809)

An experimental investigation was conducted to obtain performance data on bearings of length-diameter ratios of 1, 1/2, and 1/4 for comparison with theoretical curves. A 1.375-inch-diameter bearing was tested at speeds up to 6000 rpm and with unit loads from 0 to 900 pounds per square inch. Experimental data for eccentricity ratio and friction followed single lines when plotted against a theoretically derived capacity number, which is equal to Sommerfeld number times the square of the length-diameter ratio. The form of the capacity number indicates that under certain conditions the eccentricity ratio is theoreti-

Copies obtainable from NACA, Washington (over)

1. Friction and Lubrication - Theory and Experiment (3.8.1)
2. Bearings, Sleeve (3.8.2.1)

I. DuBois, George B.
II. Ocvirk, F. W.
III. NACA TN 2809
IV. Cornell U.

NACA TN 2809
National Advisory Committee for Aeronautics.
EXPERIMENTAL INVESTIGATION OF ECCENTRICITY RATIO, FRICTION, AND OIL FLOW OF SHORT JOURNAL BEARINGS. G. B. DuBois and F. W. Ocvirk, Cornell University. November 1952. 79p. diagrs., photos., 4 tabs. (NACA TN 2809)

An experimental investigation was conducted to obtain performance data on bearings of length-diameter ratios of 1, 1/2, and 1/4 for comparison with theoretical curves. A 1.375-inch-diameter bearing was tested at speeds up to 6000 rpm and with unit loads from 0 to 900 pounds per square inch. Experimental data for eccentricity ratio and friction followed single lines when plotted against a theoretically derived capacity number, which is equal to Sommerfeld number times the square of the length-diameter ratio. The form of the capacity number indicates that under certain conditions the eccentricity ratio is theoreti-

Copies obtainable from NACA, Washington (over)

1. Friction and Lubrication - Theory and Experiment (3.8.1)
2. Bearings, Sleeve (3.8.2.1)

I. DuBois, George B.
II. Ocvirk, F. W.
III. NACA TN 2809
IV. Cornell U.

NACA TN 2809
National Advisory Committee for Aeronautics.
EXPERIMENTAL INVESTIGATION OF ECCENTRICITY RATIO, FRICTION, AND OIL FLOW OF SHORT JOURNAL BEARINGS. G. B. DuBois and F. W. Ocvirk, Cornell University. November 1952. 79p. diagrs., photos., 4 tabs. (NACA TN 2809)

An experimental investigation was conducted to obtain performance data on bearings of length-diameter ratios of 1, 1/2, and 1/4 for comparison with theoretical curves. A 1.375-inch-diameter bearing was tested at speeds up to 6000 rpm and with unit loads from 0 to 900 pounds per square inch. Experimental data for eccentricity ratio and friction followed single lines when plotted against a theoretically derived capacity number, which is equal to Sommerfeld number times the square of the length-diameter ratio. The form of the capacity number indicates that under certain conditions the eccentricity ratio is theoreti-

Copies obtainable from NACA, Washington (over)

1. Friction and Lubrication - Theory and Experiment (3.8.1)
2. Bearings, Sleeve (3.8.2.1)

I. DuBois, George B.
II. Ocvirk, F. W.
III. NACA TN 2809
IV. Cornell U.

NACA TN 2809
National Advisory Committee for Aeronautics.
EXPERIMENTAL INVESTIGATION OF ECCENTRICITY RATIO, FRICTION, AND OIL FLOW OF SHORT JOURNAL BEARINGS. G. B. DuBois and F. W. Ocvirk, Cornell University. November 1952. 79p. diagrs., photos., 4 tabs. (NACA TN 2809)

An experimental investigation was conducted to obtain performance data on bearings of length-diameter ratios of 1, 1/2, and 1/4 for comparison with theoretical curves. A 1.375-inch-diameter bearing was tested at speeds up to 6000 rpm and with unit loads from 0 to 900 pounds per square inch. Experimental data for eccentricity ratio and friction followed single lines when plotted against a theoretically derived capacity number, which is equal to Sommerfeld number times the square of the length-diameter ratio. The form of the capacity number indicates that under certain conditions the eccentricity ratio is theoreti-

Copies obtainable from NACA, Washington (over)

1. Friction and Lubrication - Theory and Experiment (3.8.1)
2. Bearings, Sleeve (3.8.2.1)

I. DuBois, George B.
II. Ocvirk, F. W.
III. NACA TN 2809
IV. Cornell U.

cally independent of bearing diameter. A method of plotting oil flow data as a single line is shown. Methods are also discussed for approximating a maximum bearing temperature and evaluating the effect of deflection or misalinement on the eccentricity ratio at the ends of the bearings.

Copies obtainable from NACA, Washington

NACA TN 2809

cally independent of bearing diameter. A method of plotting oil flow data as a single line is shown. Methods are also discussed for approximating a maximum bearing temperature and evaluating the effect of deflection or misalinement on the eccentricity ratio at the ends of the bearings.

Copies obtainable from NACA, Washington

NACA TN 2809

cally independent of bearing diameter. A method of plotting oil flow data as a single line is shown. Methods are also discussed for approximating a maximum bearing temperature and evaluating the effect of deflection or misalinement on the eccentricity ratio at the ends of the bearings.

Copies obtainable from NACA, Washington